

Electronic Thesis and Dissertation Repository

4-15-2024 10:30 AM

Investigation of Segregation in Mixing Pharmaceutical Powders using Passive Acoustic Emissions in a V-blender

Omar Salem, *The University of Western Ontario*

Supervisor: Tribe, Lauren A., *The University of Western Ontario*

A thesis submitted in partial fulfillment of the requirements for the Master of Engineering Science degree in Chemical and Biochemical Engineering

© Omar Salem 2024

Follow this and additional works at: <https://ir.lib.uwo.ca/etd>

 Part of the [Chemical Engineering Commons](#)

Recommended Citation

Salem, Omar, "Investigation of Segregation in Mixing Pharmaceutical Powders using Passive Acoustic Emissions in a V-blender" (2024). *Electronic Thesis and Dissertation Repository*. 10001.
<https://ir.lib.uwo.ca/etd/10001>

This Dissertation/Thesis is brought to you for free and open access by Scholarship@Western. It has been accepted for inclusion in Electronic Thesis and Dissertation Repository by an authorized administrator of Scholarship@Western. For more information, please contact wlsadmin@uwo.ca.

Abstract

Powder mixing is a crucial and complex step in pharmaceutical production. Mixing and segregation processes can be monitored using process analytical technologies to improve product quality. Passive acoustic emissions were examined during mixing in a V-blender. Vibrations from the emissions were measured through an accelerometer affixed to the outer V-shell arm lid. Horizontal and vertical loading configurations of particles were examined. Stable mixtures were reached when the measured amplitude plateaued around the approximate weighted average of the particles in the outer V-shell arm. Horizontal loading trials mixed faster and reached stable mixtures in fewer revolutions. Fill level impacted mixing and segregation efficiency inside the V-blender. Passive acoustic emissions examination with different loading orders and fill levels emphasized how to improve mixing efficiency and mitigate segregation. Passive acoustic emissions confirm its effectiveness for monitoring powder mixing and segregation in pharmaceutical production which can enhance product quality and manufacturing efficiency.

Keywords

Pharmaceutical industry, process analytical technologies, passive acoustic emissions, mixing, segregation, vibrations, V-blender, powder processing, loading configuration

Summary for Lay Audience

Tablets and capsules are the most common dosage forms produced of all pharmaceuticals. During tablet and capsule production, several powders are mixed together until the needed uniformity is reached. Mixing is crucial during pharmaceutical production to prevent quality issues such as incorrect concentration of active constituents. Powder mixing must be monitored to ensure that products meet quality standards. Pharmaceutical industry currently uses monitoring methods that are expensive, invasive, destructive, and inefficient. Passive acoustic emissions are non-invasive, non-destructive method and offer effective monitoring of powder mixing at low cost.

Passive acoustic emissions were measured using an accelerometer attached to the lid of the outer arm of the V-shell. During powder mixing, segregation can develop and affect product quality. Segregation occurs when ingredients with different properties start to separate from each other. Experiential trials were completed to evaluate the effect of different loading configurations and fill levels of particles on mixing and segregation. One particle size was loaded on the bottom of the V-shell and the second particle size was loaded on top in case of horizontal loading and one particle size was loaded in the inner arm and the second one in the outer arm in case of vertical loading. Initially, the amplitude measured was similar to the particle loaded on top and in the outer arm. While mixing, the amplitude begins to change moving towards the amplitude of the particle loaded on the bottom and in the inner arm, before reaching a stable mixture and plateauing around the weighted average amplitude based on the relative fractions of the two particle sizes in the outer V-shell arm.

The results showed that horizontal loading mixed faster and reached stable mixtures in fewer revolutions. Also, by increasing the fill level the segregation decreased and the mixing efficiency was impacted. The results from this research can help develop ways to improve mixing efficiency and mitigate segregation in pharmaceutical production. Overall, this research helps support the potential for passive acoustic emissions to be used for monitoring powder mixing and segregation to improve final product quality.

Acknowledgments

I would first like to thank and express my gratitude to my supervisor Dr. Lauren Tribe. Without Dr. Tribe's unwavering support, mentorship, and expertise the completion of my thesis would not have been possible.

I would like to acknowledge the Natural Sciences and Engineering Research Council (NSERC) of Canada and Western Graduate Research Scholarship (WGRS) for their financial contributions.

I would also like to thank Dr. Lars Rehmann and Dr. Paul Charpentier for serving on my advisory committee.

Lastly, I would like to thank my family and friends for their support, love, and encouragement throughout my research period.

Table of Contents

Abstract.....	ii
Keywords.....	iii
Summary for Lay Audience.....	iv
Acknowledgments.....	v
List of Abbreviations.....	xi
List of Tables.....	xiii
List of Figures.....	xv
List of Appendices.....	xviii
1 Introduction.....	1
1.1 Foundations of Powder Mixing.....	2
1.2 Pharmaceutical Powder Mixing Process.....	2
1.3 Mixing Mechanisms.....	3
1.4 Types of Mixtures.....	5
1.4.1 Segregated Mixture.....	5
1.4.2 Random Mixture.....	6
1.4.3 Ordered Mixture.....	6
1.5 Powder Mixing Modes.....	7
1.5.1 Batch Mixing Process.....	7
1.5.2 Continuous Mixing Process.....	9
1.6 Mixture Homogeneity Assessment.....	10
1.7 Mixers Geometries and Types.....	11
1.8 V-blender.....	12
1.9 Segregation.....	14

1.9.1	Mechanisms of Segregation	15
1.9.2	Factors Affecting Segregation	18
1.9.2.1	Handling Processes	19
1.9.2.2	Material Characteristics	19
1.9.2.3	Environmental Conditions	21
1.9.2.4	Mixer Operational Parameters	22
1.10	Mixing Monitoring Methods.....	22
1.10.1	Offline Monitoring.....	22
1.10.2	Quality by Design	24
1.11	Process Analytical Technologies	26
1.12	Thesis Objectives and Overview	27
1.13	Reference	29
2	Process Analytical Technologies Review	37
2.1	Passive Acoustic Emissions	38
2.1.1	Passive Acoustic Emissions Advantages	43
2.1.2	Passive Acoustic Emissions Disadvantages.....	44
2.2	Spectroscopic Techniques.....	44
2.2.1	Near-Infrared Spectroscopy	44
2.2.1.1	NIR Advantages.....	46
2.2.1.2	NIR Disadvantages	47
2.2.2	Raman Spectroscopy.....	47
2.2.2.1	Raman Spectroscopy Advantages.....	49
2.2.2.2	Raman Spectroscopy Disadvantages	49
2.3	Tomographic Techniques.....	49

2.3.1	X-ray Computed Tomography	50
2.3.1.1	X-ray Computed Tomography Advantages	51
2.3.1.2	X-ray Computed Tomography Disadvantages.....	51
2.3.2	Magnetic Resonance Imaging	51
2.3.2.1	Magnetic Resonance Imaging Advantages	52
2.3.2.2	Magnetic Resonance Imaging Disadvantages	53
2.4	Velocimetric Techniques	53
2.4.1	Optical Image Analysis.....	53
2.4.1.1	Optical Image Analysis Advantages	55
2.4.1.2	Optical Image Analysis Disadvantages	55
2.4.2	Positron Emission Particle Tracking.....	56
2.4.2.1	Positron Emission Particle Tracking Advantages	57
2.4.2.2	Positron Emission Particle Tracking Disadvantages	57
2.5	Conclusions.....	57
2.6	References.....	60
3	Investigating Particle Loading Configuration in a V-blender during Powder Mixing Using Passive Acoustic Emissions.....	75
3.1	Introduction.....	75
3.2	Materials and Methods.....	79
3.2.1	Materials	79
3.2.2	Equipment.....	80
3.2.3	Experimental Trials.....	82
3.2.3.1	Individual Particle Size Cuts.....	83
3.2.3.2	Horizontal Loading Configuration.....	84

3.2.3.3	Vertical Loading Configuration	85
3.2.3.4	Intensifier Bar Addition	85
3.3	Results.....	86
3.3.1	Individual Particle Size Cuts.....	86
3.3.2	Horizontal Loading Configuration.....	90
3.3.3	Vertical Loading Configuration	98
3.3.4	Intensifier Bar Addition	111
3.4	Discussion.....	113
3.5	Conclusions.....	128
3.6	References.....	130
4	Effect of Fill Level on Powder Mixing and Segregation in a V-blender Using Passive Acoustic Emissions	140
4.1	Introduction.....	140
4.2	Materials and Methods.....	144
4.2.1	Materials	144
4.2.2	Equipment.....	145
4.2.3	Experimental Trials.....	146
4.2.3.1	Fill Level for Individual Size Fractions	146
4.2.3.2	Fill Level for Mixture Combinations	147
4.3	Results.....	148
4.3.1	Fill Level for Individual Size Fractions	148
4.3.2	Fill Level for Mixture Combinations	148
4.4	Discussion.....	156
4.5	Conclusion	162

4.6	References.....	163
5	Conclusion	166
5.1	General Discussion and Conclusions.....	166
5.2	Future Work and Recommendations	168
5.3	References.....	170
	Appendices.....	172
	Curriculum Vita	177

List of Abbreviations

Abbreviation	Meaning	Page
API	Active Pharmaceutical Ingredient	1
QbD	Quality by Design	24
FDA	Food and Drug Administration	24
ICH	International Council of Harmonization	24
CPP	Critical Process Parameter	25
CQA	Critical Quality Attribute	25
PAT	Process Analytical Technology	25
NIR	Near Infra-Red	37
MRI	Magnetic Resonance Imaging	38
PAE	Passive Acoustic Emission	43
SNV	Standard Normal Variate	45
MSC	Multiplicative Scatter Correction	45
DT	De-Trending	45
PLS	Partial Least Square	45
PCA	Principal Component Analysis	45
HPLC	High Performance Liquid Chromatography	48
FTIR	Fourier Transform Infrared Raman	48
X-ray CT	X-ray Computed Tomography	50
NMR	Nuclear Magnetic Resonance	51
PEPT	Positron Emission Particle Tracking	56
RPT	Radioactive Particle Tracking	56
RPM	Rotation Per Minute	80

STD

Standard Deviation

96

List of Tables

Table 2.1: Summary of the available literature on applications using passive acoustic emission	40
Table 2.2: Some of the available literature that used NIR spectroscopy in mixing.....	45
Table 2.3: Summary of some of the available literature that used Raman spectroscopy in powder mixing	48
Table 2.4: Some of the available literature that used X-ray CT in mixing	50
Table 2.5: Some previous studies that used MRI analysis in mixing monitoring	52
Table 2.6: Some of the available studies that used optical image analysis in mixing ...	54
Table 2.7: Some of the available literature that used PEPT in mixing	56
Table 2.8: Comparison and summary of major PATs currently under development and their applications	58
Table 3.1: Summary of particles and their characteristics	80
Table 3.2: Trials conducted for starch granules binary mixtures and their loading configurations	83
Table 3.3: Sieving results in the outer arm of the V-shell for different size cut trials...	93
Table 3.4: Minimum mixing required to reach stable mixtures for different trials horizontally loaded in the V-blender and their loading order	97
Table 3.5: Sieving data in the outer arm of the V-shell for different trials.....	102
Table 3.6: Minimum mixing required to reach stable mixtures for different trials vertically loaded in the V-blender and their loading order	105

Table 3.7: Vertical versus horizontal loading trials and their average minimum mixing in revolutions required to reach stable mixtures	110
Table 3.8: Sieving results of Cut#1 and Cut#4 binary mixture loaded horizontally in the V-blender with and without intensifier bar additions	112
Table 4.1: Summary of particles used and their characteristics.....	145
Table 4.2: Sieving results of Cut#1 and Cut#4 binary mixture in the outer arm of the V-shell at different fill levels	152

List of Figures

Figure 1.1: Types of different mixtures (adapted from Archer, 2017 (12))	7
Figure 1.2: 16-quart schematic Patterson Kelly V-blender used in this research.....	13
Figure 3.1: Schematic diagram for the V-blender (A) showing its dimensions and (B) showing accelerometer location.....	81
Figure 3.2: Average vibration amplitude of different-sized glass beads in V-shell with trendline	87
Figure 3.3: Average vibration amplitudes of starch granules with trendline and R ² value	87
Figure 3.4: Amplitude distribution of Cut#1 starch granules across three trials of 50 revolutions each	88
Figure 3.5: Cut#1 isolated filtered raw signal after 1 V-shell revolution	89
Figure 3.6: Filtered acoustic signals of Cut#1 starch granules	90
Figure 3.7: Visual observations of different starch granule size fractions horizontally loaded in the V-blender.....	92
Figure 3.8: Acoustic profile of combined trials of Cut#1 (2.00 – 2.36 mm) and Cut#4 (0.006 – 1.18 mm).....	94
Figure 3.9: Acoustic profile of combined trials of Cut#2A (1.70 – 2.00 mm) and Cut#3 (1.18 – 1.40 mm).....	95
Figure 3.10: Calculation of the minimum mixing time needed to reach a stable mixture using +/- 1 STD.....	98
Figure 3.11: Average minimum mixing time in revolutions for horizontal loading trials vs size difference between cuts in millimeters	98

Figure 3.12: Visual observation of Cut#1 and Cut#4 binary mixtures vertically loaded in the V-blender	100
Figure 3.13: Visual observation of Cut#2A and Cut#3 binary mixtures vertically loaded in the V-blender	101
Figure 3.14: Acoustic profile of combined trials of Cut#1 (2.00 – 2.36 mm) and Cut#4 (0.006 – 1.18 mm).....	103
Figure 3.15: Acoustic profile of combined trials of Cut#2A (1.70 – 2.00 mm) and Cut#3 (1.18 – 1.40 mm).....	104
Figure 3.16: Average minimum mixing in revolutions for vertical loading trials vs size difference between cuts in millimeters	106
Figure 3.17: Horizontal versus vertical loadings of Cut#1 and Cut#4 binary mixture	107
Figure 3.18: Vertical versus horizontal loadings of Cut#1 and Cut#4 binary mixture	107
Figure 3.19: Horizontal versus vertical loadings of Cut#2A and Cut#3 binary mixture	108
Figure 3.20: Vertical versus horizontal loadings of Cut#2A and Cut#3 binary mixture	109
Figure 3.21: Average minimum mixing time in revolutions for horizontal and vertical loading trials vs size difference between cuts in millimeters	111
Figure 3.22: (A) Small and (B) large intensifier bar additions with their dimensions	112
Figure 3.23: Schematic diagram for particle motion in the few initial rotations with (A) particles loaded horizontally and (B) particles loaded vertically in the V-blender	118
Figure 3.24: Schematic diagram for particle motion in the vertical direction of mixing in the V-blender	123

Figure 3.25: Estimation of minimum mixing time required in revolutions to reach a stable mixture for binary mixture of Cut#2A and Cut#3 using +/- 1 STD.....	124
Figure 3.26: Schematic diagram showing particle trajectories based on size when (A) V-shell was inverted and (B) V-shell was in an upright position	125
Figure 3.27: (A) Schematic diagram of the support arm protruding into the inner V-shell arm and (B) trajectory segregation of larger particles flow path inside the V-blender.....	127
Figure 4.1: (A) Schematic diagram for the V-blender and its properties and (B) schematic diagram showing accelerometer location.....	145
Figure 4.2: Average vibration amplitudes of individual Cut#1 and Cut#4 at different fill levels with vertical error bars representing +/- 1 STD values	148
Figure 4.3: Visual observation of Cut#1 and Cut#4 binary mixture at varying fill levels in the V-blender	150
Figure 4.4: Effect of fill level on sieving of Cut#4 in the outer arm of the V-shell with trendlines and R ² and P-values.....	153
Figure 4.5: Acoustic profile of combined trials of Cut#1 (2.00 – 2.36 mm) and Cut#4 (0.006 – 1.18 mm) at 10% fill level.....	154
Figure 4.6: Acoustic profile of combined trials of Cut#1 (2.00 – 2.36 mm) and Cut#4 (0.006 – 1.18 mm) at 30% fill level.....	155
Figure 4.7: Acoustic profile of combined trials of Cut#1 (2.00 – 2.36 mm) and Cut#4 (0.006 – 1.18 mm) at 70% fill level.....	156
Figure 4.8: Filtered raw signals of binary mixtures of Cut#1 and Cut#4 at (A) 10% and (B) 70% fill levels by mass ratio of the V-shell.....	161

List of Appendices

Appendix A: Sieving data for different horizontal loading trials in the outer arm of the V-shell.....	172
Appendix B: Sieving data for different vertical loading trials in the outer arm of the V-shell.....	173
Appendix C: Starch granules combined trials with 50-50% binary mixture by mass ratio, Cut#2B (1.40 – 1.70 mm), Cut#4 (0.006 – 1.18 mm) horizontally loaded in the V-blender.....	174
Appendix D: Starch granules combined trials with 50-50% binary mixture by mass ratio, Cut#1 (2.00 – 2.36 mm), Cut#3 (1.18 – 1.40 mm) horizontally loaded in the V-blender.....	174
Appendix E: Starch granules combined trials with 50-50% binary mixture by mass ratio, Cut#2A (1.70 – 2.00 mm), Cut#4 (0.006 – 1.18 mm) horizontally loaded in the V-blender.....	175
Appendix F: Starch granules combined trials with 50-50% binary mixture by mass ratio, Cut#2B (1.40 – 1.70 mm), Cut#4 (0.006 – 1.18 mm) vertically loaded in the V-blender.....	175
Appendix G: Starch granules combined trials with 50-50% binary mixture by mass ratio, Cut#1 (2.00 – 2.36 mm), Cut#3 (1.18 – 1.40 mm) vertically loaded in the V-blender.....	176
Appendix H: Starch granules combined trials with 50-50% binary mixture by mass ratio, Cut#2A ((1.70 – 2.00 mm), Cut#4 (0.006 – 1.18 mm) vertically loaded in the V-blender.....	176

Chapter 1

1 Introduction

Pharmaceutical formulations are commonly developed as capsules and tablets; these solid dosage forms account for approximately 80% of all available pharmaceutical formulations. Capsules and tablets offer a convenient route for drug administration due to their ease of use, transport, stability, and cost-effectiveness (1,2). To make tablets or capsules, the process entails mixing two or more powder ingredients and compressing them into tablets or filling the mixture into capsules. A tablet or capsule must contain an active constituent responsible for the therapeutic effect of the medication, called the Active Pharmaceutical Ingredient (API). Other constituents may be added to the API named additives or excipients. The addition of the excipients may aid in the manufacturing process, protect the oral dosage form, also it may enhance the stability and bioavailability of the product. Additionally, the excipients may act as fillers, surfactants, binders, and lubricants.

During the production of tablets and capsules, several mixing procedures are done to make sure that the API is well distributed in the formulation. Tablet formulation is a multi-stage manufacturing process. The process commonly involves the addition of the API and the excipients, mixing the powder materials altogether, and then granulating the mixture. After the granulation process is finished, the materials are dried to remove excess water, then compressed followed by coating and packaging of the final product. Since most of these ingredients are chemical compounds and can be toxic at high doses if over-administered and can lead to serious adverse events, the API in a formulation must contain a calculated pre-specified dose to be able to deliver its specific therapeutic effect. Moreover, if the dose is inadequately low and is under-administered, it will not give the desired therapeutic effect. The tablet may be produced with quality, texture, composition inconsistency and variations in colors and shapes, which is why it is very important to account for proper mixing and control of the tablet and capsule ingredients to ensure high quality, effective and safe oral dosage forms (3).

1.1 Foundations of Powder Mixing

Powder mixing is a particularly important process in many industries and fields such as the food industry in freeze-dried products, the cosmetics industry in makeup and creams, and the pharmaceutical industry in drug preparations, yet it is very challenging and not completely understood (9). The final product must have specific features, qualities and specifications that match and are agreed upon, one of these specifications is uniform composition. This is especially important in the pharmaceutical industry where the quality index and expectations for the final product are extremely strict, and it must involve accurate drug content and dosage. The main goal of performing powder mixing is to make all the constituents added mixed to a specified level based on the characteristics of the mixed materials until reaching the level of homogeneity suitable for the product's end use. However, the mixing process faces many difficulties due to the diversity and characteristics of the powders that are being mixed.

1.2 Pharmaceutical Powder Mixing Process

Pharmaceutical powder mixing and sampling are considered important in tablet and capsule dosage forms. In the normal mixing process, the API and added excipients are all mixed until the required mixture is reached, then the mixed materials are emptied into a vessel onto a tableting press machine to compress the tablets or a machine to fill the capsules reaching the final stage of the product. If insufficient mixing occurs along the way, it may result in poor powder product quality and the whole batch can be rejected. Controlling the powder mixing process is especially important in the pharmaceutical industry. Reaching the desired homogeneity and uniformity of the final product at the desired scale will help in attaining the required characteristics and quality of the product. The quality control and assurance of the products must be validated at every step of the process to ensure that the final product will meet all the expected standards and specifications. That is why achieving homogenous materials that can result in the final product with certain quality and specifications is a very crucial step in the pharmaceutical industry, especially in formulations with small amounts of potent active constituents (43,44).

The production of all solid dosage forms that include powder mixing requires optimal mixing which plays a crucial role in establishing content uniformity. Optimal powder mixing depends on powder behavior and characteristics which are considered important factors needed to be able to understand and control the mixing process. However, due to a poor understanding of powder mixing, it is still not a clear and efficient process, as many factors can influence and interfere with powder mixings, such as particle diameter, density, shape, flowability, hygroscopicity, segregation, and size distribution, as well as the type of mixer used. Process design and operation are very challenging and have traditionally relied on judgment and experience rather than real scientific data. That is why the mixing process is still considered more of an art rather than science.

There are two main classes of materials: cohesive materials and cohesionless materials. The cohesive materials are considered non-free-flowing materials that can acquire their cohesiveness due to chemical or physical reasons. Individual particulates can stick to other particulates forming a large, agglomerated mixture that eventually may lead to agglomerate segregation. Cohesive materials are not easy to handle in bulk.

Cohesionless materials are considered free-flowing materials that move easily and have a well-defined path of movement. Cohesionless materials are easy to handle in bulk. However, cohesionless materials can cause segregation while being mixed due to different powder characteristics such as shape, size, mass, density, and flowability (4,41).

1.3 Mixing Mechanisms

Powder mixing mechanisms in any mixing apparatus are classified into two groups. The first group is based on the driving force for mixing while the second one is based on the scale that mixing occurs. The first group that is based on the driving force for mixing can be done through three primary mechanisms which are convective mixing, dispersive mixing, and shear mixing. Convective mixing involves the bulk movement of particles inside the mixer whether by tumbling under rotational effects or by a force of action from an impeller or shaft (4). Convective mixing is a rapid process that is easy to scale up, but it has a major drawback which is the segregation of flow structures that lead to random mixture creation (10). Dispersive mixing is a slow process which

involves small random motions of individual particles that result in a more homogenous mixing. It is like diffusion in fluids with the exception that there is a dispersion coefficient instead of the diffusion coefficient for fluids. The dispersion coefficient is seen due to the non-ideal flow patterns of the particles. The dispersion coefficient can be scale-dependent making this type of mixing challenging to be scaled up (4,5,6,10). Shear mixing involves blending by the addition of the materials travelling along driven slip planes of the mixer and there is a velocity gradient within the streams of the powder (5). Often shear mixing decreases agglomeration and can lead to a product with a good consistency. However, it is very challenging to scale up (4,10).

The second group that is based on the scale that mixing can be categorized as macro-mixing or micro-mixing. Macro-mixing involves completely mixing different components or particles at a larger scale, typically at the level of the entire mixture or batch. It is done by convective mixing. In contrast, micro-mixing involves the complete mixing of different components or particles at a small scale, typically at the level of individual particles, which helps to ensure that the final product has uniform composition and properties (7,8).

In the mixing vessels, the type of mixer determines the predominant mechanism of mixing. However, most of the powder mixing processes involve the first group of mixing which relies on the driving force for mixing and the three mechanisms mentioned happen simultaneously and together across the length and time scales. This indicates that the process is unlikely to be dominated by a single mixing mechanism, but a combination of mechanisms that produces homogeneous mixtures. When powders are mixed, the aim is to obtain a uniform mixture in which each particle is evenly distributed throughout the mixture. Various mixing techniques and equipment may be used to achieve this purpose. The type of mixer used in mixing can determine the basic mixing method. For example, some mixers rely on convective mixing, in which particles are transported throughout most of the mixture. Other mixing techniques rely on mixing dispersion, in which particles move due to the positioning of the mixtures. However, regardless of the mixing method used, most powder mixers have an initial

mixing mechanism, which is based on a mixing driving force. This driving force can also include shear, gravity, or electrostatic force. (10,11).

There are two types of homogeneity, long-range and short-range homogeneity. Micro-mixing and macro-mixing can be used to differentiate between the two types of homogeneity. Long-range homogeneity is the variation within a material batch, while the short-term is the variation within the particle level. Micro-mixing is the randomly normal mixed variance mentioned previously. As a result of the presence of expected sampling errors, while measuring the expected variance it is advised to use small samples and increase the expected variance value to account for the errors that may result in incomplete homogeneous mixing. However, the increase in the expected variance can lead to the masking of long-range variations that can give wrong results (36,40). When it comes to sampling, it is important to account for sampling for micro and macro-mixing to account for detecting long-term and short-term variation. This can be achieved by making large samples to check and test for long-range variations and making small samples to be able to recognize and address the agglomeration of materials. It is possible to reduce the effect of the final issue by increasing the mixing process, but for the current issue, different techniques like increasing shear may be needed (36,39,40). This relates to the scale of scrutiny of powder mixing. Danckwerts introduced the term “scale of scrutiny” to describe the minimum size of the regions of segregation in a particular mixture, which would cause it to be regarded as insufficiently mixed. A poor mixture will have a large scale of segregation and a good mixture will have a small scale of segregation.

1.4 Types of Mixtures

The three main types of mixtures are segregated, random, and ordered mixtures.

1.4.1 Segregated Mixture

If differences in the physical properties or the nature of particles are present in the mixer, segregation can occur. Segregation can be seen due to the sticking of some particles to other particles resulting in agglomeration. When the particles agglomerate, they result in a certain degree of homogeneity that is more than the random mixture.

This is the ideal scenario, but usually what happens is that the particles get distributed and stick to each other and the number of one particle to the other varies. This can result in a homogeneity mixture which is lower than that of the random mixture. Figure 1.1-A shows an example of a segregated mixture system (13).

1.4.2 Random Mixture

In a two-ingredient system, both types of particles have a chance of being sampled equally to their average composition. This is known as a random mixture. A random mixture is challenging to reach if the used material has strong interparticle interactions. Figure 1.1-B shows an example of a random mixture of almost equal gray and black tile spots. It is created with noninteracting particles that have almost identical characteristics. In pharmaceuticals, the mixing usually occurs with materials that have different characteristics. It is difficult to achieve this type of mixture in a complete and uniform pattern (13).

1.4.3 Ordered Mixture

The ordered or perfect mixture was named to describe a completely homogenized mixture where the ingredients are uniformly distributed, and units are in order. The mixture should contain the exact ratio of the two ingredients. However, the perfect mixture is an ideal situation that can rarely happen in industry or nature as materials are only mixed to a specific level needed for the level of scale of scrutiny. Figure 1.1-C shows an example of an ordered mixture (13).

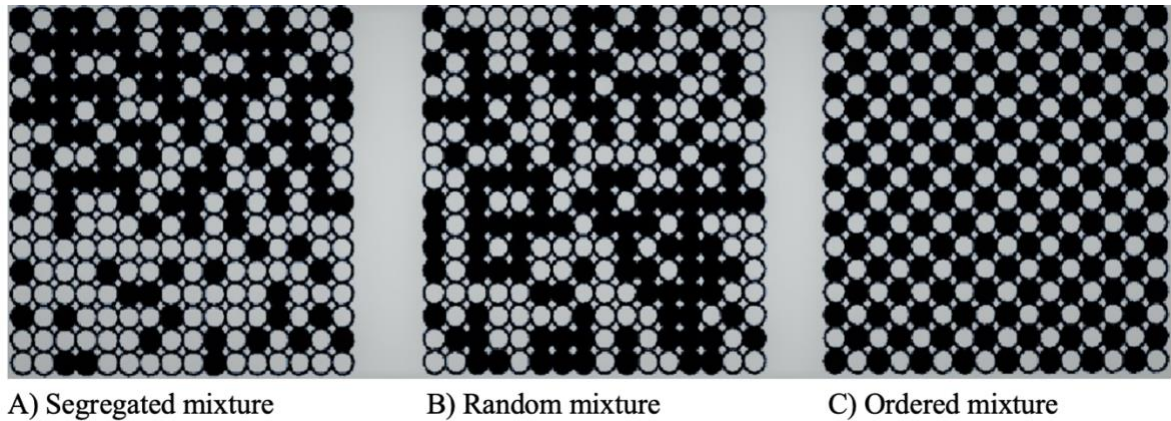


Figure 1.1: Types of different mixtures (adapted from Archer, 2017 (12))

1.5 Powder Mixing Modes

Powder mixing and blending are done through two main methods which are batch and continuous mixing.

1.5.1 Batch Mixing Process

Batch mixing is a process used in many industries. It involves adding a specific number of raw materials into a mixer, subject to certain conditions, and allowing the mixture to blend for a specified period. After the mixture has been blended, it is discharged from the mixer and tested using offline analysis methods to ensure the quality product. This process can be used in a variety of industries, including food and beverage, chemical, and pharmaceutical industries. After the resulting mixture is tested and ensured it is desired, it can proceed to the next step (14).

A batch mixer can be a large cylinder which can be closed appropriately upon adding the constituents and then rotated until the desired time. A typical mixer size used in the pharmaceutical industry ranges from approximately 1 L to over 4000 L. Mixing occurs with rotations of the mixer. Batch mixing results in more precise control over the process than continuous mixing, allowing for extra accuracy and consistency in the results as the net resulting product is extensively tested after each step. Additionally, batch mixing can be more cost-effective since it requires less equipment and material

handling (14,15,16). However, batch mixing has some drawbacks when compared to continuous mixing such as:

- 1) Product variations in the quality of the final products can happen in a batch process due to several factors such as temperature and/or pressure change, mixing times, and materials ratio. This can lead to batch differences which can eventually lack product quality and standards consistency. The temperature change can result in changing the chemical or physical properties of the mixed materials which can lead to unacceptable results in the final product like changes in color, shape, and texture. Also, pressure change and mixing times may lead to changes in the composition of the final product. These are some of the examples of why the whole batch can be discarded if the final products do not match the expected quality and standards needed which can lead to more waste products (16,17).
- 2) Batch processes often lack real-time information resulting in mixtures being allowed to operate for a longer period than what is needed, thereby possibly causing product damage. If the mixing time is too long or too short, the final product may not reach the required consistency or homogeneity or even damage the final product impacting its quality and effectiveness (14,16).
- 3) Thief probe monitoring is often used as part of offline monitoring; however, thief probe sampling can result in disturbing the bed, and loss of product due to over-testing and analysis, and can lead to sampling errors (4,16,18,19). Thief probe sampling is regarded as an inaccurate sampling method because it provides a small sample size that can lead to inaccuracies while analyzing the materials. Moreover, thief probes can be difficult to clean properly which can result in cross-contamination when used and this can impact the product quality. In the pharmaceutical industry, accurate and precise measurements, analyses, and proper equipment cleaning are crucial to avoid several consequences due to sampling measurement errors (44).
- 4) Batch processes do not have enough accepted mathematical models due to the lack of process control and quality, and a lack of choices for process optimization is present. This can lead to an increase in waste, and production of products with inadequate quality, standards, and yield (16,21).

- 5) Batch processes need more mixing time for the same materials than continuous processes, the reason is due to the lack of real-time monitoring that can lead to larger constituents added in the first place or more mixing time than needed. Batch mixing usually uses large machines such as vessels, tanks and mixers which use more time and energy to be loaded, cleaned, and prepared for every batch run. Furthermore, the batch mixing process needs the production line to be stopped between runs limiting the overall throughput and consuming more time (14,16).
- 6) Scaling up is particularly challenging due to the large equipment used in the batch mixing processes. As the batch size increases, the dimensions of the integration vessel and the amount of material being mixed also increase. This can cause demanding situations in terms of device design, processing time, and combining performance (13). Another undertaking in scaling up batch mixing strategies is the processing time. As the batch size increases, the processing time required to attain a homogenous mixture additionally increases. This can cause longer processing times, which may be a problem if the process is time-sensitive or if there is limited production capacity.

1.5.2 Continuous Mixing Process

Continuous mixing is a process where the materials are continually supplied unmixed in the mixer, mixing occurs inside the mixer and on the other side of the mixer, the materials are continually removed in a well-mixed pattern. The mixer does not need to be stopped between the batches like batch mixing process. Continuous mixing is an ongoing process. Most of the mixers have impellers inside the vessel that help the powder to move along the mixer by the action of convection which puts a lot of force on the powder to blend. (13,14). There are some factors for the continuous mixing process to be implemented such as real-time, accurate monitoring, and quality control checks over different periods while the mixing process is happening (16). Continuous mixing has some advantages over batch mixing such as:

- 1) Real-time information control and online monitoring are more easily incorporated (13).

- 2) Continuous mixing processes consume less time than batch processes due to the lack of distinct and separate loading and discharge operations (14,16,21).
- 3) Continuous mixing processes have widely used and accepted mathematical models that can result in improving the quality and standards of the final products by enhancing the product quality, production rate, mixing time and reducing waste. The flow rate of the materials is constant allowing for more optimization and control of the materials. (16,21).
- 4) Continuous processes are easier to scale up than batch processes due to the smaller types of equipment used that allow for efficient production of the required materials without stopping the processes like in batch systems (13).
- 5) In continuous mixing processes, there is a lower risk for segregation than in batch processes due to its automated discharge cycle that makes the products move from one stage to the next to be processed easily and smoothly. There is no need to stop the production line to add materials or clean the mixer like in a batch system process. Moreover, the presence of a wide variety of blenders in the continuous mixing process makes it superior in mixing highly segregating powders (13,16,20).
- 6) Continuous mixers make it easier to change process settings, enhancing the process's adaptability and reducing waste from improperly mixed products (16,20).

1.6 Mixture Homogeneity Assessment

There are several methods to assess the homogeneity of the materials being mixed. One of the accepted and used methods to evaluate the relative homogeneity of a mixture in the industry is by taking multiple samples from the mixer randomly and then determining the composition variance of the mixture. If the results of the composition variance are low, that means the mixture is homogenous (the lower the variance, the more homogenous the mixture). An equation can be used to calculate the expected variance of the mixture composition being analyzed since the nature of the particles used may vary differently. The expected variance can be limited for different natures of particles (36,40). The equation can be described as follows:

$$\sigma^2 = \frac{p(1-p)}{N} \quad (\text{Equation 1.1})$$

Where σ is the expected variance, p is the overall fraction number of one of the components, and N is the number of particles withdrawn randomly from the mixture.

1.7 Mixers Geometries and Types

There are several types, geometries, and shapes for mixers in the pharmaceutical industry that are used to mix various materials. There are two main classifications for mixers: moving or rotating mixers which are also called tumbling mixers and fixed or stationary shell mixers (4.16).

The first type of mixer is the moving or tumbling mixer which consists of a moving shell piece that rotates while the powder is present inside it. In these types of mixers, the main mixing mechanisms used are shear, mixing, and diffusion. Tumbling mixers are easy to clean and used in the cosmetics, food, and pharmaceutical industries (4,16). Some examples that fall under the umbrella of this type of mixer are:

- 1) Double-cone blender. A double-cone blender is a batch mixer that consists of two conical parts linked at the base (4).
- 2) Tote blender. Tote blenders are sealed, attached on an axis, and rotated to allow mixing. Tote blenders are used with an asymmetrical angle to make irregular mixing patterns for the sake of improving the mixing process by breaking up any flow happening inside it while mixing (4).
- 3) V-shell blender. This type of blender is one of the widely used blenders in the pharmaceutical industry. V-blenders consist of two inclined cylinders attached in a "V" shape. A V-blender is a usually used kind of mixer in batch processing. The V-formed vessel creates a natural flow pattern that promotes mixing (4). More details about V-blender will be discussed in Section 1.8 of this Chapter.

The second type of mixer is the fixed or stationary shell mixer also called the convective blender. A convective blender consists of a non-moving shell with a rotating central shaft that helps to mix the powders. Convective blenders use convection as the mixing mechanism (4,16). Some examples of stationary shell mixers are:

- 1) The ribbon mixer. This type of mixer consists of one or two spiral blades. If there are two spiral blades, the first one will be rotating in an axial direction towards the center of the mixer, while the second one will be rotating in the opposite direction near the walls of the mixer (4).
- 2) The orbiting screw blender. It looks like an inverted cone with a screw at the base. It is operated by convection and diffusion mixing mechanisms (4).
- 3) The centrifugal mixers. This type of mixer is also called a planetary mixer. The centrifugal mixer consists of a vessel with a central rotating shaft with mixing blades attached to it. There are two types of centrifugal mixers: the vertical-axis centrifugal mixer and the horizontal-axis centrifugal mixer. The vertical-axis centrifugal mixer is more suitable for cohesive materials and agglomerate formation and treatment than the horizontal-axis centrifugal mixer (4).

1.8 V-blender

A V-blender was used for all the experimental trials of this research (Figure 1.2). The V-blender is a type of tumbling mixer that is commonly used in many industries. It is quite common in the pharmaceutical industry to mix various materials such as powders and granules (16,27). It consists of two inclined cylinders attached to form a “V” shaped shell which is rotated on a horizontal axis. The materials to be mixed are loaded through the top opening of the shell. By the action of mechanical transmission, the powder materials inside the shell of a V-mixer are tumbled and moved back and forth to reach the desired mixing pattern of the powder inside with the help of the two shell arms. While mixing, the tumbling process is considered gentle on the powder to minimize possible physical damage to fragile particles. The normal average cycle time of a V-blender is in the range of 10-15 minutes. The mixing cycle is dependent upon several factors such as the rotation rate, fill level, and the powder material characteristics being mixed (16,27).

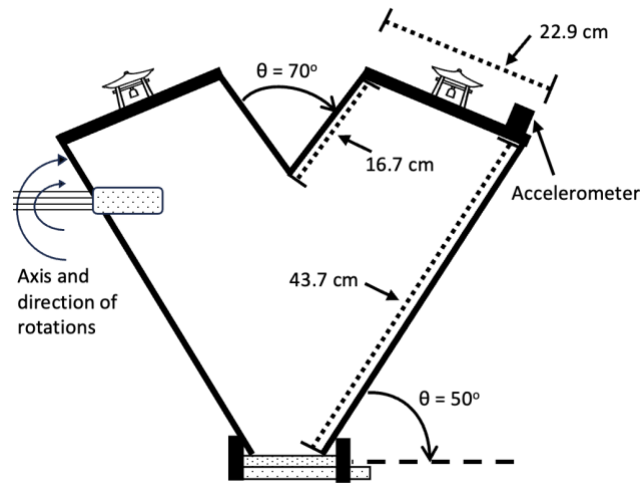


Figure 1.2: 16-quart schematic Patterson Kelly V-blender used in this research

The number of revolutions and speed are crucial factors to get the desired homogeneity of a mixture. The final quality of the mixed product can be affected by the mixing time. The homogeneity of the final mixture product will not be reached if the mixing period is not long enough to allow for proper material mixing. However, if the powder is left to mix for a prolonged period it may cause the materials to be damaged or de-mix (16,27,28). Certain parameters can be changed to ensure the desired mixing outcome is reached such as the filling rate of the mixer, rotation rate, rotation speed, materials loading pattern, and the size of the V-blender used (16,30). There are various materials and sizes for the outer shells of a V-blender and usually, the joint angle ranges between 70° to 90° (16,27,28). Some designs can have blades or baffles to improve the mixing process especially if the mixed materials are cohesive (45).

Due to the uncomplicated design of the shells of the V-blender, they are considered easy to clean and use. Also, the V-blenders can be used with various materials such as granules and powders making them widely used (4,27,46). However, V-blenders have some drawbacks even though they are commonly used in many industries because of the geometry of their shells. For example, in the V-shell arms, there is a lack of mixing due to the angle that results in a dead-end area where mixing is hard to occur. Most of the material mixing in a V-blender occurs in each shell arm. When the V-blender

reaches 180° to 360° angle, that is the only time when the materials in the two arm shells interact with each other at the base of the V-blender (4,16,22,27). Another drawback for the V-blenders is that they can induce segregation of the materials that are being mixed inside them. The induced segregation can be a result of the dead ends that are found at the corner of the V-shell where the material does not mix properly which can lead to the formation of agglomerated materials that can induce segregation. Also, as the V-blender starts to tumble and the materials inside get mixed, the larger particles more likely tend to settle at the base of the V-shaped shell. In contrast, the smaller particles tend to stay at the top of the V-shell. The separation of the particles based on their size can further induce segregation. This is considered one of the biggest problems that are faced in the industry and contributes to a lot of significant issues such as segregation development (4,22,29).

1.9 Segregation

Segregation is a process in which the materials or powder separate or de-mix. Segregation is a phenomenon that occurs when the particles of a powder mixture separate from each other, leading to a non-uniform distribution of particle sizes, densities, and/or chemical composition within the mixture. This can result in uneven flow, mixing, or processing, and affect the quality and consistency of the final product (16,32,42). Segregation occurs due to the tendency of materials that are different in the process and particle properties that tend to segregate (29). It was discovered that the properties of these particles that have the major effect on segregation are density, shape, cohesivity, and size. Due to the difference in these properties, the particles condense and segregate into separate parts in the mixer (4,16,29,32). Mixer design and geometry are key factors in promoting or decreasing segregation. For example, mixers such as orbiting screw mixers, tote blenders, V-blenders, and planetary mixers have been shown to promote segregation (4,22). Upon mixing, segregation of materials can also happen when particles with distinctive characteristics tend to stick to each other forming certain shapes. The more the difference in the characteristics between the particles, the more segregation can occur (16,29).

1.9.1 Mechanisms of Segregation

All powder materials have a certain tendency to de-mix and segregate while being operated in a mixer which can lead to non-homogeneous and not well-mixed powder material resulting in poor-quality products. Different known factors can lead to materials segregation and de-mixing including agglomeration degree, differences in particle shape, size, density and flowability, and mixer design and geometry (32,36). There are two main types of mechanisms for powder segregation which are:

- 1) Trajectory mechanism. This type of segregation happens when mixing a powder with high momentum and another powder with low momentum. While moving the powder particles with varying masses and/or sizes, acceleration and deceleration will occur making the smaller particles accumulate in the center of the mixer while the bigger particles will move toward the outside of the mixer, thus leading to powder separation.
- 2) Percolation mechanism. In the percolation mechanism, gravity makes the smaller particles accumulate in the gaps found between the bigger particles which leads to powder segregation based on the particle size. Upon vibration of the powder inside the mixer, the smaller particles move in a pattern that makes them fall through the gaps of the bigger particles which can lead to de-mixing or separation of the particles based on the size difference.

Trajectory segregation is defined as segregation that occurs while mixing particles with high inertia. Due to inertia, particles with smaller diameters tend to separate from particles with larger diameters of the granular mixture. Particles that tend to have higher inertia or momentum will tend to follow a more straight-line trajectory, while particles with lower inertia or momentum will tend to follow a more curved trajectory. As a result, particles of different densities or sizes may separate into different regions in the used mixer or blender, leading to uneven distribution and potential segregation. The faster the rotations of the V-shell of the V-blender, the higher the inertia of the particles will acquire. At first, the mixtures with slower speeds of rotations will induce the smaller particles with low inertia to accumulate near the walls of the V-shell due to the friction, and the larger particles will accumulate near the base of the V-shell in the

center due to the higher inertia. After some rotations, the opposite will happen with the larger and smaller particles switching places due to the force of inertia increasing leading to a decrease in the friction between the particles making the larger particles present near the walls of the V-shell and the smaller particles near the center of the V-shell. That is why trajectory segregation decreases at the wall by increasing the rotational rates. All these factors are the reason for the identification of the four types of segregation patterns (16,29,33).

The literature discussed the mechanism and pattern formation of segregations in different mixers. Alexander et al, (2003) used a 1.8 L V-blender filled with glass beads at 50% fill capacity. There were two size ranges of glass beads, one of size 150-250 micrograms and the other one of size 700-850 micrograms. It was observed that four main types of segregation mechanisms occurred during powder mixing which are “Small-out phenomena,” “Left-right phenomena,” “Stripes phenomena,” and “Inverse stripes phenomena” (16,29,33). The segregation mechanisms depend on the fill rate of the mixer and the rotation speed, also the density and velocity of the materials being mixed vary throughout the wall and the shell joint which can influence the pattern formation and the mechanism of mixing. Trajectory segregation can happen in a mixer which controls the mixture development and that is for the V-shell joint and the surface wall.

The first phenomenon is the “small-out” which represents a core of bigger particles arising with smaller particles at the sides next to the outer shell. It is a pattern where the small material particles move in a horizontal pattern to reach the arms shells on the outer side, while the bigger particles are left in the base of the V-shell, which can result in almost no mixing of the materials and leads to major segregation in the V-blender. This phenomenon usually happens when the particle velocity at the shell joint and the wall is slow, also it may occur due to the fill level and rotational rates that correspond to 30 – 60 % fill level of the materials in the mixer and 4 - 12 rpm of rotational rates, respectively (16,29,33).

The second phenomenon is the “stripes”. It is a pattern formed in which the smaller particles accumulate in the center of each arm shell of the V-blender and the bigger particles are left on both sides of the smaller ones of each arm shell. The literature has shown that the stripes pattern phenomenon can occur when there are high fill levels of 62 – 80 % of the materials in the V-blender and with high rotation rates that were found to range from 4 – 30 rounds per minute. This pattern phenomenon is formed when the velocity of the particles is fast at the surface wall and slow at the V-shell joint (16,29,33).

The third phenomenon is the “inverse stripes”. This is the opposite of the stripes phenomenon, the pattern formed is the bigger particles accumulate in the center of each arm shell of the V-blender and the smaller ones are left on both sides of the bigger particles of each arm shell. The inverse stripes pattern phenomenon is seen where the rotation rate of the V-blender ranges between 6 – 12 rounds per minute and the fill rate is about 30 – 45 % of the V-shell. It usually happens when the particle velocity is slow at the wall surface and fast at the V-shell joint which is the opposite of the stripes pattern discussed above (16,29,33).

The fourth phenomenon is the “left-right.” This pattern is described by the accumulation of the smaller particles in the outer arm shell and the bigger particles in the inner arm shell of the V-blender. However, the left-right pattern is not completely understood, and some mixing mechanisms and theories are going on and investigated as to why this pattern is formed while mixing the materials. The main problem in this pattern formation is not the segregation issue but the concentration of particles that are affected in each arm shell of the V-blender and the concentration can be affected by the factors of operation and the characteristics of the used materials. This left-right segregation pattern can be seen with a rotational rate of 6 – 30 rounds per minute and at a fill level ranging between 30 – 80 %. The pattern is seen when the velocity of the particles that are being mixed is fast at the V-shell joint and the surface of the wall (16,29,33).

There is a transitional pattern that is seen temporarily while the left-right segregation pattern is being formed which is called the “Big-out” pattern. This temporary big-out pattern is characterized by the bigger particles moving horizontally to the outer arm sides of the V-blender and the smaller particles are seen in the base of the V-blender. The literature and previous research found that the big-out pattern can be seen after 50 revolutions, and it switches back at approximately 250 revolutions.

Wilson and Briens (2022) used starch granules that were sieved into four different size ranges and tried binary mixtures of different size combinations to observe the segregation of the particles. One of the size fractions of the starch granules was dyed to distinguish between other particles allowing for visual observation of segregation. The mixture was 50-50% by mass ratio, and the mixture was loaded and tumbled in a V-blender. It was found that the mixtures with larger differences in the size range exhibited more segregation patterns than others. (16).

The mixing time, fill level, axis of rotation and loading pattern are all factors that contribute to the mixing quality. Top-bottom loading pattern was shown to increase the homogeneity and results in well-mixed powders rather than a side-to-side loading pattern. Moreover, allowing the mixer to mix in a direction that is perpendicular to the axis of rotation also increases the mixing homogeneity and produces a mixture with a prominent level of mixing qualities, while a high fill level of the mixer was seen to decrease the mixture homogeneity and adversely impacted the mixing process (37).

1.9.2 Factors Affecting Segregation

Many factors affect the segregation of powders during mixing. Those factors can be classified into four main groups which are:

- 1) Handling processes
- 2) Material characteristics
- 3) Environmental conditions
- 4) Mixer operational parameters

1.9.2.1 Handling Processes

While handling the materials that are being mixed, different segregation patterns are observed. Segregation can occur while filling the materials inside the mixer or discharging the materials from the mixer. It can happen while mixing, upon deposition, and/or during packing. During the filling process, three segregation mechanisms can be seen which are sieving, fluidization, and trajectory. Sieving and trajectory segregations are seen mainly when a heap is formed. Fluidization segregation can be seen due to the free fall height and/or the use of fine particles. To be able to minimize different segregation patterns, different methods can be used such as using different inserts and distributors to prevent heap formation or reduce free fall height and heap size (62).

1.9.2.2 Material Characteristics

The main material characteristics that play a role in promoting segregation are particle shape, density, cohesivity, surface texture, flowability, adhesion, elasticity, ability to absorb moisture, chemical and physical affinities, brittleness, morphology, particle size, distribution, use of fine particles, and size ratio. All those material features can contribute to segregation, some play a significant role in impacting segregation while others have minimal roles. Physical characteristics are considered one of the key features that can impact segregation and have received more attention than other characteristics. Particle shape, the concentration of fine particles used, particle density, size ratio, distribution, and mean size are all considered to be from the physical characteristics that contribute primarily to powder segregation (62).

Particle shape is one of the physical characteristics that can promote segregation as well as affect the flowability of the particle. Mixtures with multiple particles that have irregular particle shapes are more prone to segregate when compared with regular similarly shaped particles. Tang et al, (2003) stated that segregation is drastically higher in a binary mixture containing irregular coarse-shaped particles with spherical-shaped fine powder compared to when a mixture is used containing spherical-shaped particles that are both fine and coarse. This segregation notice that was found can be explained as the irregularly shaped particles can settle between the void gaps and when

comparing the void gaps that are formed from the irregularly shaped coarse particles and the spherical-shaped particles, it was found that the void gaps from the irregularly shaped coarse particles are significantly larger than spherically shaped ones. The authors agreed that the influence of the particle shape on segregation is smaller than the influence of the size ratio effect (64).

The size ratio of the particle is considered one of the physical characteristics that affect the segregation of a mixture to a great extent. When the particle size ratio increases for free-flowing particles, the segregation potential is increased. For sieving segregation to be seen, the particle size ratio needs to be at least 2:1 to 3:1. Mean particle size is another physical characteristic that can promote segregation. As the particle size decreases the chance of segregation to occur decreases, typically segregation decreases with a mean particle size below 500 μm . Due to decreasing particle size, the different inter-particle forces between the particles such as Van der Waals, capillary, mechanical, and electrostatic forces dominate due to the surface tension. The inter-particle forces are dominating instead of the gravity force. It was found that a minimum mean particle size from 70 to 200 μm in range prevents sieving segregation from appearing. Another characteristic is the fine particle concentration. If the mixture contains 15-30% of fine particles, sieving segregation will appear significantly. Sieving segregation usually can be seen with lower fine particle concentration compared to fluidization segregation which can be seen when the fine particles are over 60-80% of the mixture. When the level of fine particle concentration reaches 60%, segregation starts to decrease noticeably and can reach almost zero (63,64).

Particle density can affect the segregation of the mixture. The higher the particle density, the higher segregation can occur. For example, fine particles with higher particle density have a higher segregation rate than fine particles with lower particle density. One more important characteristic that is related to segregation and can have an impact on segregation is particle flowability. Free-flowing granule materials that have wide particle size distribution can often be segregated. Cohesive particles can initiate a segregation pattern with the particles moving to stick to each other and moving together forming a thick agglomerate patch. Many small agglomerates of

individual mixtures retain their structure during the mixing process which can lead to a small segregation pattern but with high intensity.

The last physical characteristic that can affect the segregation of a mixture is the particle size distribution. However, there are few studies in the literature that quantitatively and effectively linked the effect of the segregation with the particle size distribution, but most researchers reached a common point of view that is considered accepted which is the wider size distribution the particles have, the more segregation can appear (62-64).

1.9.2.3 Environmental Conditions

Segregation can be impacted by environmental conditions such as temperature, vibration, and humidity. Humidity and vibration are widely studied and found in the literature. Humidity or an increase in moisture content can affect the segregation. Generally, increasing humidity can lead to increasing the likelihood of segregation because of the increased moisture content that can affect the particle surface properties resulting in the agglomeration and the powder sticking to each other. Furthermore, if the particles have different characteristics such as different sizes, densities, and shapes, increasing the humidity can lead to the smaller particle accumulating on the bottom of the mixer, while the larger particle remains on the top because of gravitational settling. These mechanisms can result in the segregation of the mixture. However, humidity effect on the segregation of a powder mixture can be dependable on many circumstances such as the type of mixer used, mixer design, mixing rate, mixing time, and properties of the particles being mixed. Increasing moisture content can lead in some scenarios to decrease the segregation probabilities specifically if the mixed mixture can agglomerate and stick to each other if not provided with enough moisture content. Vibrations can cause large particles to move upwards through a mass or finer particles which can lead to an increase in segregation with increasing acceleration but at a constant frequency. Temperature changes can influence segregation development by increasing the tendency of particles to agglomerate. Also, temperature changes can induce chemical reactions within the material being mixed which may result in alteration of the properties of the particles leading to segregation (62,65).

1.9.2.4 Mixer Operational Parameters

Some operational parameters are related and can affect the segregation such as free fall height, size of the heap, feed rate, and velocity rate. The velocity rate can change in the various positions in the mixer. Usually, the velocity in the center of the mixer is much faster compared with the velocity at the wall of the mixer. That velocity gradient in the mixer can lead to potential segregation because of interparticle motion and movement. The velocity gradient and the inter-particle motion that is present inside the mixer can lead to material variability before and after the mixing of the powder. Feed rate is one of the important operational parameters that can affect segregation. The increase in the feed rate will lead to less segregation. Lawrence and Beddow (1969) reported that segregation is reduced when the fill rate and time are reduced. The last parameter is the heap size. It is extremely hard to quantitatively know and estimate the effect of the heap size on segregation. However, it is qualitatively considered that increasing the heap size can result in increasing the potentiality of segregation (62). Prescott and Hossfeld (1994) reported that in the center of the mixer, the velocity is five times more than at the walls which eventually leads to segregation.

Mehrotra et al, (2009) employed a mathematical model to compare mixing rates under various conditions, such as different fill levels, mixer types, and loading patterns. The findings revealed that mixing rates were more efficient when a top-bottom loading pattern was used in comparison with a side-to-side loading pattern. The mixing performance was improved when blenders with the dual axis of rotation were employed in mixing compared with blenders with or without baffles. Furthermore, when the fill levels were low compared to a high fill level, it resulted in an improvement in the mixing performance of the mixtures.

1.10 Mixing Monitoring Methods

1.10.1 Offline Monitoring

In the pharmaceutical industry, different techniques are used to check the quality and standards of the product that is being produced. These methods are considered essential in all industries, especially in industries like the pharmaceutical industry. The thief

probe is considered one of the most common sampling methods within the pharmaceutical industry that is used in the analysis of the powder mixing process and the product quality. (4,16,18). The thief probe consists of an inner rod and an outer rod containing openings or holes to account for sample collection. When the thief probe is used to collect a sample from a mixture, the inner rod is rotated allowing the powder to be filled in the rod openings or holes then the sample can be analyzed. (16,18,49). To use the thief probe in analysis, samples are withdrawn from the powder mixture from several locations from the mixer and then analyzed through different tests. Several types of thief probes are used such as the groove thief probe, plug thief probe, and globe-pharma thief probe. The groove thief probe is considered the least one that may result in errors (16,48,49).

Thief probes are commonly used in the pharmaceutical industry, but they possess some drawbacks that make their use result in inaccurate and error-prone data. Some of the drawbacks are:

- 1) Thief probes disturb the bed while withdrawing the sample from the mixture which may lead to channeling which disrupts the internal structure of the powder materials leading to de-mixing (18,50).
- 2) Thief probes are prone to errors while sampling. One of the main errors is that the withdrawn sample from the mixture may not represent the entire mixture (16,18)
- 3) In the thief probe, the sample withdrawn from the mixture is susceptible to damage and product loss due to the destructive testing methods required such as UV spectroscopy. (16,47).
- 4) The excessive cost of the sampling due to the loss of the product due to using highly destructive testing methods. Furthermore, if the batch does not meet the required standards and qualities, it will be thrown away resulting in more cost and waste products (16,47).
- 5) Thief probes can result in inaccurate results if the materials being mixed are cohesive due to the inability of the cohesive materials to flow well in the rod holes resulting in inaccuracies while sampling (16).

In powder mixing processes, there must be new sampling methods and techniques that must be improved to allow for more accurate, easy, and precise sampling and analysis. Thief probes hinder real-time information and analysis from being available due to their offline nature which may lead to throwing away the unaccepted batches resulting in increased costs and increased waste products (16).

1.10.2 Quality by Design

Quality by design (QbD) is defined as an organized and systematic process for developing pharmaceutical products in a way where the quality of the product is designed and checked along the manufacturing and developing processes as a core focus through the process. Dr. Joseph M. Juran was the first one to introduce the theory of quality by design. Dr. Juran thought that a product's quality should be designed from the start of the development process and most of the errors or quality problems that happen are initially due to a problem in the design of the product. Quality is not a secondary consideration or a performance indicator that is only considered during testing; rather, the whole product or process is created to retain and exceed high standards of quality (16,51). The US Food and Drug Administration (FDA) recommends the adoption and use of the QbD approach and process in the pharmaceutical industry and drug manufacturing, regulation, and development to ensure that the products meet the required qualities. FDA stresses using QbD as the product quality must be initially designed in the product (51). Woodcock (52) defined a product with high quality as a product that is free of contamination and delivers its therapeutic effect.

Pharmaceutical QbD has issued some documents and systems along the way to guide the industry and provide directions to improve product quality, some of those documents are produced by the International Council of Harmonization (ICH) and include ICHQ8 (R2) (Pharmaceutical Development), ICH Q9 (Quality Risk Management), and ICH Q10 (Pharmaceutical Quality System). These documents give directions on how to use and imply QbD in industrial processes for the sake of designing and implementing product quality to be able to develop pharmaceutical products (53-55). The main aims of pharmaceutical QbD are to improve product

development and manufacturing practices, to reach product quality standards that rely upon clinical performance, to increase root cause analysis, and to enhance the product design, understanding, control, and quality by decreasing the variability of the product, decreasing the errors, and enhancing the process capability. These aims can be attained by making a link to the quality of the product and the required clinical performance followed by designing a valid formulation and manufacturing process to be able to reach and produce the desired quality of the product (51).

QbD involves determining Critical Process Parameters (CPPs) and Critical Quality Attributes (CQAs). CPPs can be determined when the process variations are known which can affect the product quality, while the CQAs include the product characteristics which have the most impact on the product quality. CQAs can be chemical, physical, or microbiological features of a material which can impact product quality. That is why a design process should be implemented to make sure that these factors are controlled (51,53). The key elements of QbD are:

- 1) Risk Assessment. To be able to determine possible variability and error sources in the production process and define the critical quality attributes and critical process parameters, a risk assessment must be used in the first step.
- 2) Experiment Design. In the second step after determining the CPPs and CQAs, an experiment design needs to be executed to know how the product quality is affected by these factors.
- 3) Process Analytical Technologies. Process analytical technologies (PATs) are used to ensure that the QbD process philosophy is followed to be able to check, control, and observe the production process in real-time, which helps prevent errors that may occur.
- 4) Regulatory Compliance. QbD is considered a systematic process that is aligned with regulatory authorities. As mentioned previously, the FDA recommends the use of QbD processes in the development and manufacturing of pharmaceutical products to improve product consistency, quality, and production. Nevertheless, it decreases the production variabilities, rejections, and defects and decreases the cost and the waste from unapproved batches.

This introduction to QbD in the pharmaceutical industry does not cover all the aspects and details. More details can be found in the study by Yu et al., (2014).

1.11 Process Analytical Technologies

Process analytical technologies (PATs) are defined as a “system for designing, analyzing, and controlling manufacturing through timely measurements (i.e., during processing) of critical quality and performance attributes of raw and in-process materials and processes to ensure final product quality” (56). PATs rely on the QbD process that is used in many industries such as the pharmaceutical industry. By using PATs in QbD processes, the pharmaceutical manufacturing process can be monitored and controlled in many aspects, which can result in more improvement in the quality of the product in addition to reducing the variabilities and errors that can happen along the production stages (51,53).

The main goal of the PATs is to design and develop well-understood processes that will result in a more consistent quality final product. A well-understood process is defined when all main causes of variation and variability are explained, recognized, and controlled. Lastly, the product quality characteristics can be anticipated precisely and effectively across the design that is specified for the utilized materials and production process (57). Some PATs are not fully developed and utilized. The processes are under development to improve the production process and increase the quality of the powder mixture used in the pharmaceutical industry. Moreover, if PATs are employed well, it may help shift the pharmaceutical processes to continuous processing which can help in improving the efficiency of the tablet manufacturing process and can lower the cost and waste generated in the industry. When PATs are used in monitoring and improving the quality of the powder mixture, it aids in addressing some of the thief probes sampling drawbacks such as inaccurate results and analysis, the need to use destructive testing techniques, and disturbing the bed when a sample is withdrawn (16,57). There are many PATs available and in development for implementation in the industry to improve the powder mixing process. PATs can be different in the monitoring way that is used for powder mixing. Each method has advantages and disadvantages that can allow or restrict the use of the method in the industry. PATs can be classified into four

main groups: Passive acoustic emissions, Spectroscopic, Tomographic, and Velocimetric. Each PAT method will be discussed further in detail regarding its application, advantages, disadvantages, and other features in Chapter 2 of this thesis.

1.12 Thesis Objectives and Overview

The mixing process in the pharmaceutical industry is not fully understood as many factors can influence and interfere with powder mixing. Process design and operation are challenging and have traditionally relied on judgment and experience rather than real scientific data. That is why the mixing process is still considered more of an art rather than science. Further research is required to better understand the process and to develop techniques for its control and monitoring. Also, the mechanism of some segregation patterns is not fully understood, and it remains challenging to monitor their processes and minimize their development. Additionally, more studies and research are needed to investigate and evaluate passive acoustic emissions applications in monitoring powder mixing and segregation in the pharmaceutical industry which is the main motive and aim behind the research conducted in this thesis.

The main objectives of the research completed in this thesis were to expand further on the application of passive acoustic emissions for monitoring powder mixing and segregation in the pharmaceutical industry. This included extended experiments for the different-sized binary mixture combinations and how they mix and behave inside a V-blender. Also, different loading configurations, orders, and patterns were applied for particle loading to evaluate the effect of loading configurations on powder mixing and segregation development as well as identifying stable mixtures with different loadings. Moreover, trials were completed using different intensifier bars attached to the V-blender inner shell arm to test the effect of the little arm that projects in the inner V-shell arm on segregation development. Additionally, experimental trials were completed to understand the effect of different process parameters on mixing and segregation such as V-blender fill level which led to more information extracted from the emission processes and provided more information on powder mixing and segregation while changing V-blender fill levels. With more measurement analysis, improvement and further research, the mixing process and ways to improve and

monitor the process and how to avoid some disruption that may be seen while mixing like segregation could be improved and implemented. The objectives of the research completed in this thesis are addressed over the subsequent chapters, as follows:

Chapter 3 discusses the use of glass beads and starch granules in the V-blender with different loading configurations, patterns, and orders. In addition to the usage of different-sized intensifier bars to monitor mixing and segregation processes while using passive acoustic emissions and exploring its application to the pharmaceutical industry.

Chapter 4 discusses the effect of process parameters on mixing and segregation mainly the effect of different V-shell fill levels of starch granules on powder mixing and segregation development in the V-blender.

Chapter 5 discusses the work completed to date as well as discussing potential future work.

1.13 Reference

1. F. J. Muzzio, T. Shinbrot, and B. J. Glasser, "Powder technology in the pharmaceutical industry: the need to catch up fast," *Powder Technology*, vol. 124, no. 1–2, pp. 1–7, Apr. 2002, doi: [https://doi.org/10.1016/s0032-5910\(01\)00482-x](https://doi.org/10.1016/s0032-5910(01)00482-x).
[https://doi.org/10.1016/s0032-5910\(01\)00482-x](https://doi.org/10.1016/s0032-5910(01)00482-x).
2. N. Debotton and A. Dahan, "Applications of Polymers as Pharmaceutical Excipients in Solid Oral Dosage Forms," *Medicinal Research Reviews*, vol. 37, no. 1, pp. 52–97, Aug. 2016, doi: <https://doi.org/10.1002/med.21403>.
3. G. Léonard, F. Bertrand, J. Chaouki, and P. M. Gosselin, "An experimental investigation of effusivity as an indicator of powder blend uniformity," *Powder Technology*, vol. 181, no. 2, pp. 149–159, Feb. 2008, doi: <https://doi.org/10.1016/j.powtec.2006.12.007>.
4. J. Bridgwater, "Mixing of powders and granular materials by mechanical means—A perspective," *Particuology*, vol. 10, no. 4, pp. 397–427, Aug. 2012, doi: <https://doi.org/10.1016/j.partic.2012.06.002>.
5. E. Ortega-Rivas, *Unit Operations of Particulate Solids: Theory and Practice*. Taylor & Francis, 2011. <https://library.oapen.org/handle/20.500.12657/40119>
6. P. J. Cullen, R. J. Romañach, N. Abatzoglou, and C. D. Rielly, *Pharmaceutical Blending and Mixing*. John Wiley & Sons, 2015.
7. D. Brone, A. Alexander, and F. J. Muzzio, "Quantitative characterization of mixing of dry powders in V-blenders," *AIChE Journal*, vol. 44, no. 2, pp. 271–278, Feb. 1998, doi: <https://doi.org/10.1002/aic.690440206>.
8. M. Lemieux, F. Bertrand, J. Chaouki, and P. Gosselin, "Comparative study of the mixing of free-flowing particles in a V-blender and a bin-blender," *Chemical Engineering Science*, vol. 62, no. 6, pp. 1783–1802, Mar. 2007, doi: <https://doi.org/10.1016/j.ces.2006.12.012>.
9. M. Poux, P. Fayolle, J. Bertrand, D. Bridoux, and J. Bousquet, "Powder mixing: Some practical rules applied to agitated systems," *Powder Technology*, vol. 68, no. 3, pp. 213–234, Dec. 1991, doi: [https://doi.org/10.1016/0032-5910\(91\)80047-M](https://doi.org/10.1016/0032-5910(91)80047-M).
10. J. C. Williams, "The mixing of dry powders," *Powder Technology*, vol. 2, no. 1, pp. 13–20, Sep. 1968, doi: [https://doi.org/10.1016/0032-5910\(68\)80028-2](https://doi.org/10.1016/0032-5910(68)80028-2).

11. M. Poux, "Powder mixing: Some practical rules applied to agitated systems," *Powder Technology*, Jan. 1991.
https://www.academia.edu/108702009/Powder_mixing_Some_practical_rules_applied_to_agitated_systems?uc-sb-sw=14805524
12. A. R. Archer, "An Experimental and Statistical Study of 2D Hopper Flow of Binary Mixtures." Order No. 10268766, Iowa State University, United States -- Iowa, 2017.
13. S. Oka and F. J. Muzzio, "Chapter 4 - Continuous powder mixing and lubrication," *ScienceDirect*, Jan. 01, 2022.
<https://www.sciencedirect.com/science/article/abs/pii/B9780128134795000136>
14. Ralf Weinekötter, "Mixing of Solid Materials," *Particle technology series*, pp. 291–326, Jan. 2016, doi: https://doi.org/10.1007/978-3-319-20949-4_9.
15. H. G. Merkus and Gabriel M.H. Meesters, *Production, Handling and Characterization of Particulate Materials*. Springer Nature (Netherlands), 2016. doi: <https://doi.org/10.1007/978-3-319-20949-4>
16. K. Wilson, "Application of Passive Acoustic Emissions for Inline Monitoring of Segregation Prone Mixtures in a V-Blender." Aug. 2022.
17. M. Asachi, E. Nourafkan, and A. Hassanpour, "A review of current techniques for the evaluation of powder mixing," *Advanced Powder Technology*, vol. 29, no. 7, pp. 1525–1549, Jul. 2018, doi: <https://doi.org/10.1016/j.apr.2018.03.031>.
18. F. J. Muzzio et al., "Sampling and characterization of pharmaceutical powders and granular blends," *International Journal of Pharmaceutics*, vol. 250, no. 1, pp. 51–64, Jan. 2003, doi: [https://doi.org/10.1016/S0378-5173\(02\)00481-7](https://doi.org/10.1016/S0378-5173(02)00481-7).
19. D. S. Hausman, R. T. Cambron, and A. Sakr, "Application of Raman spectroscopy for on-line monitoring of low dose blend uniformity," *International Journal of Pharmaceutics*, vol. 298, no. 1, pp. 80–90, Jul. 2005, doi: <https://doi.org/10.1016/j.ijpharm.2005.04.011>.
20. W. Engisch and F. Muzzio, "Using Residence Time Distributions (RTDs) to Address the Traceability of Raw Materials in Continuous Pharmaceutical Manufacturing," *Journal of Pharmaceutical Innovation*, vol. 11, no. 1, pp. 64–81, Nov. 2015, doi: <https://doi.org/10.1007/s12247-015-9238-1>.

21. K. Plumb, "Continuous Processing in the Pharmaceutical Industry," *Chemical Engineering Research and Design*, vol. 83, no. 6, pp. 730–738, Jun. 2005, doi: <https://doi.org/10.1205/cherd.04359>.
22. Van der Wel "P. Powder Mixing. Powder Handl Process"11: 83-86. 1999.
23. A. U. Vanarase and F. J. Muzzio, "Effect of operating conditions and design parameters in a continuous powder mixer," *Powder Technology*, vol. 208, no. 1, pp. 26–36, Mar. 2011, doi: <https://doi.org/10.1016/j.powtec.2010.11.038>.
24. A. U. Vanarase, J. G. Osorio, and F. J. Muzzio, "Effects of powder flow properties and shear environment on the performance of continuous mixing of pharmaceutical powders," *Powder Technology*, vol. 246, pp. 63–72, Sep. 2013, doi: <https://doi.org/10.1016/j.powtec.2013.05.002>.
25. L. Pernenkil and C. L. Cooney, "A review on the continuous blending of powders," *Chemical Engineering Science*, vol. 61, no. 2, pp. 720–742, Jan. 2006, doi: <https://doi.org/10.1016/j.ces.2005.06.016>.
26. H. P. Kuo, R. C. Hsu, and Y. C. Hsiao, "Investigation of axial segregation in a rotating drum," *Powder Technology*, vol. 153, no. 3, pp. 196–203, Jun. 2005, doi: <https://doi.org/10.1016/j.powtec.2005.03.018>.
27. D. Brone, C. Wightman, K. Connor, A. Alexander, F. J. Muzzio, and P. Robinson, "Using flow perturbations to enhance mixing of dry powders in V-blenders," *Powder Technology*, vol. 91, no. 3, pp. 165–172, May 1997, doi: [https://doi.org/10.1016/s0032-5910\(96\)03231-7](https://doi.org/10.1016/s0032-5910(96)03231-7).
28. G. G. Pereira and P. W. Cleary, "De-mixing of binary particle mixtures during unloading of a V-blender," *Chemical Engineering Science*, vol. 94, pp. 93–107, May 2013, doi: <https://doi.org/10.1016/j.ces.2013.02.051>.
29. A. Alexander, F. J. Muzzio, and T. Shinbrot, "Segregation patterns in V-blenders," *Chemical Engineering Science*, vol. 58, no. 2, pp. 487–496, Jan. 2003, doi: [https://doi.org/10.1016/s0009-2509\(02\)00530-4](https://doi.org/10.1016/s0009-2509(02)00530-4).
30. M. Lemieux, F. Bertrand, J. Chaouki, and P. Gosselin, "Comparative study of the mixing of free-flowing particles in a V-blender and a bin-blender," *Chemical Engineering Science*, vol. 62, no. 6, pp. 1783–1802, Mar. 2007, doi: <https://doi.org/10.1016/j.ces.2006.12.012>.

31. D. Brone, A. Alexander, and F. J. Muzzio, "Quantitative characterization of mixing of dry powders in V-blenders," *AIChE Journal*, vol. 44, no. 2, pp. 271–278, Feb. 1998, doi: <https://doi.org/10.1002/aic.690440206>.
32. S. Oka, A. Sahay, W. Meng, and F. Muzzio, "Diminished segregation in continuous powder mixing," *Powder Technology*, vol. 309, pp. 79–88, Mar. 2017, doi: <https://doi.org/10.1016/j.powtec.2016.11.038>.
33. A. Alexander, T. Shinbrot, B. Johnson, and F. J. Muzzio, "V-blender segregation patterns for free-flowing materials: effects of blender capacity and fill level," *International Journal of Pharmaceutics*, vol. 269, no. 1, pp. 19–28, Jan. 2004, doi: [https://doi.org/10.1016/s0378-5173\(03\)00296-5](https://doi.org/10.1016/s0378-5173(03)00296-5).
34. J. Swarbrick, *Encyclopedia of pharmaceutical science and technology*. Boca Raton: Crc Press, Taylor & Francis Group, 2013.
35. A. Alexander, T. Shinbrot, and F. J. Muzzio, "Scaling surface velocities in rotating cylinders as a function of vessel radius, rotation rate, and particle size," *Powder Technology*, vol. 126, no. 2, pp. 174–190, Jul. 2002, doi: [https://doi.org/10.1016/s0032-5910\(02\)00010-4](https://doi.org/10.1016/s0032-5910(02)00010-4).
36. R. Hogg, "Mixing and Segregation in Powders: Evaluation, Mechanisms and Processes," *KONA Powder and Particle Journal*, vol. 27, no. 0, pp. 3–17, 2009, doi: <https://doi.org/10.14356/kona.2009005>.
37. A. Mehrotra and F. J. Muzzio, "Comparing mixing performance of uniaxial and biaxial bin blenders," *Powder Technology*, vol. 196, no. 1, pp. 1–7, Nov. 2009, doi: <https://doi.org/10.1016/j.powtec.2009.06.008>.
38. J. Mosby, S. R. de Silva, and G. G. Enstad, "Segregation of Particulate Materials – Mechanisms and Testers," *KONA Powder and Particle Journal*, vol. 14, no. 0, pp. 31–43, 1996, doi: <https://doi.org/10.14356/kona.1996008>.
39. P. Tang and V. M. Puri, "Methods for Minimizing Segregation: A Review," *Particulate Science and Technology*, vol. 22, no. 4, pp. 321–337, Oct. 2004, doi: <https://doi.org/10.1080/02726350490501420>.
40. R. Hogg, "Characterization of relative homogeneity in particulate mixtures," *International Journal of Mineral Processing*, vol. 72, no. 1–4, pp. 477–487, Sep. 2003, doi: [https://doi.org/10.1016/s0301-7516\(03\)00121-2](https://doi.org/10.1016/s0301-7516(03)00121-2).

41. N. Harnby, "An engineering view of pharmaceutical powder mixing," *Pharmaceutical Science & Technology Today*, vol. 3, no. 9, pp. 303–309, Sep. 2000, doi: [https://doi.org/10.1016/s1461-5347\(00\)00283-2](https://doi.org/10.1016/s1461-5347(00)00283-2).
42. Ko Higashitani, H. Makino, and Shuji Matsusaka, *Powder Technology Handbook*, Fourth Edition. CRC Press, 2019.
43. H. Berthiaux, K. Marikh, and C. Gatumel, "Continuous mixing of powder mixtures with pharmaceutical process constraints," *Chemical Engineering and Processing: Process Intensification*, vol. 47, no. 12, pp. 2315–2322, Nov. 2008, doi: <https://doi.org/10.1016/j.cep.2008.01.009>.
44. F. J. Muzzio, P. Robinson, C. Wightman, and Dean Brone, "Sampling practices in powder blending," *International Journal of Pharmaceutics*, vol. 155, no. 2, pp. 153–178, Sep. 1997, doi: [https://doi.org/10.1016/s0378-5173\(97\)04865-5](https://doi.org/10.1016/s0378-5173(97)04865-5).
45. "Perry's chemical engineers' handbook," *Choice Reviews Online*, vol. 35, no. 06, pp. 35–307935–3079, Feb. 1998, doi: <https://doi.org/10.5860/choice.35-3079>.
46. D. M. Parikh, *Handbook of pharmaceutical granulation technology*. New York, N.Y.: Informa Healthcare, 2007.
47. G. J. Vergote et al., "In-line monitoring of a pharmaceutical blending process using FT-Raman spectroscopy," *European Journal of Pharmaceutical Sciences*, vol. 21, no. 4, pp. 479–485, Mar. 2004, doi: <https://doi.org/10.1016/j.ejps.2003.11.005>.
48. R. Deveswaran, S. Bharath, BV. Basavaraj, S. Abraham, S. Furtado, S. Madhavan, "Concepts and Techniques of Pharmaceutical Powder Mixing Process: A Current Update," *Research Journal of Pharmacy and Technology*, vol. 2, no. 2, pp. 245–249, 2014.
49. T. P. Garcia, S. J. Wilkinson, and J. F. Scott, "The Development of a Blend-Sampling Technique to Assess the Uniformity of a Powder Mixture," *Drug Development and Industrial Pharmacy*, vol. 27, no. 4, pp. 297–307, Jan. 2001, doi: <https://doi.org/10.1081/ddc-100103729>.
50. D. S. Hausman, R. T. Cambron, and A. Sakr, "Application of Raman spectroscopy for on-line monitoring of low dose blend uniformity," *International Journal of Pharmaceutics*, vol. 298, no. 1, pp. 80–90, Jul. 2005, doi: <https://doi.org/10.1016/j.ijpharm.2005.04.011>.

51. L. X. Yu et al., “Understanding Pharmaceutical Quality by Design,” *The AAPS Journal*, vol. 16, no. 4, pp. 771–783, May 2014, doi: <https://doi.org/10.1208/s12248-014-9598-3>.
52. J. Woodcock, “The concept of pharmaceutical quality” *American Pharmaceutical Review* 1-3, Nov, 2004.
53. Center for Drug Evaluation and Research, “Q8(R2) Pharmaceutical Development,” U.S. Food and Drug Administration, 2019. <https://www.fda.gov/regulatory-information/search-fda-guidance-documents/q8r2-pharmaceutical-development>
54. C. for D. E. and Research, “Q9(R1) Quality Risk Management,” U.S. Food and Drug Administration, Jun. 15, 2022. <https://www.fda.gov/regulatory-information/search-fda-guidance-documents/q9r1-quality-risk-management>
55. Center for Drug Evaluation and Research, “Q10 Pharmaceutical Quality System,” U.S. Food and Drug Administration, 2019. <https://www.fda.gov/regulatory-information/search-fda-guidance-documents/q10-pharmaceutical-quality-system>
56. Center for Drug Evaluation and Research, “Q8(R2) Pharmaceutical Development,” U.S. Food and Drug Administration, Center for Biologics Evaluation and Research (CBER), 2019. Guidance for Industry. <https://www.fda.gov/regulatory-information/search-fda-guidance-documents/q8r2-pharmaceutical-development>
57. A. S. Rathore, R. Bhambure, and V. Ghare, “Process analytical technology (PAT) for biopharmaceutical products,” *Analytical and Bioanalytical Chemistry*, vol. 398, no. 1, pp. 137–154, May 2010, doi: <https://doi.org/10.1007/s00216-010-3781-x>.
58. Bruneau M. “Fundamentals of Acoustics”, London, England: ISTE Ltd; 70. 2006.
59. Fabien Anselmet and Pierre-Olivier Mattei, *Acoustics, aeroacoustics and vibrations*. London: Iste ; Wiley, 2016.
60. J. Boyd and J. Varley, “The uses of passive measurement of acoustic emissions from chemical engineering processes,” *Chemical Engineering Science*, vol. 56, no. 5, pp. 1749–1767, Mar. 2001, doi: [https://doi.org/10.1016/s0009-2509\(00\)00540-6](https://doi.org/10.1016/s0009-2509(00)00540-6).
61. A. Crouter and L. Briens, “Methods to Assess Mixing of Pharmaceutical Powders,” *AAPS PharmSciTech*, vol. 20, no. 2, Jan. 2019, doi: <https://doi.org/10.1208/s12249-018-1286-7>.

62. P. Tang and V. M. Puri, "Methods for Minimizing Segregation: A Review," *Particulate Science and Technology*, vol. 22, no. 4, pp. 321–337, Oct. 2004, doi: <https://doi.org/10.1080/02726350490501420>.
63. T. Deng, V. Garg, H. Salehi, and M. S. A. Bradley, "Correlations between segregation intensity and material properties such as particle sizes and adhesions and novel methods for assessment," *Powder Technology*, vol. 387, pp. 215–226, Jul. 2021, doi: <https://doi.org/10.1016/j.powtec.2021.04.023>.
64. Tang, P., V. M. Puri, and P. H. Patterson. "Design, development and performance of second generation primary segregation shear cell for size-segregation," *Particulate Systems Analysis* 10-12: 2003.
65. A. Crouter and L. Briens, "The Effect of Moisture on the Flowability of Pharmaceutical Excipients," *AAPS PharmSciTech*, vol. 15, no. 1, pp. 65–74, Oct. 2013, doi: <https://doi.org/10.1208/s12249-013-0036-0>.
66. L. R. Lawrence and J. K. Beddow, "Powder segregation during die filling," *Powder Technology*, vol. 2, no. 5, pp. 253–259, Jun. 1969, doi: [https://doi.org/10.1016/0032-5910\(69\)80036-7](https://doi.org/10.1016/0032-5910(69)80036-7).
67. P. J. K., "Maintaining product uniformity and uninterrupted flow to direct-compression tableting presses," *Pharmaceutical Technology*, vol. 18, pp. 99–114, 1994.
68. D. M. Koller et al., "Continuous quantitative monitoring of powder mixing dynamics by near-infrared spectroscopy," *Powder Technology*, vol. 205, no. 1–3, pp. 87–96, Jan. 2011, doi: <https://doi.org/10.1016/j.powtec.2010.08.070>.
69. A. C. Kak, M. Slaney, and G. Wang, "Principles of Computerized Tomographic Imaging," *Medical Physics*, Jan. 2001, doi: <https://doi.org/10.1137/1.9780898719277>.
70. A. W. Chester, J. A. Kowalski, M. E. Coles, E. L. Muegge, F. J. Muzzio, and D. Brone, "Mixing dynamics in catalyst impregnation in double-cone blenders," *Powder Technology*, vol. 102, no. 1, pp. 85–94, Apr. 1999, doi: [https://doi.org/10.1016/S0032-5910\(98\)00193-4](https://doi.org/10.1016/S0032-5910(98)00193-4).
71. R. Liu et al., "Visualization and quantitative profiling of mixing and segregation of granules using synchrotron radiation X-ray microtomography and three dimensional

- reconstruction,” *International Journal of Pharmaceutics*, vol. 445, no. 1–2, pp. 125–133, Mar. 2013, doi: <https://doi.org/10.1016/j.ijpharm.2013.02.010>.
72. A. Crouter and L. Briens, “Passive acoustic emissions from particulates in a V-blender,” *Drug Development and Industrial Pharmacy*, vol. 41, no. 11, pp. 1809–1818, Feb. 2015, doi: <https://doi.org/10.3109/03639045.2015.1009913>.
73. A. Cameron and L. Briens, “Monitoring Magnesium Stearate Blending in a V-Blender Through Passive Vibration Measurements,” *AAPS PharmSciTech*, vol. 20, no. 7, Jul. 2019, doi: <https://doi.org/10.1208/s12249-019-1469-x>.

Chapter 2

2 Process Analytical Technologies Review

Powder mixing in the pharmaceutical industry is one of the most important processes and this process requires the mixing of several powder components. Mixing is a very complicated process and is dependent on many factors like particle properties, mixer type and design, and environmental factors. Monitoring methods are needed during powder mixing to ensure that the final product will meet the high-quality requirements and good manufacturing practices for pharmaceutical production. Nowadays powder mixing in the pharmaceutical industry is primarily monitored through offline monitoring methods like thief probes. Offline monitoring methods can result in inaccurate and unreliable data. Thief probe analysis employs the withdrawal of a powder sample from the powder bed using a probe and analyzing the sample using destructive methods. Thief probe comes with some disadvantages as this method is invasive and destructive, and sampling error is usually present (1-5). Even with careful considerations and strict adherence to procedures while sampling, there are still several error risks present (6-8).

Process Analytical Technologies (PATs) are potential methods to be used in the pharmaceutical industry and there are some methods currently being used such as Near-Infra-Red (NIR) spectroscopy. PATs are methods used for analyzing, monitoring, and controlling manufacture during the processing of critical quality and performance features of raw and in-process materials and processes to ensure the quality of the final product. The application of these technologies enables the acquisition of real-time, in-line of critical information regarding powder behaviors and the quality of mixtures (9,10). The absence of real-time, inline monitoring methods restricts the transition of pharmaceutical processing from batch to continuous processing. Shifting the pharmaceutical industry from batch to continuous processing can result in many advantages including decreasing equipment size, cost, waste, segregation development, and mixing times. Moreover, mathematical models can be employed in continuous

processes by understanding the behavior and motion of the particles while mixing that can lead to improving the quality and monitoring of the mixing process (11,12,13).

Continuous processing is very challenging without accurate real-time and inline monitoring techniques. PATs application in the industry can help improve process designs and operation parameters to further improve the quality, efficiency, and safety of the mixing processes. Although PATs are supported by different regulatory groups like FDA and have some studies in the literature and their use supports the Quality by Design (QbD) philosophy, the industry has been hesitant to adopt the use and application of PATs (9,10). Expanding and providing more studies that support PATs application and advantages may help to encourage the industry to adopt PATs more readily.

PATs can be classified into four main groups: Passive acoustic emissions, Spectroscopic, Tomographic, and Velocimetric. Passive acoustic emissions rely on the released acoustic emission when the particles and the mixer wall or different particles collide with each other. (14-16). Spectroscopic PATs rely on electromagnetic radiation. The specific resonance wavelength of the particles is recorded when the particles are exposed to electromagnetic radiation. NIR spectroscopy and Raman spectroscopy are examples of spectroscopic PATs (17). Tomographic PATs rely on the reflectivity and conduction of the energy wave applied to the bulk powder material. X-ray computed tomography and magnetic resonance imaging (MRI) are examples of tomographic PATs (18). Velocimetric PATs rely on tracking the particles while mixing through the particle bed. Optical image analysis and positron emission particle tracking are examples of velocimetric PATs (20).

2.1 Passive Acoustic Emissions

Acoustic emissions are the result of the generation of waves as an energy source then transmission of the energy followed by receiving the energy in the form of vibrational waves of the matter. Acoustics can be identified as the study of vibrations and sound (21,22). The fundamental mechanics of wave transmission and the transmission principle are the two main factors on which acoustics are based upon. The transmission

principle is the change in the position of a particle due to its equilibrium. The fundamental mechanics of wave transmission can address the propagation concept upon expansion of the transmission principle. If a source triggers a particle to move out of equilibrium, this particle will behave as a source for the particles next to it followed by shifting positions for these particles to become a source for other particles nearby and so on. Following this pattern, the waves can be propagated throughout the medium (21,23). Passive acoustic emissions have the potential to be a monitoring mixing method by measuring the stress waves that are generated upon the collision of particles with each other or with the walls of the mixer. The stress waves generated can be recorded and measured using sensors that can be placed externally on the mixer. The energy released from the collision of the particles is affected by several factors such as the powder flow and particle characteristics (14-16).

Acoustic waves can travel through liquids, solids, and gases. The waves produced upon collision of the particles can be classified as longitudinal, transverse, and Rayleigh waves. The acoustic waves would be longitudinal if the waves travel through liquids, solids, or gases. Upon hitting the matter, the propagation of the wave energy by the vibration of the particle is parallel to the wave direction leading to compressions which are regions with high-pressure and high-density wave series. Rarefactions are also formed which is the opposite of compression that have regions of low pressure and low density. The propagation of the wave energy by the vibration of the particle is perpendicular to the wave direction resulting in a transverse wave. Transverse waves can only exist in the solid phase and propagate perpendicularly to the energy source. Rayleigh waves are a mixture of longitudinal and transverse waves forming an ellipse in a semi-infinite medium (21,23). In the experiments conducted in this research, the acoustic waves were transmitted and travelled through a solid object and measured. A combination of both longitudinal and transverse acoustic waves was formed by the source upon transmission through the object. Velocity and displacement can be used as particle diameters when defining the acoustic wave magnitude.

All waves can be characterized by several features such as frequency, speed, amplitude, and wavelength. The wavelength is defined as the distance between two consecutive

points on the wave that is in phase with each other. The wavelength of a wave is represented by the symbol (λ), also named lambda. The frequency of the wave is defined as the number of cycles or oscillations of the wave that happen per unit of time. The frequency of a wave is represented by the symbol (f). The frequency can be classified into three magnitude regions; infrasonic (<20Hz), audible (20-20,000 Hz), and ultrasonic (>20,000 Hz) and is the reciprocal of the period of the wave (21,23). The amplitude is defined as the maximum displacement of the wave from its equilibrium position or the maximum amplitude of its oscillations. The amplitude of a wave is represented by the symbol (A). The amplitude is a crucial wave feature in passive acoustic emission analysis. The energy released upon collision of the particles is proportional to the wave amplitude squared. A percentage of the energy transferred after particle collision is diminished. This diminishing happens through particle rotation, sound, heat, and scattering. If the particle collision happened away from the sensor, more diminishing of the wave will be seen due to the necessity of the wave to travel further. The change in amplitude of the wave needs to be measured and analyzed to be able to monitor a powder mixture (23,24). Speed is the rate at which the wave's energy travels across a medium or through space. The speed of a wave is represented by the symbol (c). The speed of a wave is related to its wavelength and frequency and can be described by the following equation:

$$c = \lambda * f \quad \text{(Equation 2.1)}$$

Passive acoustic emissions have been measured in many different processes including mixing, granulation, compaction, fluidization, drying, direct energy deposition, powder bed fusion, absorption, pneumatic and hydro transport (Table 2.1).

Table 2.1: Summary of the available literature on applications using passive acoustic emission

Reference	Mixer	Powder components	Application	Objectives
Boyd and Varley (22)	V-blender	Glass beads, Magnesium stearate, Pharmaceutical granules	Mixing	To monitor passive acoustic emissions in the mixing process of particles with added lubricant

Tily et al. (25)	Kenwood blender	Many components were used	Mixing	To monitor powder mixing
Cameron and Briens (26)	V-blender	Pharmaceutical granules, Glass beads, Magnesium stearate	Mixing	To determine the effect of the fill level of the mixer and loading configuration on pharmaceutical granules and magnesium stearate mixture
Cameron and Briens (16)	V-blender	Pharmaceutical granules, Glass beads, Magnesium stearate	Mixing	To determine passive vibration reliability and effectiveness in monitoring the mixing process of particles with added lubricant
Crouter and Briens (27)	V-blender	Pharmaceutical granules, Sugar spheres, Magnesium stearate	Mixing	To assess the ability of passive acoustic emissions to monitor the mixing process of particles with added lubricant
Bellamy et al. (28)	High shear blender	Cellulose, Aspirin	Mixing	To determine the benefits of using passive acoustics compared to NIR in powder mixing monitoring
Allen et al. (29)	Convective mixer with three blades	Aspirin, Microcrystalline cellulose, Citric acid	Mixing	To monitor powder mixing and to determine the effectiveness of passive acoustics in monitoring the effects of the mixtures with secondary compounds
Whitaker et al. (30)	Non-available	Lactose monohydrate, Microcrystalline cellulose, Aqueous polyvinylpyrrolidone solution	Granulation	To monitor the changes in physical properties
Hansuld et al. (31)	Non-available	Cornstarch, Microcrystalline cellulose, Mannitol, Croscarmellose sodium, Hypromellose 2910	Granulation	To monitor the changes in process conditions

Hansuld et al. (32)	Non-available	MCC spheres, Sugar spheres, Anhydrous dextrose, Microcrystalline cellulose, Mannitol, Croscarmellose sodium, Hypromellose 2910	Granulation	To monitor the relationship between particle size
Hansuld et al. (33)	Non-available	Microcrystalline cellulose Magnesium stearate, Mannitol, Maize starch, Anhydrous dextrose, Croscarmellose sodium, Hypromellose 2910	Granulation	To identify the process endpoint
Hansuld et al. (34)	Non-available	Cornstarch, Microcrystalline cellulose, Mannitol, croscarmellose sodium, Hypromellose 2910	Granulation	To monitor the density and size
Papp et al. (35)	Non-available	Microcrystalline cellulose, Hydroxypropyl, Lactose monohydrate, Deionized water	Granulation	To monitor the changes in physical properties
Briens et al. (36)	Non-available	Lactose monohydrate, Polyvinylpyrrolidone	Granulation	To monitor the granulation process
Gamble et al. (37)	Non-available	Lactose monohydrate, Povidone, Cross-linked Povidone, Microcrystalline cellulose, Deionized water	Granulation	To identify the process endpoint
Daniher et al. (38)	Non-available	Corn starch, Lactose monohydrate, Polyvinylpyrrolidone, Water	Granulation	To identify the process endpoint and monitor the changes in granule characteristics
Vervloet et al. (39)	Non-available	Lactose monohydrate, Microcrystalline cellulose, Croscarmellose, HPMC, USP distilled water	Fluidization	To monitor the changes in process conditions

Tsujimoto et al. (40)	Non-available	Crystalline cellulose	Fluidization	To monitor fluidization during granulation
Hou et al. (41)	Non-available	Silica flour	Pneumatic transport	To monitor the changes in process conditions
Albion et al. (42)	Non-available	Glass beads, Polyethylene pellets, Polyvinylchloride	Pneumatic transport	To identify the flow regime
Albion et al. (43)	Non-available	Glass beads, Polyvinylchloride	Pneumatic transport	To identify the flow regime
Albion et al. (44)	Non-available	Oblong tablets	Pneumatic transport	To identify the breakage of tablets
Albion et al. (45)	Non-available	Rocks, Silica sand slurry	Hydro transport	To identify the defects of oversized components
Kouprianoff et al. (46)	Non-available	Ti6Al4V ELI pre-alloyed gas atomized powder	Powder Bed Fusion	To monitor the real-time defect detection and balling effect
Briens et al. (47)	Non-available	Stainless steel gas atomized powder	Drying	To monitor the mass flow rate
Serris et al. (48)	Non-available	Aspirin AC 360, Cornstarch, Saccharose	Compaction	To identify process defects
Hansuld et al. (49)	Non-available	Ceramic Raschig rings, Ceramic intalox saddles, Glass marbles, Water	Absorption	To monitor absorption processes
Whiting et al. (50)	Non-available	Stainless steel gas atomized powder	Direct energy deposition	To monitor the mass flow rate

2.1.1 Passive Acoustic Emissions Advantages

Passive acoustic emissions (PAE) have several advantages over other monitoring methods. PAE is a non-invasive method because the sensors can be attached outside the mixer which allows the measurements to be recorded compromising the integrity of the mixer. PAE can be used to extract information regarding powder mixing. PAE is a non-destructive method as the measurements recorded are passive acoustics generated by the process itself. Also, the product being analyzed is not lost due to the requirement of destructive testing processes like other methods. All that makes PAE a less expensive monitoring method to set up compared to other spectroscopic and radiation methods. The sensor can be attached to the equipment without changing the design or alteration

of the equipment making PAE a method that can be used in several applications and fields.

2.1.2 Passive Acoustic Emissions Disadvantages

PAE results in a large volume of data produced that requires proper handling and analyzing to be able to extract the relevant data and information needed for monitoring. Moreover, it needs more processing and space for storage due to the need for high frequencies to make sure that the vibrations and emissions are recorded within the desired range. The application of PAE in pharmaceutical powder mixing is relatively new and there is a lack of guidelines for the research making this method a potential for more research and discovery which is the current motivation behind the work and research presented in this dissertation.

2.2 Spectroscopic Techniques

Spectroscopic techniques rely on the interaction of electromagnetic radiation generated with an object. Upon the interaction of the object with electromagnetic radiation, electromagnetic energy is generated that leads to vibration of the molecules because of photons' absorption and emission. Every individual component has a unique wavelength that resonates, making the components in a mixture identifiable. Near-infrared spectroscopy (NIR) and Raman spectroscopy are examples of spectroscopic techniques that are used in some industries such as the pharmaceutical industry (16).

2.2.1 Near-Infrared Spectroscopy

NIR spectroscopy can help in identifying the components in a mixture and monitoring the mixing process. This can be achieved by analyzing how the particles react when exposed to the NIR light. Upon exposure of the molecules to the NIR light, the molecules absorb some of the NIR light causing the molecules to vibrate. Each molecule vibrates in a way that is different from others due to different bond compositions between molecules making them absorb energy differently. The vibrations of the molecules can result in compression, stretching, and bending between the bonds of the molecules changing the bond angle and distance (17,51,52).

During the use of NIR spectroscopy, the main bonds seen are C-H, N-H, S-H, and O-H bonds with a wavelength range of NIR light of 780 nm to 2500 nm (53-55). The NIR spectra collected can have variations in vibrations measured and a large amount of overlapping data that needs more analysis and pre-treatment to be used in assessing the homogeneity of a mixture in a mixing process. The NIR spectra pre-treatment is used to correct the overlapping and weak absorption bands generated and decrease the spectral contributions that are seen because of the physical characteristics of the used materials such as particle density and size. It also counts for the measurement volume (17,56).

The pre-treatment of the NIR spectra data can be done through several methods such as normalization, Standard Normal Variate (SNV), Savitzky–Golay algorithm, Multiplicative Scatter Correction (MSC), and De-Trending (DT). The DT method is commonly used with the SNV pre-treatment method (57,62,63). Post-treatment methods can be used on NIR spectra data such as Partial Least Squares (PLS) and Principal Component Analysis (PCA). Those are two methods that are commonly used. Other post-treatment methods include relative standard deviation, moving block standard deviation, and principal component regression. NIR usage in the observation of mixing and homogeneity has been studied and applied in several different processes and various mixer types (Table 2.2).

Table 2.2: Some of the available literature that used NIR spectroscopy in mixing

Reference	Mixer	Powder components	Pre-treatment	Post-treatment	Objectives	Result and conclusion
Berntsson et al. (55)	Nauta mixer	Two powders, one coarse and one fine	MSC, mean spectrum	PLS	New in-line method for monitoring powder mixtures using NIR spectroscopy	The results indicated that the new NIR method can be used for inline real-time monitoring of mixture homogeneity

Scheibelhofer et al. (66)	Stainless steel mixing vessel with four bladed stirrers	Acetylsalicylic acid, α -lactose monohydrate	Wave-number averaging, cutting of the spectral band, SNV	PLSR	Monitoring mixing behavior in the powder bed using a multi-probe NIR	The results showed that the multi-probe NIR is successful in monitoring blending, particle motion, and segregation
Portillo et al. (68)	Continuous horizontal stationary angled drum mixer	Milled acetaminophen, Lactose 100M, Lactose 125M	Un-specified	Relative standard deviation	Determine the effect of changing process parameters	The results confirm the potentiality of using NIR to monitor process parameters
El-Hagrasy et al. (71)	Batch V-blender	Salicylic acid, Fast-Flo lactose, Methanol	Second derivative	Multiterm linear regression, principal component regression, PLS	Determine blend homogeneity	The results showed that the calibrated model proposed was effective in using NIR to predict the blend homogeneity
Quinones et al. (73)	Continuous low-shear tumble mixer	Naproxen sodium, Lactose monohydrate, Magnesium stearate	Relative standard deviation and roots mean standard error of prediction	PCA, PLS, MCS	Determine the effectiveness of the proposed model strategy for inline modelling	The results of the proposed model strategy for NIR showed effectiveness in controlling the process of mixing

2.2.1.1 NIR Advantages

NIR spectroscopy is one of the methods used in the pharmaceutical industry for mixing procedures. It can provide an effective way to monitor in-line mixing by using the correct and appropriate calibrations. Previous research and studies confirmed that the NIR spectroscopy method can determine endpoints, detect multi-component compositions, assess homogeneity, and utilize various optimization strategies. NIR spectroscopy can identify the chemical compositions of the particles and can be

integrated with other methods. Moreover, NIR spectroscopy can be used for both offline and online monitoring systems, allowing for a wide application scope.

2.2.1.2 NIR Disadvantages

NIR spectroscopy has a wide application scope; however, this method comes with some disadvantages. NIR spectroscopy is a very expensive method that involves high costs, labour, and regulatory steps. This is because it requires equipment modifications such as ports or windows and probes added to different places for accurate sensor measurements. As well, it requires many pre- and post-processing treatments that make data analysis and interpretation more difficult and time-consuming (75,76). The interpretation of NIR spectra is challenging. The NIR probe measurements collected can be impacted by mixing process factors such as polymorphism, moisture content, particle size, and material characteristics. The sensor port and probe must be clear to record and produce accurate measurements. This is a challenging process to control in a pharmaceutical mixing process, specifically in a tablet mixing process with cohesive, fine, and hygroscopic powders.

2.2.2 Raman Spectroscopy

Raman spectroscopy is a monitoring method that involves the powder mixture being exposed to radiation by monochromatic light and detecting the scattered light with various frequencies to the incident beam. Raman spectroscopy is based on differences in light scattering. Upon exposure of the powder mixture to the monochromatic light, the light will initially scatter in the sample elastically then the particles in the mixture will absorb some of the light and the remaining light will be scattered differently depending on the particle characteristics, polarizability, and molecular composition (77,78). The spectral lines have unique peaks that are specific to every particle sample. Raman spectrum is known as the spectrum produced from the scattered light which can help to identify the mixture composition (79,80). Raman spectroscopy can be used to monitor the differences in the homogeneity of mixtures by the measurements and specific vibrational frequencies of each molecular composition.

Raman spectroscopy has been studied and used in some of the pharmaceutical production processes such as granulation (81,82), fluidization (83), tablet analysis (84), mixing (3,85-87), coating (88,89), and freeze-drying (90). However, there are limited studies and publications on monitoring powder mixing using Raman spectroscopy (Table 2.3). The available literature on mixing focuses on proving and expanding the effectiveness of Raman spectroscopy and comparing it to other monitoring methods such as High-Performance Liquid Chromatography (HPLC), acoustic emission, and NIR spectroscopy and few studies are available on powder mixing and identifying homogeneity endpoint (3,85,87,91). The most common light wavelengths used are between 532 and 1064 nm with probes using 785 nm light wavelength.

Table 2.3: Summary of some of the available literature that used Raman spectroscopy in powder mixing

Reference	Mixer	Powder components	Wavelength	Objectives	Result and conclusion
Bridgewater J. (3)	Planetary mixer	Paraffinic wax, Drum dried corn starch, Sodium starch glycolate, Drug pellets	1064 nm	To assess the effectiveness of Fourier Transform Infrared Raman (FTIR) spectroscopy for in-line powder mixing monitoring	The results showed that FTIR is effective as a powder-mixing monitoring method
Vergote et al. (85)	V-blender	Azimilide dihydrochloride, Spray-dried lactose, Crospovidone, Magnesium stearate	785 nm	To assess the effectiveness of Raman spectroscopy using univariate and multivariate methods for low-dose mixtures	The results showed that Raman spectroscopy is effective in monitoring low-dose mixtures
De Beer et al. (86)	Gral™ 10 high shear mixing system	Diltiazem hydrochloride, Avicel PH 102, lactose DCL 21, Silicium dioxide	785 nm	To determine the endpoint for monitoring powder mixing by using a new strategy through Raman spectroscopy	The results showed that Raman spectroscopy is an effective method to determine the endpoint and mixture homogeneity

2.2.2.1 Raman Spectroscopy Advantages

Raman spectroscopy can be used in the automation of controlling batch processes helping with improving the quality and efficiency of the processes. Raman spectroscopy allows for real-time inline monitoring. This method is considered to have more advantages over other spectroscopic methods such as NIR spectroscopy. It is considered less expensive and time-efficient than NIR spectroscopy due to the minimal pre-treatment processes and sample preparation required. Also, Raman spectroscopy uses simpler methods than NIR spectroscopy. Moreover, it can be used with various mixtures such as mixtures with crystalline compounds, several compounds, and moist powders. Raman spectroscopy can detect sensitive features within a mixture and can be used with polymorphic compounds. The measured peaks produced from Raman spectroscopy are more intense and sharper than other spectroscopic methods resulting in higher chemical specificity therefore it can be used for several component mixtures.

2.2.2.2 Raman Spectroscopy Disadvantages

Raman spectroscopy has some similar disadvantages to NIR spectroscopy such as the use of windows or ports to be attached to the mixing vessel, the addition of several probes to allow for accurate monitoring that increases the cost, fouling of the probe tip, and more extensive analysis is needed due to the use of multiple measurements. Fluorescence can be seen and interfere masking the peaks obtained. The Raman signals produced are relatively weak compared to other spectroscopic methods which can limit the sensitivity, especially for samples with weak Raman scattering and low concentrations.

2.3 Tomographic Techniques

Tomographic techniques are imaging techniques that use the information from the transmission and reflection of energy waves that penetrate a sample to reconstruct image cross-sections. X-ray computed tomography and magnetic resonance imaging are examples of tomographic techniques.

2.3.1 X-ray Computed Tomography

X-ray computed tomography (X-ray CT) is one of the available tomographic techniques used. X-ray CT is an imaging technique that uses X-ray to pass through the materials being analyzed to generate images. X-ray CT can be used for inline monitoring. This technique utilizes a high form of electromagnetic energy that is used to generate images. Every particle has a different atomic number and density and the X-rays absorbed can vary producing different images of the powder bed depending on the particles used. X-ray CT has shown the potential to monitor mixing processes and several studies have been conducted confirming the use and effectiveness of this application in powder mixing monitoring (Table 2.4). X-ray CT was used in monitoring different mixing applications including monitoring mixture homogeneity, segregation of powders, and mixing dynamics. The quality of the powder mixture used and analyzed can be affected by fill level, rotation speed, and material characteristics such as particle shape, size, and density.

Table 2.4: Some of the available literature that used X-ray CT in mixing

Reference	Mixer	Powder components	Objectives	Result and conclusion
Chester et al. (94)	Double-cone mixer	Pellets	To research powder mixing dynamics	The results showed that X-ray CT is effective in monitoring powder mixing dynamics and can identify several mixture features including axial and radial mixing, density gradient, and dead zones
Liu et al. (19)	Cylindrical drum mixer	Non-spherical starch granules, Spherical Celphere (Microcrystalline cellulose)	To extract more insights about mixing and assess mixture segregation and homogeneity	The results of X-ray CT produced 3D images and more information on powder mixture segregation and mixing
Yang and Fu (95)	V-blender	Celphere particles labelled with lead (II) acetate trihydrate	To develop a material labelling method	The results showed that the X-ray CT technique helped to develop a method and the impregnated particles for monitoring powder processes including mixing. Loading order and particle size effects on mixing were also identified

2.3.1.1 X-ray Computed Tomography Advantages

X-ray CT is a potential, efficient, non-invasive, non-destructive, and fast monitoring method used in mixing. This method can provide images of particles at micron resolution allowing for more detailed analysis and understanding of the particle motion in the mixer (96).

2.3.1.2 X-ray Computed Tomography Disadvantages

X-ray CT is considered an effective monitoring method in research and lab scales. However, it is not very practical when applied on a large or industrial scale due to the complicated processes, extensive equipment, and high cost associated with this monitoring method. The time required for a single scan is very long making X-ray CT in real-time mixing monitoring particularly challenging.

2.3.2 Magnetic Resonance Imaging

Magnetic resonance imaging (MRI) monitoring method uses certain frequencies of the atomic nuclei which are affected by magnetic fields. MRI is also called Nuclear Magnetic Resonance (NMR) imaging because it is based on the nuclear magnetic resonance of the particle. Atomic nuclei possess a magnetic moment around a magnetic field towards the gravity direction. There is a unique rotation frequency for each atomic nucleus within a certain magnetic field called the Larmor frequency. A known spatial difference in the magnetic field will make the nucleus at each point rotate at different Larmor frequencies. MRI analysis can monitor the spatial distribution of various nuclei in the mixture and detect mixture components (97,98). Available literature showed the use of MIR in various applications (Table 2.5). Previous studies completed using MIR analysis in mixing processes have been used in monitoring mixture concentrations, uniformity, and segregation. Also, those studies addressed how other process parameters can affect the mixing process.

Table 2.5: Some previous studies that used MRI analysis in mixing monitoring

Reference	Mixer	Powder components	Objectives	Result and conclusion
Nakagawa et al. (98)	Cylindrical Drum Mixer	Mustard seeds	To determine if MRI can be used to monitor solid mixture	The results showed that MRI is a potential method used in mixture monitoring applications and it can determine velocities, concentration, and components in a mixture
Hill et al. (99)	Cylindrical Drum Mixer	50-50 binary mixture of plastic spheres and pharmaceutical pills	To study bulk segregation	The results determined the bulk complex segregation structure
Maneval et al. (102)	Cylindrical Drum Mixer	3 mm diameter spherical particles containing liquid cores	To monitor the effects of end wall property on particle flow	The results showed that MRI is effective in identifying the effect of wall frictions on mixture flow in a cylindrical drum mixer
Sommier et al. (103)	Turbula Shaker Mixer	Sugar Beads, Sugar Beads with Silicon Oil	To monitor particle mixing and segregation	The results showed that MRI effectively monitored mixing and segregation
Kawaguchi et al. (105)	Rotating Horizontal Drum	Polystyrene spheres, Gelatin spheres filled with vitamin E liquid	To monitor axial and radial mixing and segregation	The results showed that MRI effectively monitored the mixing and segregation of the mixture
Hardy et al. (106)	Rotating Drum	Microcapsules filled with oil, Solid polymer spheres	To monitor the mixing and blend uniformity processes	The results showed that MRI effectively monitored the mixing and blending uniformity processes

2.3.2.1 Magnetic Resonance Imaging Advantages

MRI analysis can be used to indicate mixture uniformity as it can provide spatial information about a mixture. MRI is a completely non-invasive monitoring method that does not require any modification or additions of additional parts.

2.3.2.2 Magnetic Resonance Imaging Disadvantages

MRI requires extensive and expensive equipment, and it is difficult to operate, restricting its use mostly in academia. One more disadvantage of MRI is that the mixture analyzed must have a visible free proton whose distribution is representative of the mixture uniformity to be detected. Non-sensitive particles can be coated with oil to counteract this disadvantage. The oil coating must have no remarkable impact on the mixture.

2.4 Velocimetric Techniques

Velocimetric techniques can explain the mixing dynamics using a tracer particle that can be tracked and detected over time. Optical image analysis and positron emission particle tracking are examples of velocimetric techniques. Colored particles can be used as tracers in optical image analysis while in positron emission particle tracking, radioactive tracers are used.

2.4.1 Optical Image Analysis

Optical image analysis provides a non-invasive technique for inline monitoring powder mixing and homogeneity. Optical image analysis uses cameras to take images and record videos for observing and monitoring the change of colors in the mixture. Over time the endpoint can be determined with the help of the changes in the mixture color in the bed and tracer particles (23,107). The color changes in the mixture are used in studies to monitor multi-color powder mixture homogeneity while the tracer particles are used to monitor certain elements of particle motion in powder mixing. Mixtures can be observed during the mixing process. The mixers must have windows or be transparent to allow for the cameras to be incorporated and take images and videos in the mixer. The images and videos taken are then analyzed through different analysis software. Optical image analysis requires proper calibration of the software and selecting appropriate post-analysis methods is essential in the monitoring process (108,109).

Optical image analysis is one of the oldest monitoring techniques used and many research and studies have been conducted on this technique. There is a lot of literature available on the use of this monitoring technique in mixing (Table 2.6). Previous studies have been conducted using different mixer geometries, camera locations, powder materials, and types of mixers. The studies proved that optical image analysis is an effective technique to monitor powder homogeneity, mixing and segregation of mixtures.

Table 2.6: Some of the available studies that used optical image analysis in mixing

Reference	Mixer	Powder components	Camera location	Objectives	Result and conclusion
Bulent Koc et al. (107)	Batch style vessel mixer	White plaster, black and red powder dyes	Above the mixing chamber	To monitor the overall mixture	The results showed that optical image analysis was able to determine the mixture's degree of uniformity by monitoring the mixture in real-time
Le Coent et al. (110)	Glass shell with anchor and helical ribbons	Unspecified powder components	75 cm away outside the glass shell horizontally facing the center of the shell	To determine the mixing time	The results determined the mixing time by identifying the mixture uniformity endpoint
Malhotra et al. (112)	Acrylic cylindrical vessel with impeller	Glass beads	At the wall of the vessel	To study the powder mixing principles	The results provided information regarding particle motion in a vessel with an impeller
Kuo et al. (114)	Acrylic rotating drum mixer	Rigid glass beads, non-rigid rubber sphere particles	Non-available	To monitor axial segregation during powder mixing	The results showed that optical image analysis effectively monitored the segregation during powder mixing as well as the parameters that influenced segregation

Daumann et al. (115)	Discontinuous horizontal twin-shaft paddle mixer	Cement, Ultramarine blue	Above the mixing chamber	To determine the mixing time	The results showed the effectiveness of optical image analysis in determining the mixing time
Berthiaux et al. (116)	Non-available	Semolina dyed and undyed with iodine	Above the conveyor belt	To monitor and determine mixture homogeneity and ratio	The results showed that optical image analysis was able to monitor mixture homogeneity and determine some of the segregation in the mixture
Ammarcha et al. (118)	Hemi-cylindrical continuous mixer with a screw blade	Couscous dyed and undyed with iodine	Above the conveyor belt outside the mixer	To monitor the homogeneity of the mixer	The results showed that optical image analysis is an effective monitoring method to provide information about mixture segregation
Liu et al. (119)	Drum mixer with glass plate on the front end	Red and white plastic balls	In front of the mixer glass plate	To compare between different image analysis techniques	The results showed that overall image analysis should be standardized because of the possible deviances in the methods to calculate the mixing time

2.4.1.1 Optical Image Analysis Advantages

Optical image analysis has shown its effectiveness in monitoring the mixing homogeneity and segregation pattern non-invasively with low-cost equipment. Optical image analysis is a mature method that is well understood and backed up with lots of literature available.

2.4.1.2 Optical Image Analysis Disadvantages

Optical image analysis has some disadvantages including the requirement for a transparent vessel to record images and videos. Multiple windows need to be inserted into the equipment as well. This results in modifications being implemented to the equipment leading to higher costs. Optical image analysis requires the particle materials to be of various colors. Most of the pharmaceutical powder mixtures are white in color, restricting the use of optical image analysis to certain applications. One way to mitigate

this issue is to dye the powder materials. However, the properties of the powder materials must not be impacted by the dye. The image analysis results may not be representative of the full mixture as the images are taken at the powder surface or the port window (110). Multiple measurements at various locations may be needed leading to more cost increases. Some equipment may not have access to the window locations or even do not support the addition of windows.

2.4.2 Positron Emission Particle Tracking

Positron emission particle tracking (PEPT) is a radioactive monitoring technique that uses radioactive particle tracking (RPT). PEPT can be used to provide information about the mixing dynamics and flow. PEPT works by tracking the location of the tracer particle by utilizing the sensor to detect the radioactive particle disintegration. Photons are produced by the released positrons when interacting with electrons in the powder material. Sensors can detect the photons produced in the opposite direction of the bulk powder (122-124). Tracers are selected to have similar powder surfaces and physical characteristics and do not change anything in the mixture that can lead to segregation. The velocity of the tracer particle and the segregation can be determined. PEPT has been used to study the mixing dynamics and was used in various mixers with different tracers and powder components (Table 2.7). The literature available provides potential use for PEPT to be used to monitor the effects of process parameters on mixing. Also, PEPT can be used to monitor and provide essential information about particle behavior, circulation, and dispersion within a mixture.

Table 2.7: Some of the available literature that used PEPT in mixing

Reference	Mixer	Powder components	Tracer	Objective	Result and conclusion
Portillo et al. (123)	Continuous cylindrical mixer with impeller	Edible lactose, Fast Flo lactose	Ion-exchange resin tracer with absorbed ^{18}F	To determine the process parameters' effects on the powder flow during mixing	The results showed that PEPT effectively monitored the mixture providing information on understanding the process parameters effects on powder flow and particle motion during mixing. The results aided in the validation of the available literature on particle motion

Kuo et al. (124)	V-blender	Glass beads	Glass beads irradiated with ^{18}F	To monitor particle motion within the V-blender during mixing	The results showed that PEPT was effective in monitoring the particle motion giving information on particle flow pattern, circulation, and axial dispersion
Perrault et al. (125)	V-blender	MCC PH101, Spray-dried lactose	Radioactive magnesium stearate monohydrate	To monitor powder mixing with added magnesium stearate	The results showed that PEPT was effective in monitoring powder mixing and determined the effect of magnesium stearate addition and the validation of magnesium stearate as a tracer

2.4.2.1 Positron Emission Particle Tracking Advantages

PEPT monitoring can be used effectively to provide detailed and essential information for process characterization and parameters during powder mixing as well as it can be used to examine mixing dynamics. PEPT is a completely non-invasive monitoring technique used in powder mixing and no equipment modifications are required like other monitoring techniques. PEPT can accurately monitor and track small tracer particles within the mixture resulting in detailed monitoring of the tracer particle motion as particle velocity, behavior, and location.

2.4.2.2 Positron Emission Particle Tracking Disadvantages

PEPT monitoring requires appropriate sensors and radioactive trace particles to monitor processes such as mixing and segregation. Also, PEPT monitoring is not easily applicable as it only monitors the tracer particles (126). Tracer particles must be appropriately selected for their effectiveness with no impact on the mixture. Optimizations and calibrations are used to make sure that the sensors are placed in certain locations. All these factors lead to higher costs and more processing time limiting the use of PEPT to a small scale such as in laboratories.

2.5 Conclusions

Monitoring of powder mixing and mixing efficiency are key elements in the pharmaceutical manufacturing process to ensure quality, safety, content uniformity, and material distribution are met. However, it is one of the very challenging processes and

not easy to achieve. Nowadays, the pharmaceutical industry mainly uses thief probes for monitoring powder mixing. Thief probes have several disadvantages as being inaccurate, offline, destructive, invasive, and inefficient method. PATs can be used to improve powder mixing monitoring, quality, and efficiency. There are several technologies have been investigated and tested to be used in pharmaceutical powder mixing to evaluate the mixture blend uniformity, identify the required mixing time and segregation, and improve the quality of the final product. Near Infrared Spectroscopy, Raman Spectroscopy, Magnetic Resonance Imaging, X-ray Computed Tomography, Optical Image Analysis, Positron Emission Particle Tracking, and Passive Acoustic Emissions are all considered examples of PATs underdevelopment. Table 2.8 is a summary of each technology as adapted from Crouter and Briens (14).

Table 2.8: Comparison and summary of major PATs currently under development and their applications

PAT	Application	Measured Parameter	Advantages	Disadvantages
Passive Acoustic Emissions	Mixture, uniformity, and endpoint	Vibrations	Low cost, non-invasive, and non-destructive	Underdevelopment, requires more processing and storage space, and results in large volume of data
Near Infrared Spectroscopy	Mixture composition, uniformity, and endpoint	Absorbed energy	Suitable for multi-component mixture and online monitoring	Probe window fouling, equipment modification and installation, and difficult analysis
Raman Spectroscopy	Mixture composition, uniformity, and endpoint	Scattered light detection	Suitable for multi-component mixture, relatively low cost, and time efficient, and allows for online monitoring	Fluorescence can be seen in addition to probe window fouling, equipment modification and installation, and difficult analysis
X-ray Computed Tomography	Mixture, uniformity	X-ray	3D image, non-invasive, and non-destructive	Limited to one component analysis, no real time monitoring, very expensive, and particles used must be X-ray sensitive
Optical Image Analysis	Mixture uniformity and velocity profile	Color	Low cost and easy to use	Sensor window fouling, equipment modification and needs component contrast

Magnetic Resonance Imaging	Mixture uniformity and velocity profile	Magnetic field	3D image, non-invasive, and non-destructive	Limited to one component analysis, very expensive, difficult to operate, restricted to development and particles must be MRI sensitive
Positron Emission Particle Tracking	Velocity profile	Radioactive particle tracking (Positron detection)	Non-invasive	Limited to one component analysis, restricted to development, and high cost and processing time

In the experiments conducted in this research, passive acoustic emissions were used to monitor mixing and segregation in a V-blender. Passive acoustic emissions are defined in a V-blender as the kinetic energy of the particles that are transformed into vibrational waves upon hitting an object. This transformation of kinetic energy into vibrational waves can happen due to particle-particle and particle-shell collisions. Passive acoustic emissions are considered one of the PATs as the vibrational waves propagated during particle collision with each other or with the shell of the V-blender while mixing is a result of sudden changes in the localized stress. Compared to other PATs methods, passive acoustic emissions have some advantages. One of the advantages of passive acoustic emissions over other PATs is that this method is considered safe and not destructive. Another advantage is the low cost of setup for this method compared with others like spectroscopic methods. One more advantage is that passive acoustic emissions are considered a non-invasive method as the sensor that measures all the vibrational waves can be attached to the outer part of the equipment. Moreover, passive acoustic emission analysis does not require the mixture used to be exposed to any outside stimulus, such as X-rays and MRI methods. However, passive acoustic emissions have a few disadvantages such as the large volume of data produced upon measuring that needs to be precisely analyzed and extracted to gather the relevant and required information that can be used in monitoring (14,23).

2.6 References

1. F. J. Muzzio et al., "Sampling and characterization of pharmaceutical powders and granular blends," *International Journal of Pharmaceutics*, vol. 250, no. 1, pp. 51–64, Jan. 2003, doi: [https://doi.org/10.1016/S0378-5173\(02\)00481-7](https://doi.org/10.1016/S0378-5173(02)00481-7).
2. R. Deveswaran, S. Bharath, BV. Basavaraj, S. Abraham, S. Furtado, S. Madhavan, "Concepts and Techniques of Pharmaceutical Powder Mixing Process: A Current Update," *Research Journal of Pharmacy and Technology*, vol. 2, no. 2, pp. 245–249, 2014.
3. J. Bridgwater, "Mixing of powders and granular materials by mechanical means—A perspective," *Particuology*, vol. 10, no. 4, pp. 397–427, Aug. 2012, doi: <https://doi.org/10.1016/j.partic.2012.06.002>.
4. D. S. Hausman, R. T. Cambron, and A. Sakr, "Application of Raman spectroscopy for on-line monitoring of low dose blend uniformity," *International Journal of Pharmaceutics*, vol. 298, no. 1, pp. 80–90, Jul. 2005, doi: <https://doi.org/10.1016/j.ijpharm.2005.04.011>.
5. L. Susana, P. Canu, and Andrea Claudio Santomaso, "Development and characterization of a new thief sampling device for cohesive powders," *International Journal of Pharmaceutics*, vol. 416, no. 1, pp. 260–267, Sep. 2011, doi: <https://doi.org/10.1016/j.ijpharm.2011.07.003>.
6. F. J. Muzzio, P. Robinson, C. Wightman, and Dean Brone, "Sampling practices in powder blending," *International Journal of Pharmaceutics*, vol. 155, no. 2, pp. 153–178, Sep. 1997, doi: [https://doi.org/10.1016/s0378-5173\(97\)04865-5](https://doi.org/10.1016/s0378-5173(97)04865-5).
7. C. L. Burgess, "Chapter 4 Issues related to the United States v. Barr Laboratories, Inc.," *ScienceDirect*, Jan. 01, 1996.
<https://www.sciencedirect.com/science/article/abs/pii/S1464345696800068>
8. J. J. Berman, A. Schoeneman, and J. T. Shelton, "Unit Dose Sampling: A Tale of two Thieves," *Drug Development and Industrial Pharmacy*, vol. 22, no. 11, pp. 1121–1132, Jan. 1996, doi: <https://doi.org/10.3109/03639049609065948>.
9. Center for Drug Evaluation and Research, "Q8(R2) Pharmaceutical Development," U.S. Food and Drug Administration, 2019. <https://www.fda.gov/regulatory-information/search-fda-guidance-documents/q8r2-pharmaceutical-development>

10. C. for D. E. and Research, "PAT — A Framework for Innovative Pharmaceutical Development, Manufacturing, and Quality Assurance," U.S. Food and Drug Administration, Jun. 11, 2020. <https://www.fda.gov/regulatory-information/search-fda-guidance-documents/pat-framework-innovative-pharmaceutical-development-manufacturing-and-quality-assurance>
11. K. Plumb, "Continuous Processing in the Pharmaceutical Industry," *Chemical Engineering Research and Design*, vol. 83, no. 6, pp. 730–738, Jun. 2005, doi: <https://doi.org/10.1205/cherd.04359>.
12. Ralf Weinekötter and H. Gericke, *Mixing of solids*. Dordrecht ; Boston: Kluwer Academic Publishers, 2000.
13. W. Engisch and F. Muzzio, "Using Residence Time Distributions (RTDs) to Address the Traceability of Raw Materials in Continuous Pharmaceutical Manufacturing," *Journal of Pharmaceutical Innovation*, vol. 11, no. 1, pp. 64–81, Nov. 2015, doi: <https://doi.org/10.1007/s12247-015-9238-1>.
14. A. Crouter and L. Briens, "Methods to Assess Mixing of Pharmaceutical Powders," *AAPS PharmSciTech*, vol. 20, no. 2, Jan. 2019, doi: <https://doi.org/10.1208/s12249-018-1286-7>.
15. A. Crouter and L. Briens, "Passive acoustic emissions from particulates in a V-blender," *Drug Development and Industrial Pharmacy*, vol. 41, no. 11, pp. 1809–1818, Feb. 2015, doi: <https://doi.org/10.3109/03639045.2015.1009913>.
16. A. Cameron and L. Briens, "Monitoring Magnesium Stearate Blending in a V-Blender Through Passive Vibration Measurements," *AAPS PharmSciTech*, vol. 20, no. 7, Jul. 2019, doi: <https://doi.org/10.1208/s12249-019-1469-x>.
17. D. M. Koller et al., "Continuous quantitative monitoring of powder mixing dynamics by near-infrared spectroscopy," *Powder Technology*, vol. 205, no. 1–3, pp. 87–96, Jan. 2011, doi: <https://doi.org/10.1016/j.powtec.2010.08.070>.
18. A. C. Kak, M. Slaney, and G. Wang, "Principles of Computerized Tomographic Imaging," *Medical Physics*, vol. 29, no. 1, pp. 107–107, Jan. 2002, doi: <https://doi.org/10.1118/1.1455742>.
19. R. Liu et al., "Visualization and quantitative profiling of mixing and segregation of granules using synchrotron radiation X-ray microtomography and three dimensional

- reconstruction,” *International Journal of Pharmaceutics*, vol. 445, no. 1–2, pp. 125–133, Mar. 2013, doi: <https://doi.org/10.1016/j.ijpharm.2013.02.010>.
20. X. Liu, C. Zhang, and J. Zhan, “Quantitative comparison of image analysis methods for particle mixing in rotary drums,” *Powder Technology*, vol. 282, pp. 32–36, Sep. 2015, doi: <https://doi.org/10.1016/j.powtec.2014.08.076>.
21. M. Bruneau and T. Scelo, *Fundamentals of Acoustics*. New York, NY: John Wiley & Sons, 2013.
22. J. Boyd and J. Varley, “The uses of passive measurement of acoustic emissions from chemical engineering processes,” *Chemical Engineering Science*, vol. 56, no. 5, pp. 1749–1767, Mar. 2001, doi: [https://doi.org/10.1016/s0009-2509\(00\)00540-6](https://doi.org/10.1016/s0009-2509(00)00540-6).
23. K. Wilson, “Application of Passive Acoustic Emissions for Inline Monitoring of Segregation Prone Mixtures in a V-Blender.” Aug. 2022.
24. A. Cameron and L. Briens, “Monitoring lubricant addition in pharmaceutical tablet manufacturing through passive vibration measurements in a V-blender,” *Powder Technology*, vol. 364, pp. 708–718, Mar. 2020, doi: <https://doi.org/10.1016/j.powtec.2020.02.018>.
25. J. Boyd and J. Varley, “The uses of passive measurement of acoustic emissions from chemical engineering processes,” *Chemical Engineering Science*, vol. 56, no. 5, pp. 1749–1767, Mar. 2001, doi: [https://doi.org/10.1016/s0009-2509\(00\)00540-6](https://doi.org/10.1016/s0009-2509(00)00540-6).
26. A. Cameron and L. Briens, “An Investigation of Magnesium Stearate Mixing Performance in a V-Blender Through Passive Vibration Measurements,” *AAPS PharmSciTech*, vol. 20, no. 5, May 2019, doi: <https://doi.org/10.1208/s12249-019-1402-3>.
27. A. Crouter and L. Briens, “The effect of granule moisture on passive acoustic emissions in a V-blender,” *Powder Technology*, vol. 299, pp. 226–234, Oct. 2016, doi: <https://doi.org/10.1016/j.powtec.2016.05.037>.
28. P. Allan, L. J. Bellamy, A. Nordon, D. Littlejohn, J. Andrews, and P. Dallin, “In situ monitoring of powder blending by non-invasive Raman spectrometry with wide area illumination,” *Journal of Pharmaceutical and Biomedical Analysis*, vol. 76, pp. 28–35, Mar. 2013, doi: <https://doi.org/10.1016/j.jpba.2012.12.003>.

29. P. Allan, L. J. Bellamy, A. Nordon, and D. Littlejohn, "Non-invasive monitoring of the mixing of pharmaceutical powders by broadband acoustic emission," *The Analyst*, vol. 135, no. 3, p. 518, 2010, doi: <https://doi.org/10.1039/b922446g>.
30. M. P. Whitaker et al., "Application of acoustic emission to the monitoring and end point determination of a high shear granulation process," *International Journal of Pharmaceutics*, vol. 205, no. 1–2, pp. 79–91, Sep. 2000, doi: [https://doi.org/10.1016/s0378-5173\(00\)00479-8](https://doi.org/10.1016/s0378-5173(00)00479-8).
31. E. M. Hansuld, L. Briens, A. Sayani, and Joe, "The effect of process parameters on audible acoustic emissions from high-shear granulation," *Drug Development and Industrial Pharmacy*, vol. 39, no. 2, pp. 331–341, May 2012, doi: <https://doi.org/10.3109/03639045.2012.681055>.
32. E. M. Hansuld, L. Briens, A. Sayani, and J. A. B. McCann, "An investigation of the relationship between acoustic emissions and particle size," *Powder Technology*, vol. 219, pp. 111–117, Mar. 2012, doi: <https://doi.org/10.1016/j.powtec.2011.12.025>.
33. E. M. Hansuld, L. Briens, Joe A.B. McCann, and A. Sayani, "Audible acoustics in high-shear wet granulation: Application of frequency filtering," *International Journal of Pharmaceutics*, vol. 378, no. 1–2, pp. 37–44, Aug. 2009, doi: <https://doi.org/10.1016/j.ijpharm.2009.05.042>.
34. E. M. Hansuld, L. Briens, A. Sayani, and J. A. B. McCann, "Monitoring quality attributes for high-shear wet granulation with audible acoustic emissions," *Powder Technology*, vol. 215–216, pp. 117–123, Jan. 2012, doi: <https://doi.org/10.1016/j.powtec.2011.09.034>.
35. M. K. Papp, C. P. Pujara, and R. Pinal, "Monitoring of High-shear Granulation using Acoustic Emission: Predicting Granule Properties," *Journal of Pharmaceutical Innovation*, vol. 3, no. 2, pp. 113–122, May 2008, doi: <https://doi.org/10.1007/s12247-008-9030-6>.
36. L Briens, D. Daniher, and A Tallevi, "Monitoring high-shear granulation using sound and vibration measurements," *International Journal of Pharmaceutics*, vol. 331, no. 1, pp. 54–60, Feb. 2007, doi: <https://doi.org/10.1016/j.ijpharm.2006.09.012>.

37. J. F. Gamble, A. B. Dennis, and M. Tobyn, "Monitoring and end-point prediction of a small scale wet granulation process using acoustic emission," *Pharmaceutical Development and Technology*, vol. 14, no. 3, pp. 299–304, Jun. 2009, doi: <https://doi.org/10.1080/10837450802603618>.
38. D. Daniher, L. Briens, and A. Tallevi, "End-point detection in high-shear granulation using sound and vibration signal analysis," *Powder Technology*, vol. 181, no. 2, pp. 130–136, Feb. 2008, doi: <https://doi.org/10.1016/j.powtec.2006.12.003>.
39. D. Vervloet, J. Nijenhuis, and J. R. van Ommen, "Monitoring a lab-scale fluidized bed dryer: A comparison between pressure transducers, passive acoustic emissions and vibration measurements," *Powder Technology*, vol. 197, no. 1–2, pp. 36–48, Jan. 2010, doi: <https://doi.org/10.1016/j.powtec.2009.08.015>.
40. H. Tsujimoto, T. Yokoyama, C. C. Huang, and I. Sekiguchi, "Monitoring particle fluidization in a fluidized bed granulator with an acoustic emission sensor," *Powder Technology*, vol. 113, no. 1, pp. 88–96, Nov. 2000, doi: [https://doi.org/10.1016/S0032-5910\(00\)00205-9](https://doi.org/10.1016/S0032-5910(00)00205-9).
41. R. Hou, A. Hunt, and R. A. Williams, "Acoustic monitoring of pipeline flows: particulate slurries," *Powder Technology*, vol. 106, no. 1–2, pp. 30–36, Nov. 1999, doi: [https://doi.org/10.1016/s0032-5910\(99\)00051-0](https://doi.org/10.1016/s0032-5910(99)00051-0).
42. K. Albion, L. Briens, C. Briens, F. Berruti, and G. Book, "Flow regime determination in upward inclined pneumatic transport of particulates using non-intrusive acoustic probes," *Chemical Engineering and Processing - Process Intensification*, vol. 46, no. 6, pp. 520–531, Jun. 2007, doi: <https://doi.org/10.1016/j.cep.2006.06.012>.
43. K. Albion, L. Briens, C. Briens, and F. Berruti, "Flow regime determination in horizontal pneumatic transport of fine powders using non-intrusive acoustic probes," *Powder Technology*, vol. 172, no. 3, pp. 157–166, Mar. 2007, doi: <https://doi.org/10.1016/j.powtec.2006.10.040>.
44. K. Albion, L. Briens, C. Briens, and F. Berruti, "Detection of the breakage of pharmaceutical tablets in pneumatic transport," *International Journal of*

- Pharmaceutics, vol. 322, no. 1–2, pp. 119–129, Sep. 2006, doi:
<https://doi.org/10.1016/j.ijpharm.2006.05.039>.
45. K. Albion, L. Briens, C. Briens, and F. Berruti, “Modelling of oversized material flow through a horizontal hydrotransport slurry pipe to optimize its acoustic detection,” *Powder Technology*, vol. 194, no. 1–2, pp. 18–32, Aug. 2009, doi:
<https://doi.org/10.1016/j.powtec.2009.03.017>.
46. D. Koupryanoff, I. Yadroitsava, A. du Plessis, N. Luwes, and I. Yadroitsev, “Monitoring of Laser Powder Bed Fusion by Acoustic Emission: Investigation of Single Tracks and Layers,” *Frontiers in Mechanical Engineering*, vol. 7, Jun. 2021, doi: <https://doi.org/10.3389/fmech.2021.678076>.
47. L. Briens, R. Smith, and C. Briens, “Monitoring of a rotary dryer using acoustic emissions,” *Powder Technology*, vol. 181, no. 2, pp. 115–120, Feb. 2008, doi:
<https://doi.org/10.1016/j.powtec.2006.12.004>.
48. E. Serris, L. Perier-Camby, G. Thomas, M. Desfontaines, and G. Fantozzi, “Acoustic emission of pharmaceutical powders during compaction,” *Powder Technology*, vol. 128, no. 2–3, pp. 296–299, Dec. 2002, doi:
[https://doi.org/10.1016/s0032-5910\(02\)00174-2](https://doi.org/10.1016/s0032-5910(02)00174-2).
49. E. Hansuld, L. Briens, and C. Briens, “Acoustic detection of flooding in absorption columns and trickle beds,” *Chemical Engineering and Processing: Process Intensification*, vol. 47, no. 5, pp. 871–878, May 2008, doi:
<https://doi.org/10.1016/j.cep.2007.02.006>.
50. J. Whiting, A. Springer, and F. Sciammarella, “Real-time acoustic emission monitoring of powder mass flow rate for directed energy deposition,” *Additive Manufacturing*, vol. 23, pp. 312–318, Oct. 2018, doi:
<https://doi.org/10.1016/j.addma.2018.08.015>.
51. M. Asachi, E. Nourafkan, and A. Hassanpour, “A review of current techniques for the evaluation of powder mixing,” *Advanced Powder Technology*, vol. 29, no. 7, pp. 1525–1549, Jul. 2018, doi: <https://doi.org/10.1016/j.apt.2018.03.031>.
52. H. W. Siesler, O. Yukihiro, S. Kawata, and H. H. Michael, Eds., *Near-Infrared Spectroscopy: Principles, Instruments, Applications*. Wiley, Feb. 2002.

53. Wavelength Standards for the Near-Infrared Spectral Region,” *Spectroscopy*, vol. 23, no. 4, Apr. 2007, <https://www.spectroscopyonline.com/view/wavelength-standards-near-infrared-spectral-region>
54. Y. Roggo, P. Chalus, L. Maurer, C. Lema-Martinez, A. Edmond, and N. Jent, “A review of near infrared spectroscopy and chemometrics in pharmaceutical technologies,” *Journal of Pharmaceutical and Biomedical Analysis*, vol. 44, no. 3, pp. 683–700, Jul. 2007, doi: <https://doi.org/10.1016/j.jpba.2007.03.023>.
55. O. Berntsson, L.-G. Danielsson, B. Lagerholm, and S. Folestad, “Quantitative in-line monitoring of powder blending by near infrared reflection spectroscopy,” *Powder Technology*, vol. 123, no. 2–3, pp. 185–193, Mar. 2002, doi: [https://doi.org/10.1016/s0032-5910\(01\)00456-9](https://doi.org/10.1016/s0032-5910(01)00456-9).
56. M. Blanco, “Monitoring powder blending in pharmaceutical processes by use of near infrared spectroscopy,” *Talanta*, vol. 56, no. 1, pp. 203–212, Jan. 2002, doi: [https://doi.org/10.1016/s0039-9140\(01\)00559-8](https://doi.org/10.1016/s0039-9140(01)00559-8).
57. M. Blanco, J. Coello, H. Iturriaga, S. Maspoch, and C. de, “Effect of Data Preprocessing Methods in Near-Infrared Diffuse Reflectance Spectroscopy for the Determination of the Active Compound in a Pharmaceutical Preparation,” vol. 51, no. 2, pp. 240–246, Feb. 1997, doi: <https://doi.org/10.1366/0003702971939947>.
58. Abraham. Savitzky and M. J. E. Golay, “Smoothing and Differentiation of Data by Simplified Least Squares Procedures,” *Analytical Chemistry*, vol. 36, no. 8, pp. 1627–1639, Jul. 1964, doi: <https://doi.org/10.1021/ac60214a047>.
59. S. Sonja. Sekulic, J. Wakeman, P. Doherty, and P. A. Hailey, “Automated system for the on-line monitoring of powder blending processes using near-infrared spectroscopy,” *Journal of Pharmaceutical and Biomedical Analysis*, vol. 17, no. 8, pp. 1285–1309, Sep. 1998, doi: [https://doi.org/10.1016/s0731-7085\(98\)00025-9](https://doi.org/10.1016/s0731-7085(98)00025-9).
60. P. Geladi, D. MacDougall, and H. Martens, “Linearization and Scatter-Correction for Near-Infrared Reflectance Spectra of Meat,” *Applied Spectroscopy*, vol. 39, no. 3, pp. 491–500, May 1985, doi: <https://doi.org/10.1366/0003702854248656>.
61. Y. Lu, Y. Qu, and M. Song, “Research on the correlation chart of near infrared spectra by using multiple scatter correction technique,” *Spectroscopy and Spectral Analysis*, vol. 27, no. 5, p. 877, May 2007.

62. R. J. Barnes, M. S. Dhanoa, and S. J. Lister, "Standard Normal Variate Transformation and De-Trending of Near-Infrared Diffuse Reflectance Spectra," *Applied Spectroscopy*, vol. 43, no. 5, pp. 772–777, Jul. 1989, doi: <https://doi.org/10.1366/0003702894202201>.
63. H. M. Heise and R. Winzen, "Chemometrics in Near-Infrared Spectroscopy," pp. 125–162, Nov. 2001, doi: <https://doi.org/10.1002/9783527612666.ch07>.
64. I. T. Jolliffe and J. Cadima, "Principal component analysis: a review and recent developments," *Philosophical Transactions of the Royal Society A: Mathematical, Physical and Engineering Sciences*, vol. 374, no. 2065, p. 20150202, Apr. 2016, doi: <https://doi.org/10.1098/rsta.2015.0202>.
65. P. A. Hailey, P. Doherty, P. Tapsell, T. Oliver, and P. K. Aldridge, "Automated system for the on-line monitoring of powder blending processes using near-infrared spectroscopy part I. System development and control," *Journal of Pharmaceutical and Biomedical Analysis*, vol. 14, no. 5, pp. 551–559, Mar. 1996, doi: [https://doi.org/10.1016/0731-7085\(95\)01674-0](https://doi.org/10.1016/0731-7085(95)01674-0).
66. O. Scheibelhofer, N. Balak, D. Koller, and J. G. Khinast, "Spatially resolved monitoring of powder mixing processes via multiple NIR-probes," *Powder Technology*, vol. 243, pp. 161–170, Jul. 2013, doi: <https://doi.org/10.1016/j.powtec.2013.03.035>.
67. A. U. Vanarase, M. Alcalà, J. I. Jerez Rozo, F. J. Muzzio, and R. J. Románach, "Real-time monitoring of drug concentration in a continuous powder mixing process using NIR spectroscopy," *Chemical Engineering Science*, vol. 65, no. 21, pp. 5728–5733, Nov. 2010, doi: <https://doi.org/10.1016/j.ces.2010.01.036>.
68. P. M. Portillo, M. G. Ierapetritou, and F. J. Muzzio, "Effects of rotation rate, mixing angle, and cohesion in two continuous powder mixers—A statistical approach," *Powder Technology*, vol. 194, no. 3, pp. 217–227, Sep. 2009, doi: <https://doi.org/10.1016/j.powtec.2009.04.010>.
69. V. Kehlenbeck, "Use of Near Infrared Spectroscopy for in- and Off-Line Performance Determination of Continuous and Batch Powder Mixers: Opportunities & Challenges," *Procedia Food Science*, vol. 1, pp. 2015–2022, Dec. 2011, doi: <https://doi.org/10.1016/j.profoo.2011.10.002>.

70. R. Besseling et al., "An efficient, maintenance free and approved method for spectroscopic control and monitoring of blend uniformity: The moving F-test," *Journal of Pharmaceutical and Biomedical Analysis*, vol. 114, pp. 471–481, Oct. 2015, doi: <https://doi.org/10.1016/j.jpba.2015.06.019>.
71. A. S. El-Hagrasy and J. K. Drennen, "A Process Analytical Technology approach to near-infrared process control of pharmaceutical powder blending. Part III: Quantitative near-infrared calibration for prediction of blend homogeneity and characterization of powder mixing kinetics," *Journal of Pharmaceutical Sciences*, vol. 95, no. 2, pp. 422–434, Feb. 2006, doi: <https://doi.org/10.1002/jps.20465>.
72. L. Martínez, A. Peinado, L. Liesum, and G. Betz, "Use of near-infrared spectroscopy to quantify drug content on a continuous blending process: Influence of mass flow and rotation speed variations," *European Journal of Pharmaceutics and Biopharmaceutics*, vol. 84, no. 3, pp. 606–615, Aug. 2013, doi: <https://doi.org/10.1016/j.ejpb.2013.01.016>.
73. L. Quiñones, C. Velazquez, and L. Obregon, "A novel multiple linear multivariate NIR calibration model-based strategy for in-line monitoring of continuous mixing," *AIChE Journal*, vol. 60, no. 9, pp. 3123–3132, Jun. 2014, doi: <https://doi.org/10.1002/aic.14498>.
74. J. Sibik, P. Chalus, L. Maurer, A. Murthy, and S. Krimmer, "Mechanistic approach in powder blending PAT: Bi-layer mixing and asymptotic end point prediction," *Powder Technology*, vol. 308, pp. 306–317, Feb. 2017, doi: <https://doi.org/10.1016/j.powtec.2016.12.038>.
75. Å. Rinnan, F. van den Berg, and S. B. Engelsen, "Review of the most common pre-processing techniques for near-infrared spectra," *TrAC Trends in Analytical Chemistry*, vol. 28, no. 10, pp. 1201–1222, Nov. 2009, doi: <https://doi.org/10.1016/j.trac.2009.07.007>.
76. Y. Sulub, M. Konigsberger, and J. Cheney, "Blend uniformity end-point determination using near-infrared spectroscopy and multivariate calibration," *Journal of Pharmaceutical and Biomedical Analysis*, vol. 55, no. 3, pp. 429–434, Jun. 2011, doi: <https://doi.org/10.1016/j.jpba.2011.02.017>.

77. Smith and G. Dent, *Modern Raman spectroscopy : a practical approach*. Hoboken, Nj Wiley, Ewen 2019.
78. J. Rantanen, "Process analytical applications of Raman spectroscopy," *Journal of Pharmacy and Pharmacology*, vol. 59, no. 2, pp. 171–177, Feb. 2007, doi: <https://doi.org/10.1211/jpp.59.2.0004>.
79. John Michael Hollas and J. Wiley, *Modern spectroscopy*. Chichester: John Wiley & Sons Ltd, Apr, 2010.
80. Smith E, Dent G. Chapter 3 The Theory of Raman Spectroscopy. In *Modern Raman Spectroscopy: A Practical Approach, Second Edition*. John Wiley & Sons Ltd 2019; 77-99.
81. G. Walker, S. E. J. Bell, M. Vann, D. S. Jones, and G. Andrews, "Fluidised bed characterisation using Raman spectroscopy: Applications to pharmaceutical processing," *Chemical Engineering Science*, vol. 62, no. 14, pp. 3832–3838, Jul. 2007, doi: <https://doi.org/10.1016/j.ces.2007.04.017>.
82. G. M. Walker, S. E. J. Bell, K. Greene, D. S. Jones, and G. P. Andrews, "Characterisation of fluidised bed granulation processes using in-situ Raman spectroscopy," *Chemical Engineering Science*, vol. 64, no. 1, pp. 91–98, Jan. 2009, doi: <https://doi.org/10.1016/j.ces.2008.09.011>.
83. Mortaza Aghbashlo, Rahmat Sotudeh-Gharebagh, Reza Zarghami, A. S. Mujumdar, and Navid Mostoufi, "Measurement Techniques to Monitor and Control Fluidization Quality in Fluidized Bed Dryers: A Review," vol. 32, no. 9, pp. 1005–1051, May 2014, doi: <https://doi.org/10.1080/07373937.2014.899250>.
84. H. Wikström, S. Romero-Torres, S. Wongweragiat, J. A. S. Williams, E. R. Grant, and L. S. Taylor, "On-Line Content Uniformity Determination of Tablets Using Low-Resolution Raman Spectroscopy," *Applied Spectroscopy*, vol. 60, no. 6, pp. 672–681, Jun. 2006, doi: <https://doi.org/10.1366/000370206777670684>.
85. G. J. Vergote et al., "In-line monitoring of a pharmaceutical blending process using FT-Raman spectroscopy," *European Journal of Pharmaceutical Sciences*, vol. 21, no. 4, pp. 479–485, Mar. 2004, doi: <https://doi.org/10.1016/j.ejps.2003.11.005>.
86. T. R. M. De Beer et al., "Raman spectroscopy as a process analytical technology (PAT) tool for the in-line monitoring and understanding of a powder blending

- process,” *Journal of Pharmaceutical and Biomedical Analysis*, vol. 48, no. 3, pp. 772–779, Nov. 2008, doi: <https://doi.org/10.1016/j.jpba.2008.07.023>.
87. D. Riolo et al., “Raman spectroscopy as a PAT for pharmaceutical blending: Advantages and disadvantages,” *Journal of Pharmaceutical and Biomedical Analysis*, vol. 149, pp. 329–334, Feb. 2018, doi: <https://doi.org/10.1016/j.jpba.2017.11.030>.
88. A. S. El-Hagrasy, S. Chang, D. Desai, and S. Kiang, “Raman spectroscopy for the determination of coating uniformity of tablets: assessment of product quality and coating pan mixing efficiency during scale-up,” *Journal of Pharmaceutical Innovation*, vol. 1, no. 1, pp. 37–42, Sep. 2006, doi: <https://doi.org/10.1007/bf02784879>.
89. J. Müller, K. Knop, J. Thies, C. Uerpmann, and P. Kleinebudde, “Feasibility of Raman spectroscopy as PAT tool in active coating,” *Drug Development and Industrial Pharmacy*, vol. 36, no. 2, pp. 234–243, Jan. 2010, doi: <https://doi.org/10.3109/03639040903225109>.
90. Saly Romero-Torres, Håkan Wikström, E. R. Grant, and L. S. Taylor, “Monitoring of mannitol phase behavior during freeze-drying using non-invasive Raman spectroscopy,” *PubMed*, vol. 61, no. 2, pp. 131–45, May 2007.
91. P. Allan, L. J. Bellamy, A. Nordon, D. Littlejohn, J. Andrews, and P. Dallin, “In situ monitoring of powder blending by non-invasive Raman spectrometry with wide area illumination,” *Journal of Pharmaceutical and Biomedical Analysis*, vol. 76, pp. 28–35, Mar. 2013, doi: <https://doi.org/10.1016/j.jpba.2012.12.003>.
92. Y. Wang, L. Fang, Y. Wang, and Z. Xiong, “Current Trends of Raman Spectroscopy in Clinic Settings: Opportunities and Challenges,” *Advanced Science*, Dec. 2023, doi: <https://doi.org/10.1002/advs.202300668>.
93. J. Breitenbach, W. Schrof, and J. Neumann, *Pharmaceutical Research*, vol. 16, no. 7, pp. 1109–1113, 1999, doi: <https://doi.org/10.1023/a:1018956304595>.
94. A. W. Chester, J. A. Kowalski, M. E. Coles, E. L. Muegge, F. J. Muzzio, and D. Brone, “Mixing dynamics in catalyst impregnation in double-cone blenders,” *Powder Technology*, vol. 102, no. 1, pp. 85–94, Apr. 1999, doi: [https://doi.org/10.1016/S0032-5910\(98\)00193-4](https://doi.org/10.1016/S0032-5910(98)00193-4).

95. C.-Y. Yang and X.-Y. Fu, "Development and validation of a material-labeling method for powder process characterization using X-ray computed tomography," vol. 146, no. 1–2, pp. 10–19, Aug. 2004, doi: <https://doi.org/10.1016/j.powtec.2004.06.011>.
96. S. R. Stock, "X-ray microtomography of materials," vol. 44, no. 4, pp. 141–164, Apr. 1999, doi: <https://doi.org/10.1179/095066099101528261>.
97. T. Kawaguchi, "MRI measurement of granular flows and fluid-particle flows," *Advanced Powder Technology*, vol. 21, no. 3, pp. 235–241, May 2010, doi: <https://doi.org/10.1016/j.appt.2010.03.014>.
98. M. Nakagawa, S. A. Altobelli, Arvind Caprihan, E. Fukushima, and Euh Duck Jeong, "Non-invasive measurements of granular flows by magnetic resonance imaging," vol. 16, no. 1, pp. 54–60, Jan. 1993, doi: <https://doi.org/10.1007/bf00188507>.
99. K. M. Hill, A. Caprihan, and J. Kakalios, "Bulk Segregation in Rotated Granular Material Measured by Magnetic Resonance Imaging," *Physical Review Letters*, vol. 78, no. 1, pp. 50–53, Jan. 1997, doi: <https://doi.org/10.1103/physrevlett.78.50>.
100. G. Metcalfe and M. Shattuck, "Pattern formation during mixing and segregation of flowing granular materials," *Physica A: Statistical Mechanics and its Applications*, vol. 233, no. 3, pp. 709–717, Dec. 1996, doi: [https://doi.org/10.1016/S0378-4371\(96\)00157-4](https://doi.org/10.1016/S0378-4371(96)00157-4)
101. Arvind Caprihan and J. D. Seymour, "Correlation Time and Diffusion Coefficient Imaging: Application to a Granular Flow System," *Journal of Magnetic Resonance*, vol. 144, no. 1, pp. 96–107, May 2000, doi: <https://doi.org/10.1006/jmre.2000.2033>.
102. J. E. Maneval, K. M. Hill, B. E. Smith, A. Caprihan, and E. Fukushima, "Effects of end wall friction in rotating cylinder granular flow experiments," *Granular Matter*, vol. 7, no. 4, pp. 199–202, Aug. 2005, doi: <https://doi.org/10.1007/s10035-005-0211-4>.
103. N. Sommier, P. Porion, P. Evesque, B. Leclerc, P. Tchoreloff, and G. Couarraze, "Magnetic resonance imaging investigation of the mixing-segregation process in a pharmaceutical blender," *International Journal of Pharmaceutics*, vol. 222, no. 2, pp. 243–258, Jul. 2001, doi: [https://doi.org/10.1016/s0378-5173\(01\)00718-9](https://doi.org/10.1016/s0378-5173(01)00718-9).

104. P. Porion, N. Sommier, A.-M. Faugère, and P. Evesque, “Dynamics of size segregation and mixing of granular materials in a 3D-blender by NMR imaging investigation,” *Powder Technology*, vol. 141, no. 1–2, pp. 55–68, Mar. 2004, doi: <https://doi.org/10.1016/j.powtec.2004.02.015>.
105. T. Kawaguchi, K. Tsutsumi, and Y. Tsuji, “MRI Measurement of Granular Motion in a Rotating Drum,” *Particle & Particle Systems Characterization*, vol. 23, no. 3–4, pp. 266–271, Oct. 2006, doi: <https://doi.org/10.1002/ppsc.200601065>.
106. E. H. Hardy, J. Hoferer, and G. Kasper, “The mixing state of fine powders measured by magnetic resonance imaging,” *Powder Technology*, vol. 177, no. 1, pp. 12–22, Aug. 2007, doi: <https://doi.org/10.1016/j.powtec.2007.02.042>.
107. A. Bulent Koc, Hasan Silleli, Caner Koc, and M. Ali Dayioglu, “Monitoring of Dry Powder Mixing With Real-Time Image Processing,” *Journal of Applied Sciences*, vol. 7, no. 8, pp. 1218–1223, Aug. 2007, doi: <https://doi.org/10.3923/jas.2007.1218.1223>.
108. X. Liu, C. Zhang, and J. Zhan, “Quantitative comparison of image analysis methods for particle mixing in rotary drums,” *Powder Technology*, vol. 282, pp. 32–36, Sep. 2015, doi: <https://doi.org/10.1016/j.powtec.2014.08.076>.
109. A. Realpe and C. Velázquez, “Image processing and analysis for determination of concentrations of powder mixtures,” *Powder Technology*, vol. 134, no. 3, pp. 193–200, Sep. 2003, doi: [https://doi.org/10.1016/s0032-5910\(03\)00138-4](https://doi.org/10.1016/s0032-5910(03)00138-4).
110. A.-L. Le Coënt, A. Rivoire, S. Briançon, and J. Lieto, “An original image-processing technique for obtaining the mixing time: The box-counting with erosions method,” *Powder Technology*, vol. 152, no. 1–3, pp. 62–71, Apr. 2005, doi: <https://doi.org/10.1016/j.powtec.2005.01.025>.
111. G. Fariss, R. Keintz, and P. okoye, “Thermal effusivity and power consumption as : PAT tools for monitoring granulation end point,” *Thermal effusivity and power consumption as : PAT tools for monitoring granulation end point*, vol. 30, no. 6, pp. 60–72 [7 p.], 2006, <https://pascal-francis.inist.fr/vibad/index.php?action=getRecordDetail&idt=17843728>

112. studies in an agitated bed of granular materials in a cylindrical vessel,” *Powder Technology*, vol. 55, no. 2, pp. 107–114, Jun. 1988, doi: [https://doi.org/10.1016/0032-5910\(88\)80093-7](https://doi.org/10.1016/0032-5910(88)80093-7).
113. C.-C. Chen and C.-K. Yu, “Two-dimensional image characterization of powder mixing and its effects on the solid-state reactions,” *Materials Chemistry and Physics*, vol. 85, no. 1, pp. 227–237, May 2004, doi: <https://doi.org/10.1016/j.matchemphys.2004.01.024>.
114. H. P. Kuo, R. C. Hsu, and Y. C. Hsiao, “Investigation of axial segregation in a rotating drum,” *Powder Technology*, vol. 153, no. 3, pp. 196–203, Jun. 2005, doi: <https://doi.org/10.1016/j.powtec.2005.03.018>.
115. Björn Daumann, A. Fath, H. Anlauf, and H. Nirschl, “Determination of the mixing time in a discontinuous powder mixer by using image analysis,” *Chemical Engineering Science*, vol. 64, no. 10, pp. 2320–2331, May 2009, doi: <https://doi.org/10.1016/j.ces.2009.01.032>.
116. H. Berthiaux, V. Mosorov, L. Tomczak, C. Gatumel, and J. F. Demeyre, “Principal component analysis for characterising homogeneity in powder mixing using image processing techniques,” *Chemical Engineering and Processing: Process Intensification*, vol. 45, no. 5, pp. 397–403, May 2006, doi: <https://doi.org/10.1016/j.cep.2005.10.005>.
117. M. Cavinato, R. Artoni, M. Bresciani, P. Canu, and A. C. Santomaso, “Scale-up effects on flow patterns in the high shear mixing of cohesive powders,” *Chemical Engineering Science*, vol. 102, pp. 1–9, Oct. 2013, doi: <https://doi.org/10.1016/j.ces.2013.07.037>.
118. Chawki Ammarcha, Cendrine Gatumel, Jean-Louis Dirion, M. Cabassud, and Henri Berthiaux, “Continuous powder mixing of segregating mixtures under steady and unsteady state regimes: Homogeneity assessment by real-time on-line image analysis,” *Powder Technology*, vol. 315, pp. 39–52, Jun. 2017, doi: <https://doi.org/10.1016/j.powtec.2017.02.010>.
119. X. Liu, C. Zhang, and J. Zhan, “Quantitative comparison of image analysis methods for particle mixing in rotary drums,” *Powder Technology*, vol. 282, pp. 32–36, Sep. 2015, doi: <https://doi.org/10.1016/j.powtec.2014.08.076>.

120. T. A. Kingston and T. J. Heindel, "Granular mixing optimization and the influence of operating conditions in a double screw mixer," *Powder Technology*, vol. 266, pp. 144–155, Nov. 2014, doi: <https://doi.org/10.1016/j.powtec.2014.06.016>.
121. B. Remy, T. M. Canty, Johannes Khinast, and B. J. Glasser, "Experiments and simulations of cohesionless particles with varying roughness in a bladed mixer," vol. 65, no. 16, pp. 4557–4571, Aug. 2010, doi: <https://doi.org/10.1016/j.ces.2010.04.034>.
122. D. J. Parker, A. E. Dijkstra, T. W. Martin, and J. P. K. Seville, "Positron emission particle tracking studies of spherical particle motion in rotating drums," *Chemical Engineering Science*, vol. 52, no. 13, pp. 2011–2022, Jul. 1997, doi: [https://doi.org/10.1016/s0009-2509\(97\)00030-4](https://doi.org/10.1016/s0009-2509(97)00030-4).
123. P. M. Portillo, A. U. Vanarase, A. Ingram, J. K. Seville, M. G. Ierapetritou, and F. J. Muzzio, "Investigation of the effect of impeller rotation rate, powder flow rate, and cohesion on powder flow behavior in a continuous blender using PEPT," *Chemical Engineering Science*, vol. 65, no. 21, pp. 5658–5668, Nov. 2010, doi: <https://doi.org/10.1016/j.ces.2010.06.036>.
124. C. J. Broadbent, J. Bridgwater, D. Parker, S.T. Keningley, and P. L. Knight, "A phenomenological study of a batch mixer using a positron camera," *Powder Technology*, vol. 76, no. 3, pp. 317–329, Sep. 1993, doi: [https://doi.org/10.1016/s0032-5910\(05\)80013-0](https://doi.org/10.1016/s0032-5910(05)80013-0).
125. H. P. Kuo, P. C. Knight, D. J. Parker, and J. P. K. Seville, "Solids circulation and axial dispersion of cohesionless particles in a V-mixer," *Powder Technology*, vol. 152, no. 1–3, pp. 133–140, Apr. 2005, doi: <https://doi.org/10.1016/j.powtec.2004.12.003>.
126. M. Perrault, F. Bertrand, and J. Chaouki, "An investigation of magnesium stearate mixing in a V-blender through gamma-ray detection," *Powder Technology*, vol. 200, no. 3, pp. 234–245, Jun. 2010, doi: <https://doi.org/10.1016/j.powtec.2010.02.030>.

Chapter 3

3 Investigating Particle Loading Configuration in a V-blender during Powder Mixing Using Passive Acoustic Emissions

3.1 Introduction

Oral dosage forms such as tablets and capsules account for approximately 80% of all available pharmaceutical formulations (1). That is due to their ease of transport, use, cost-effectiveness, and stability. During the production of oral solid dosage forms, the powder materials need to be well-mixed. Mixing is one of the essential processes in the pharmaceutical industry to ensure the tablets and capsules produced contain the desired amounts of active ingredients and other additives. Furthermore, mixing is crucial to ensure that the products have uniform weight and consistent characteristics. However, mixing is a challenging process that depends on many factors such as powder characteristics, blender design, operation, and geometry (2,3). Mixing is not a fully understood process and still requires more research to better understand the mixing process and develop techniques for its control and monitoring.

Most of the pharmaceutical tablet manufacturing is done offline using different batch processes. Process analytical technologies (PATs) are being studied as potential methods for monitoring and analyzing powder mixing in the pharmaceutical industry (9,10). These potential technologies are intended to replace the offline methods currently being used. One of the offline methods currently used in the pharmaceutical industry is using thief probes to determine mixture quality and homogeneity by analyzing samples at different time intervals. Thief probes can result in inaccurate and unreliable data and their application is limited and has several disadvantages. Moreover, thief probes are not always effective in identifying segregation in a precise and reliable way. Wilson and Briens (2022) showed more data on the sampling and analysis of thief probes and demonstrated that thief probes can give inaccurate and unreliable results (6).

The literature has studies and research for several PATs in monitoring powder mixing. Most of the research on applying PATs has focused on near-infrared (NIR) spectroscopy. Although NIR spectroscopy demonstrated potential and consideration, its use in the pharmaceutical industry is limited. It has several disadvantages such as expensive equipment modifications, sensor port issues blockage, and the long pre- and post-processing time needed to get NIR measurements (11-20).

Powder mixing in the pharmaceutical industry primarily occurs in opaque metal mixers. Equipment that is used in pharmaceutical industrial facilities would require costly modification to install windows to allow for visual observation. Furthermore, pharmaceutical powder mixtures are often made up of various powders of similar colors, mostly white, which leads to a restricted ability to visually observe and identify segregation developed in the powder mixture. Changing the color of these powders can result in various issues, such as the risk of changing the properties of the powders unintentionally and that can lead to serious side effects. As a result, visually identifying segregation in the pharmaceutical industry setup is very challenging and impractical.

There are other PATs under development and are included in several studies and research supporting their use in powder mixing, monitoring, and analysis including Raman Spectroscopy (21-27), Passive Acoustic Emissions (6,28-34), X-ray Computed Tomography (35-37), Image Analysis (38-35), and Magnetic Resonance Imaging (46,47,48). Passive acoustic emissions are defined as the formation of energy as waves produced by a source, then transmission of energy through a medium, and receiving this energy by a receiver. It is the study of vibrations and sound waves (49). In the V-blender, the energy is generated as stress waves as the result of particle-particle and particle-V-shell interactions during powder mixing (28). The stress waves generated from particle interactions are measured as vibrations by an accelerometer attached to the lid of the outer arm of the V-shell. The vibrations recorded by the accelerometer due to particle mixing and collision are dependent on several factors including particle characteristics such as size, density, and shape. Particles with larger sizes have more kinetic energy and upon collision with each other or with the V-shell, more dissipated

energy is generated leading to more vibrations as stress waves that are recorded by the accelerometer.

Passive acoustic emissions have available research in the literature discussing and supporting acoustics use in different processes such as mixing (6,28-34), granulation (50-58), fluidization (59,60), drying (61), compaction (62), direct energy deposition (63), hydro transport (64), and pneumatic transport (65-68). Previous research conducted on passive acoustic emissions determined preliminary connections and data for particle motion and behaviors inside the V-blender and provided guidelines for extracting the data needed from the recorded vibrations (6,28-31). Particle collisions with the V-shell lid where the accelerometer is attached provided the most important and reliable information regarding the particle properties and their flow within the V-shell from the recorded vibrations.

Segregation is known as areas of particles within a mixture with a high concentration of particles sharing similar properties. In the pharmaceutical industry, segregation can develop while mixing powders due to using different particles with different physical characteristics such as size, density, shape and flowability. It is crucial to account for these differences in physical characteristics to avoid segregation development. Segregation can affect mixture homogeneity and uniformity. Segregation is also known as de-mixing (69). Various factors can affect the segregation likelihood. Large differences in particle size, density, cohesiveness, and flowability can increase the probability of segregation. The more differences in the characteristics between the particles, the more segregation can be seen. (3,69,70).

The mixer type and geometry can increase the risk of segregation development.

Previous literature showed that tote mixers and V-blenders are not the best mixers to be used for segregation-prone mixtures and cohesive particles due to the motion and flow of the particles in these mixers that lead to the development of trajectory segregation (70,71). Trajectory segregation is a type of segregation that can be seen in the V-blender. It can happen when mixing a powder of high inertia with another powder of low inertia. Due to differences in inertia, the smaller diameter particles will tend to

separate from particles with larger diameters. The particles with higher inertia will flow in a straight-line path, while the particles with lower inertia will flow in a curved path (69-72).

Trajectory segregation can be further enhanced in the V-blender because of the collisions with the V-shell joint on the flow path. Segregation can develop while mixing particles inside a V-blender. The main mechanisms that can be seen while mixing particles inside a V-blender are primarily due to trajectory and percolation segregations. These types of segregation can be seen with particles that have high flowability, are subjected to a curving flow field, and have a range of various sizes. However, the starch granules used in the experimental trials completed in this research are not spherical and have irregular shapes of various diameter ranges with a spherical value of 0.70. Also, the starch granules have good flowability due to the low avalanche times below 4.8 seconds (6). The literature discussed segregation development patterns and how the physical characteristics, mixer design, fill level, and process parameters can affect the segregation pattern. It was found that the fill level and rotational speed have a significant impact on segregation pattern development in the V-blender. Four major different patterns were seen to develop in the V-blender which are “Small-out”, “Stripes”, “Inverse stripes”, and “Left-right” patterns. There is another fifth pattern seen called the “Big-out” pattern, but it is seen transiently while the “Left-right” pattern is being developed (70,71).

Passive acoustic emissions have several advantages when compared with other methods used in the pharmaceutical industry for monitoring powder mixing and segregation. Acoustic use is relatively inexpensive, non-invasive, non-destructive, requires no equipment modifications, and could be used as an in-line monitoring method. Previous research has focused on monitoring the mixing of a specific number of particles with uniform properties in one loading order. However, tablets in the pharmaceutical industry are formed from various particles and therefore it is important to develop a method that can be applied to industrial settings (6,28-31). The main aim of this research was to further investigate the potential of passive acoustic emissions for monitoring the mixing of multiple particles of different properties that are likely to

segregate and explore different loading configurations for loading these particles in the V-blender. Identifying segregation during powder mixing is crucial in the pharmaceutical industry and can result in higher quality control and assurance standards and enhance good manufacturing practices in the industry. This can be achieved by developing monitoring methods using passive acoustic emissions.

3.2 Materials and Methods

3.2.1 Materials

Experimental trials were conducted and completed using starch granules and glass beads. The starch granules were irregular in shape and had a range of different sizes. The starch granules were sieved into five different-size fraction cuts using different-size meshes. Cut#1 is the largest size fraction with a size range of 2.00 – 2.36 mm, Cut#2A has a size range of 1.70 – 2.00 mm, Cut#2B has a size range of 1.40 – 1.70 mm, Cut#3 has a size range of 1.18 – 1.40 mm, and Cut#4 is the smallest size fraction with a size range of 0.006 – 1.18 mm. Samples of starch granules from each size difference were dyed with iodine solution to allow for visual observations of any segregation that may develop while mixing. Preliminary testing trials confirmed that the dye did not significantly affect the other properties of the granules. Wilson and Briens (2022) measured the apparent density of the starch granules through estimation by volume displacement measurements using 4°C distilled water and photos of the starch granules were taken and examined with Image Pro software to estimate the circularity of the granules. Image Pro defines circularity as $\frac{\text{Perimeter}^2}{4\pi \cdot \text{Area}}$, with a perfectly circular particle having a value of 1.00 (6). The glass beads were selected as a model system because of their uniform composition and spherical size. The glass beads were selected to be in close range to the granule sizes used in the pharmaceutical industry. Experimental trials were completed using glass beads with three different diameter sizes: 1 mm, 2 mm, and 3 mm. All starch granule and glass bead experimental trials were completed in triplicate with average values reported. Table 3.1 shows the particle characteristics.

Table 3.1: Summary of particles and their characteristics

Particle	Size (mm)	Average size (mm)	Apparent density (g/cm ³)	Sphericity (-)
Starch granules Cut#1	2.00 – 2.36	2.18	1.3	0.70
Starch granules Cut#2A	1.70 – 2.00	1.85	1.3	0.70
Starch granules Cut#2B	1.40 – 1.70	1.55	1.3	0.70
Starch granules Cut#3	1.18 – 1.40	1.29	1.3	0.70
Starch granules Cut#4	0.006 – 1.18	0.593	1.3	0.70
Glass beads	1.00	1.00	2.5	1.00
Glass beads	2.00	2.00	2.5	1.00
Glass beads	3.00	3.00	2.5	1.00

3.2.2 Equipment

A Patterson-Kelly V-blender with a fixed rotation speed of 25 Rotations Per Minute (RPM) was used in all the experimental trials completed in this research. A 16-quart (15.1 liter) transparent acrylic V-shell was used. The V-shell was filled by particle mass corresponding to approximately 25% fill level ratio by mass. The V-shell of the blender has inner and outer arms with two lids attached to them and a bottom plate. Figure 3.1 shows a schematic diagram of the V-blender with all its properties.

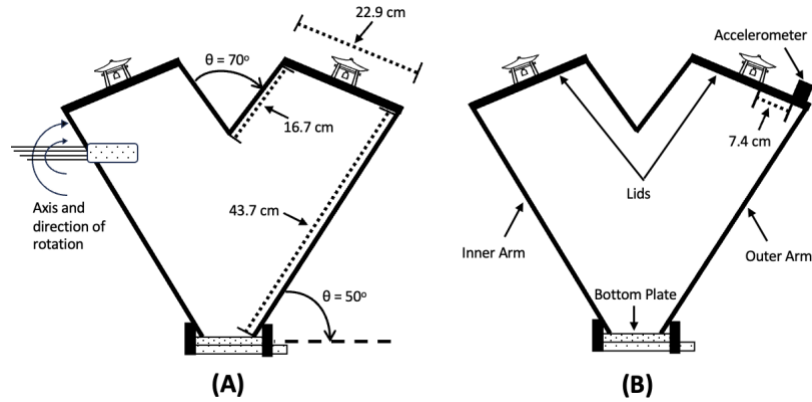


Figure 3.1: Schematic diagram for the V-blender (A) showing its dimensions and (B) showing accelerometer location

PCB Piezotronics Accelerometer of model 353B3 combined with an ICP signal conditioner of model 480E0 were used to measure the vibrations generated from passive acoustic emissions. The accelerometer combined with the signal conditioner was attached to the lower front center of the outer arm of the V-shell at a radial position of $r/R = 0.74$ using adhesive wax. Figure 3.1-B shows the location of the accelerometer. Labview with a National Instruments DAQ-6036E card was used to record the vibrations from passive acoustic emissions. The vibrations were recorded at an acquisition frequency of 40,000 Hz. The choice of an acquisition frequency of 40,000 Hz was used to exceed the Nyquist frequency of the signal of interest. The Nyquist-Shannon Sampling Theorem states that to accurately construct a signal, the sampling frequency must be at least twice the highest frequency present in the signal. In the case of audio signals, where the human hearing range is up to 20,000 Hz, a common choice is to use a sampling frequency of at least 40,000 Hz to ensure that all audible frequencies are adequately captured and avoid aliasing and to make sure that the signal preserves the original characteristics of the analog signal (76,77).

Daubechies wavelet filter in Matlab was used to filter the measurements recorded to remove the V-shell oscillations motion to primarily focus on the vibrations generated from the particle collision inside the V-shell. Noise generated due to the oscillation motion of the V-shell can interfere with the wavelets recorded. That is why it was

important to remove wavelets coming from V-shell oscillations to be able to focus on the wavelets needed that are generated from particle collisions (78).

3.2.3 Experimental Trials

Experimental trials were conducted using various size fractions of starch granules and glass beads as well as different intensifier bar additions to the inner V-shell arm. The starch granules were sieved into five different size fractions as shown in Table 3.1. One of the starch granule size fractions were dyed using iodine solution to allow for visual observations of any segregation that may develop. All size fractions were in a 50-50% ratio by mass and the mixture combinations were loaded horizontally and vertically in the V-blender at a 25% fill level by mass ratio and tumbled. Rotations of different size fractions were completed allowing for mixing and segregation patterns were photographed. All segregation for different size fraction combinations was observed and photographed. Individual particle material trials for each particle size of starch granules and glass beads shown in Table 3.1 were conducted. Table 3.2 shows the experimental trials conducted for starch granules binary mixtures and the loading configuration used. All starch granules and glass beads trials were conducted in triplicate for reproducibility and confirmation of the results obtained; however, as replicates were similar, only one trial was shown for each condition.

The weighted average amplitude was determined in all trials based on the percentage of small and large particles in the outer V-shell arm of the V-blender. This was done by sieving and weighing the particles in the outer V-shell arm after 100 revolutions. The percentages found in the outer V-shell arm along with the average amplitude recorded of each size fraction were then used to determine an approximate weighted average amplitude value. The percentage of the large particles found in the outer arm was multiplied by the average amplitude recorded of the large particles and then summed up to the percentage of the small particles found in the outer arm multiplied by the average amplitude recorded of the small particles giving the weighted average value for every trial. The weighted average was determined in each set of trials and demonstrated on the graph. Each trial was done in triplicate therefore the weighted average was

calculated three times. The total weighted average for all trials is much of a zone seen on the graph that corresponds to three trials completed.

Table 3.2: Trials conducted for starch granules binary mixtures and their loading configurations

Trial	Binary mixture (50-50% by mass ratio)	Loading configuration
I	Cut#1 and Cut#4, where Cut#1 on top	Horizontal loading
II	Cut#1 and Cut#4, where Cut#4 on top	Horizontal loading
III	Cut#1 and Cut#3, where Cut#1 on top	Horizontal loading
IV	Cut#1 and Cut#3, where Cut#3 on top	Horizontal loading
V	Cut#2A and Cut#4, where Cut#2A on top	Horizontal loading
VI	Cut#2A and Cut#4, where Cut#4 on top	Horizontal loading
VII	Cut#2A and Cut#3, where Cut#2A on top	Horizontal loading
VIII	Cut#2A and Cut#3, where Cut#3 on top	Horizontal loading
IX	Cut#2B and Cut#4, where Cut#2B on top	Horizontal loading
X	Cut#2B and Cut#4, where Cut#4 on top	Horizontal loading
A	Cut#1 and Cut#4, where Cut#1 in inner arm	Vertical loading
B	Cut#1 and Cut#4, where Cut#4 in inner arm	Vertical loading
C	Cut#1 and Cut#3, where Cut#1 in inner arm	Vertical loading
D	Cut#1 and Cut#3, where Cut#3 in inner arm	Vertical loading
E	Cut#2A and Cut#4, where Cut#2A in inner arm	Vertical loading
F	Cut#2A and Cut#4, where Cut#4 in inner arm	Vertical loading
G	Cut#2A and Cut#3, where Cut#2A in inner arm	Vertical loading
H	Cut#2A and Cut#3, where Cut#4 in inner arm	Vertical loading
I	Cut#2B and Cut#4, where Cut#2B in inner arm	Vertical loading
J	Cut#2B and Cut#4, where Cut#4 in inner arm	Vertical loading

3.2.3.1 Individual Particle Size Cuts

Vibration measurements were recorded and completed with individual particle size cuts of starch granules and glass beads. The starch granules and glass beads were separately

loaded in the 16-quart transparent acrylic V-shell in a 100% ratio at a 25% fill level based on mass. The accelerometer was attached to the outer arm lid of the V-shell as shown in Figure 3.1-B. The vibrations were measured and recorded over 50 revolutions of the V-shell. After the vibrations were measured, the measurements were filtered and analyzed using Matlab.

3.2.3.2 Horizontal Loading Configuration

Vibration measurements were recorded and completed with binary mixtures of the starch granules. The binary mixture of starch granules was loaded in the 16-quart transparent acrylic V-shell in a 50–50% ratio at a 25% fill level based on mass. The starch granules were loaded into the V-shell in a horizontal loading configuration. The main objective of this horizontal loading configuration was to obtain a symmetrical top-bottom loading pattern for the geometry of the V-blender shells. The accelerometer was attached to the outer arm lid of the V-shell as indicated in Figure 3.1-B. The vibrations were measured and recorded over 100 revolutions of the V-shell. After the vibrations were measured, the measurements were filtered and analyzed using Matlab.

While the V-blender was tumbling and rotating, the V-shell was stopped at different revolutions to take photos and sieve the mixture inside. Sieving of the mixture was done for both inner and outer V-shell arms using different size meshes based on starch granule size fraction cuts in the mixture. This was performed to observe the extent of segregation developed and quantify the amount of smaller and larger particles seen in each arm of the V-shell. Photos of the dyed starch granules mixture allowed for visual observations of any segregation pattern development and monitored the mixing stage. Moreover, the sieving data allowed for confirmation of mixing and segregation observed in each arm of the V-shell. In the sieving analysis, the V-shell was stopped while inverted, and the inner and outer arms were unloaded separately. Each arm emptied contained a mixture which was then sieved to determine the percentage composition by weight of each particle component. The mixtures from each arm were unloaded after 100 revolutions. Preliminary trials were conducted, and stable mixtures were determined in all trials.

3.2.3.3 Vertical Loading Configuration

Vibration measurements were recorded and completed with binary mixtures of the starch granules. The binary mixture of starch granules was loaded in the 16-quart transparent acrylic V-shell in a 50–50% ratio at a 25% fill level based on mass. A technique for proper and repeatable vertical loading of binary mixtures was developed and the starch granule size fraction cuts were loaded in a vertical configuration into the V-shell. The V-shell was stopped in a position that was parallel to the ground and then the particles were loaded in each V-shell arm. Then the V-blender was returned to its upright position with particles inside reaching a vertical loading configuration. The main objective of this vertical loading configuration was to obtain a symmetrical side-to-side loading pattern for the geometry of the V-blender shells. The accelerometer was attached to the outer arm lid of the V-shell as indicated in Figure 3.1-B. The vibrations were measured and recorded over 100 revolutions of the V-shell. After the vibrations were measured, the measurements were filtered and analyzed using Matlab.

The V-shell was stopped to take photos and sieve the mixture inside. Sieving of the mixture was done for both the inner and outer V-shells. This was performed to observe the extent of segregation developed and quantify the amount of smaller and larger particles seen in each arm of the V-shell. The sieving data allowed for confirmation of mixing and segregation to be observed in V-shell arms. In the sieving analysis, the V-shell was stopped while inverted and the inner and outer arms were unloaded separately after 100 revolutions and sieved. Preliminary trials were conducted, and stable mixtures were determined in all trials as done in horizontal loading trials in Section 3.2.3.2.

3.2.3.4 Intensifier Bar Addition

Vibration measurements were recorded for binary mixtures of the starch granules. The binary mixture of starch granules was loaded in the 16-quart transparent acrylic V-shell in a 50-50% ratio at a 25% fill level based on mass. Cut#1 was dyed using iodine solution to observe any segregation pattern that may develop while mixing. The starch granule particles were loaded in a horizontal loading configuration in the V-shell with the addition of different intensifier bars to examine their effects on mixing and

segregation. Particles were loaded in a horizontal configuration to obtain a symmetrical top-bottom loading pattern for the geometry of the V-blender shells. The accelerometer was attached to the outer arm lid of the V-shell as indicated in Figure 3.1-B. The vibrations were measured and recorded over 50 revolutions of the V-shell. After the vibrations were measured, the measurements were filtered and analyzed using Matlab. Sieving of the binary mixture was completed by stopping the V-shell after 50 revolutions to take photos and sieve the mixture inside. Sieving of the mixture was done for both inner and outer V-shell arms as performed with horizontal loading trials in Section 3.2.3.2.

3.3 Results

3.3.1 Individual Particle Size Cuts

Experimental trials were performed using different starch granules and glass beads size cuts. Each size fraction cut of starch granules and glass beads was loaded separately in the V-blender at a 25% fill level by mass and trials were completed over 50 revolutions. The vibration amplitudes were recorded for different glass bead size fractions. Figure 3.2 shows the average vibration amplitude recorded varied nearly linearly with the glass beads. Vertical bars showing the average maximum and minimum amplitudes were added that correspond to three trials over 50 revolutions for each trial; however, the values were very small and almost negligible which makes them not visible on the graph. The vibration amplitude recorded was seen to increase with increasing the size of glass beads with a significant well-fitting linear trend as indicated by an R^2 value > 0.99 and a P-value of 0.04 (Figure 3.2). The average vibration amplitudes were recorded for different starch granule size cuts. Figure 3.3 shows the average amplitude and average granule size for each cut for three trials of 50 revolutions each. Vertical bars show the maximum and minimum amplitudes and horizontal bars show the maximum and minimum granule size. The increase in vibration amplitude with granule size was not quite linear (Figure 3.3); the trend was significant and slightly exponential as indicated by R^2 of 0.97 and a P-value of 0.02. Figure 3.4 shows an example of individual Cut#1 amplitude distributions recorded over 150 revolutions across three trials of 50 revolutions for each trial and their vibration distribution.

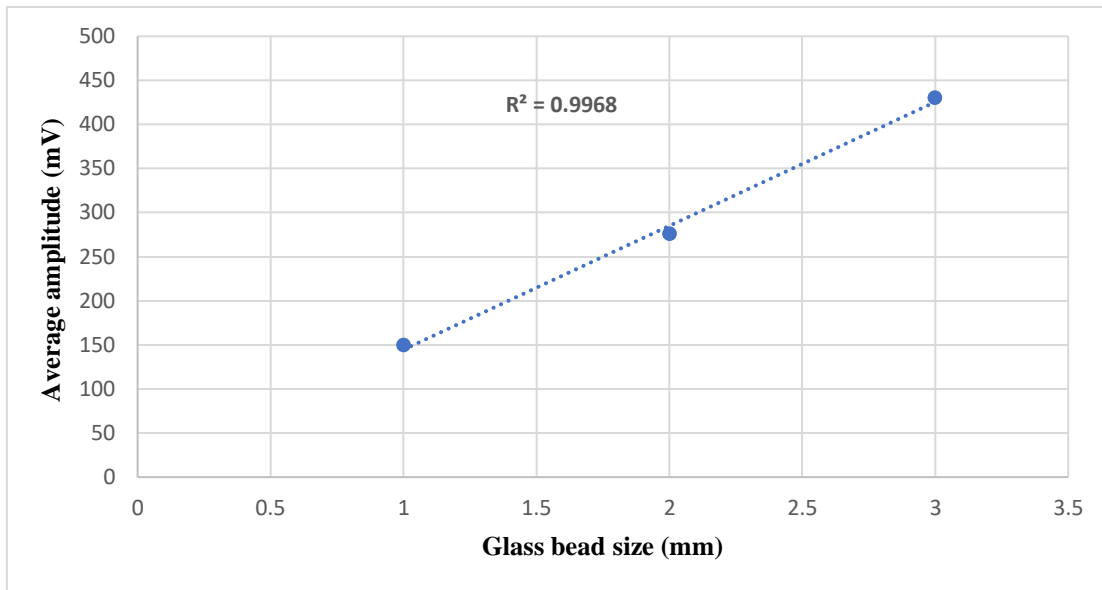


Figure 3.2: Average vibration amplitude of different-sized glass beads in V-shell with trendline

R^2 and P-values were calculated and showed significant values for a linear trendline with average amplitude increasing with increasing the glass bead size

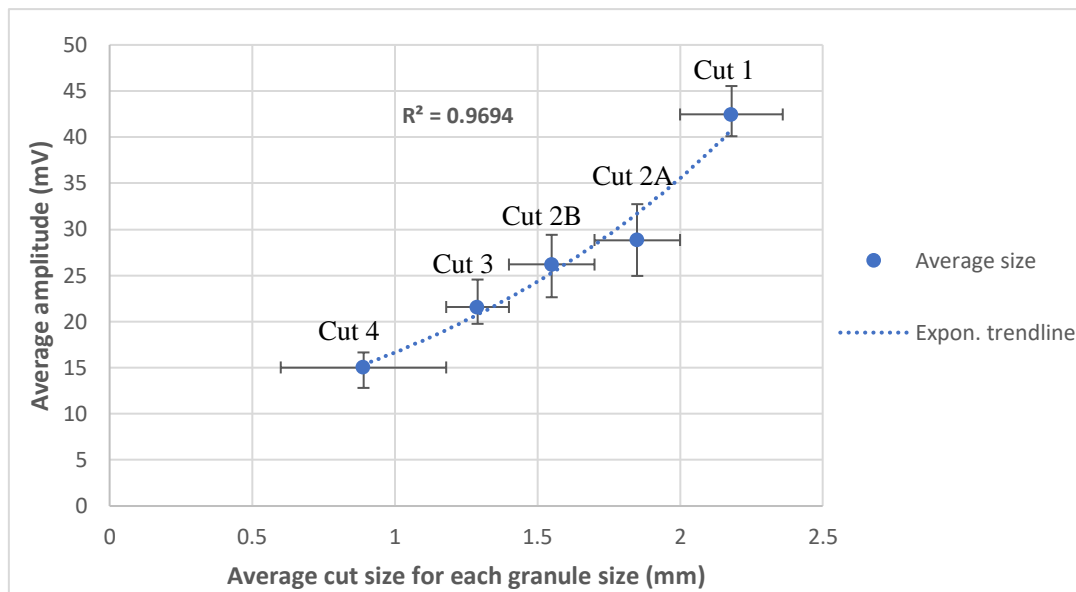


Figure 3.3: Average vibration amplitudes of starch granules with trendline and R^2 value

Horizontal bars represent the maximum and minimum cut size values and vertical bars represent the maximum and minimum amplitudes

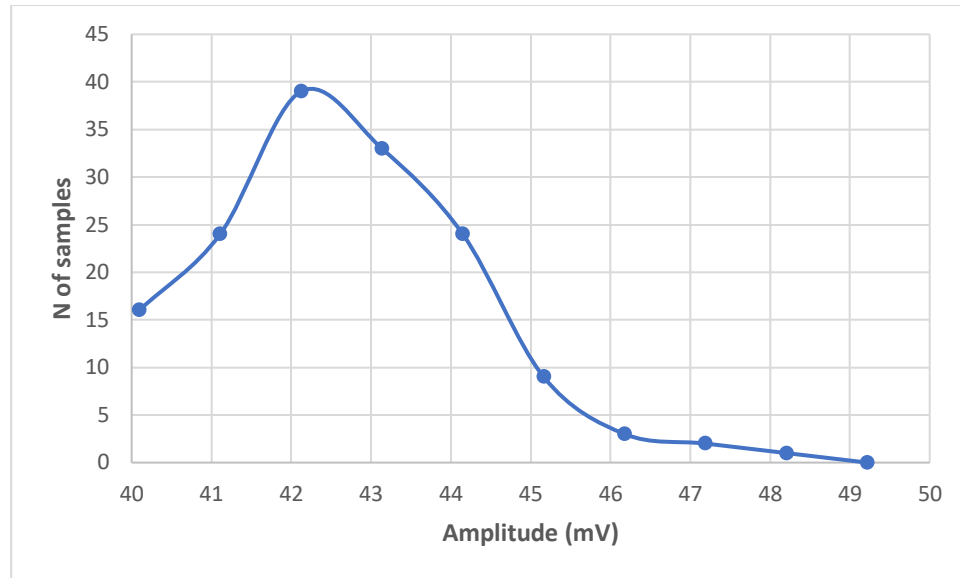


Figure 3.4: Amplitude distribution of Cut#1 starch granules across three trials of 50 revolutions each

There are different features for each signal based on the flow of particles inside the V-shell and how particles move and interact with V-shell walls and with each other. The flow of particles in the V-shell can be classified into three main parts. The first part is associated with the flow of particles while the V-shell is inverted and is called Feature#1. The second part is associated with the flow of particles along the V-shell arms of the outer side and is called Feature#2. The third part is associated with the flow of particles reaching the V-shell base and is called Feature#3 as shown in Figure 3.5.

Feature #1 consists of three sub-features. Initially, particles interact with the inner arms of the V-shell flowing along these arms towards the V-shell lids (Feature 1a). Then collisions occur between particles that are accumulating in the upper V-shell arms and the V-shell lids (Feature 1b). Finally, particles accumulating in the upper V-shell arms flow past the lids towards the outer arms of the V-shell. These three events occur continuously with overlapping durations (4).

Figure 3.6 shows the filtered raw signals of Cut#1 starch granules after 10 revolutions recorded by the accelerometer attached to the outer V-shell arm as shown in Figure 3.1-B. Signals were recorded and filtered with each full signal corresponding to one V-shell

rotation. While the V-shell is rotating, energy is dissipated as stress waves as particles collide with each other and with the V-shell walls. This energy is recorded by the accelerometer which translates into amplitudes. For each revolution, the average of the largest amplitudes in Feature 1b corresponds to one amplitude value for each V-shell revolution. This was continued for 50 revolutions resulting in 50 recorded amplitude values. The amplitude value recorded corresponds to the energy dissipated after 50 revolutions. Individual-sized particles were rotated over 50 revolutions in the V-shell, and 50 amplitude were recorded. The average of these 50 amplitude values was calculated and plotted on the graph versus the size range of different starch granules as shown in Figure 3.3.

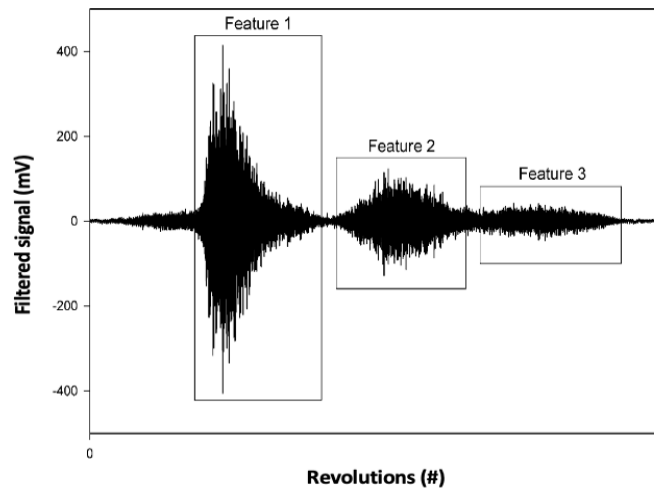


Figure 3.5: Cut#1 isolated filtered raw signal after 1 V-shell revolution

The granules were loaded at a 25% fill level in the V-shell and the filtered signal show different features of particle motion in the V-blender

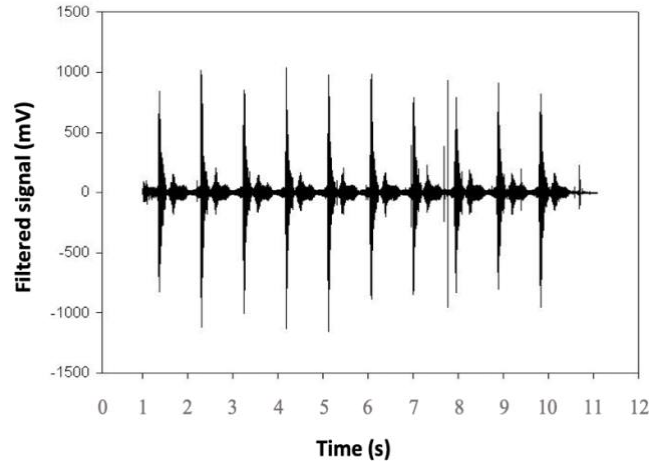


Figure 3.6: Filtered acoustic signals of Cut#1 starch granules

Filtered signals were recorded at 10 V-shell rotations and granules were loaded at 25% fill level

3.3.2 Horizontal Loading Configuration

All starch granule size fractions were in a 50-50% by mass ratio and the mixture combinations were loaded horizontally in the V-blender at 25% fill level by mass and tumbled. Rotations of different size fractions were completed, and mixing and segregation patterns were photographed. The segregation pattern was observed to be larger for mixtures with larger differences in their fraction size. The photos and sieving data confirmed the results. Visual observations of the starch granule mixtures confirm that segregation was higher with larger differences in the fraction size. Segregation for all different size fraction combinations was observed and photographed. Stable mixtures were reached and identified in all different size fraction trials. A stable mixture is generally defined as the combination of substances that remain without changing their properties over a certain time under defined conditions.

Figure 3.7 shows the extent of segregation between different size combinations of starch granules every 10 revolutions. Figure 3.7, column A shows a large difference in size fraction cuts, the larger size fraction Cut#1 (2.00 – 2.36 mm) was mixed with the smaller size fraction Cut#4 (0.006 – 1.18 mm). The larger undyed starch granules were loaded horizontally on top of the smaller dyed starch granules. The smaller dyed starch granules segregated towards the outer arm of the V-blender, and the larger undyed

starch granules segregated towards the inner arm. Figure 3.7, column B shows a small difference in starch granule size fraction cuts, Cut#2A (1.7 – 2.00 mm) was mixed with Cut#3 (1.18 – 1.40 mm). The larger dyed starch granules were loaded horizontally on top of the smaller undyed starch granules. The smaller undyed starch granules segregated towards the outer arm of the V-blender and the larger dyed starch granules towards the inner arm. This segregation pattern is named "left-right" segregation, which is seen in Figure 3.7 after around 20 revolutions. Experimental trials continued for 100 revolutions and showed that this left-right segregation pattern remained stable with no changes.

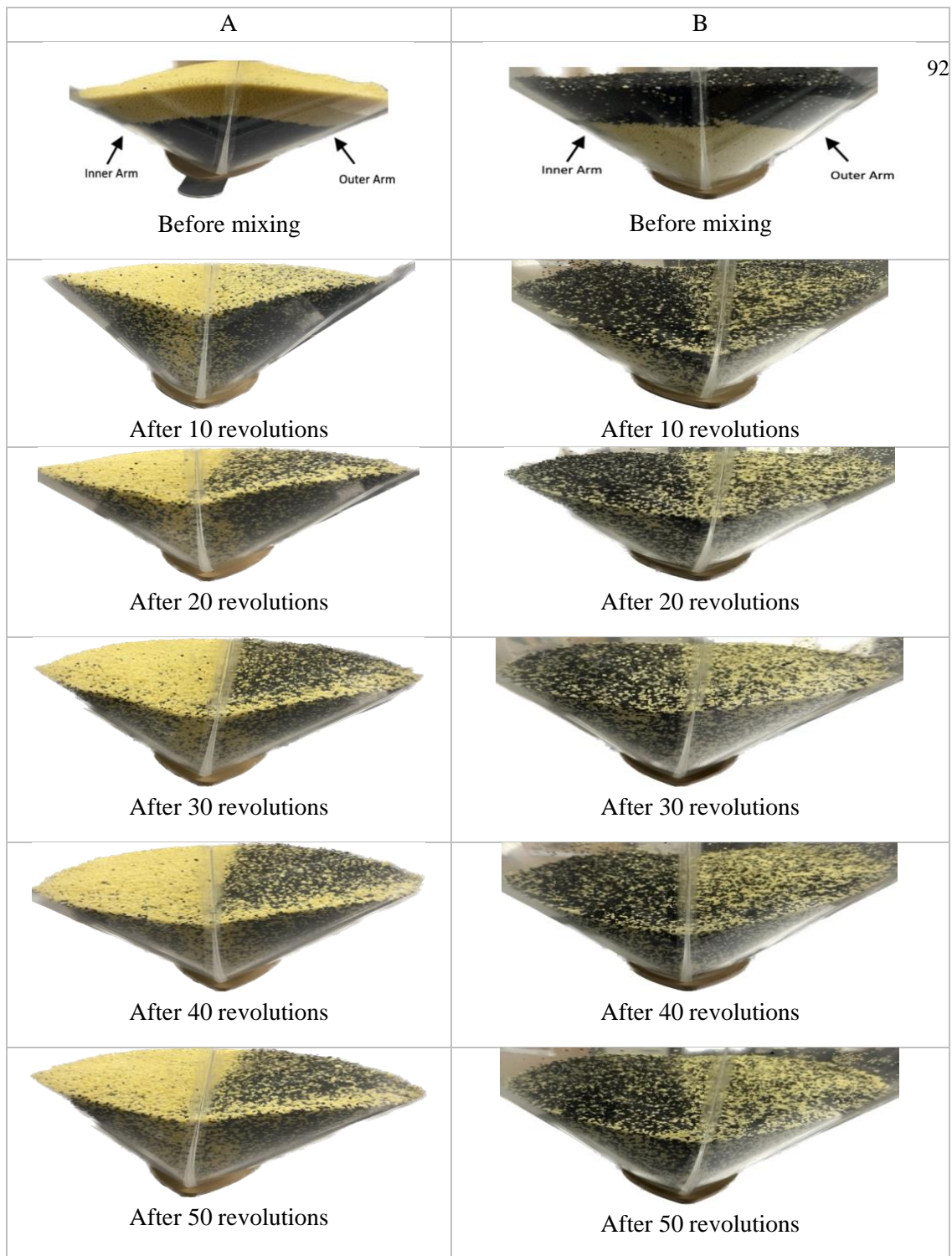


Figure 3.7: Visual observations of different starch granule size fractions horizontally loaded in the V-blender

Mixtures were in a 50-50% by mass ratio, Column A: Cuts 1 and 4 where undyed Cut#1 (yellow) loaded on top of dyed Cut#4 (black) and Column B: Cuts 2A and 4 where dyed Cut#2A (black) loaded on top of undyed Cut#3 (yellow)

Sieving of the mixtures was completed for both V-shell arms using various-sized meshes based on starch granule size fraction cuts used in each mixture. In the sieving analysis, the V-shell was stopped while inverted and both the inner and outer arms were unloaded separately. Each arm emptied contained a mixture which was then sieved to determine the percentage of each size fraction in each V-shell arm. The sieving results showed that smaller size fraction cuts were seen with higher percentages in the outer arm of the V-shell and the larger size fraction cuts were seen to segregate towards the inner arm with higher percentages. These results confirm the visual observations seen in Figure 3.7 with different starch granule size fraction mixtures. Table 3.3 shows the sieving results for different starch granule mixtures and their percentages in the outer arm of the V-shell. Table 3.3 shows only sieving results for the trials conducted for the largest and smallest combination mixtures; Cut#1 and Cut#4 and Cut#2A and Cut#3 binary mixtures, respectively. All other sieving data for remaining size fraction combination mixtures are reported in the Appendix section of this thesis.

Table 3.3: Sieving results in the outer arm of the V-shell for different size cut trials

Trial	Size cuts	Loading order	Loading configuration	Sieving results in outer arm (%)
I	Cut#1 and Cut#4	Cut#1 on top and Cut#4 on bottom	Horizontal loading	Trial 1: Cut#4 (68), Cut#1 (32) Trial 2: Cut#4 (70), Cut#1 (30) Trial 3: Cut#4 (67), Cut#1 (33) Average: Cut#4 (68), Cut#1 (32)
II	Cut#1 and Cut#4	Cut#1 on bottom and Cut#4 on top	Horizontal loading	Trial 1: Cut#4 (66), Cut#1 (34) Trial 2: Cut#4 (67), Cut#1 (33) Trial 3: Cut#4 (70), Cut#1 (30) Average: Cut#4 (68), Cut#1 (32)
VII	Cut#2A and Cut#3	Cut#2A on top and Cut#3 on bottom	Horizontal loading	Trial 1: Cut#3 (55), Cut#2A (45) Trial 2: Cut#3 (61), Cut#2A (39) Trial 3: Cut#3 (58), Cut#2A (42) Average: Cut#3 (58), Cut#2A (42)
VIII	Cut#2A and Cut#3	Cut#2A on bottom and Cut#3 on top	Horizontal loading	Trial 1: Cut#3 (53), Cut#2A (47) Trial 2: Cut#3 (57), Cut#2A (43) Trial 3: Cut#3 (57), Cut#2A (43) Average: Cut#3 (56), Cut#2A (44)

The vibration amplitude profiles of starch granule size fraction cuts were recorded. All trials were conducted with 50-50% binary mixtures by mass ratio. Figure 3.8 shows the acoustic vibration amplitude profiles recorded of the largest and the smallest starch granule size fractions of Cut#1 and Cut#4 and their binary mixtures, respectively. When Cut#4 was loaded horizontally on top of Cut#1, the initial mixture vibration amplitude recorded was around 15 mV which was similar to the amplitude of the small size fraction of Cut#4. The vibration amplitude then increased to around 27 mV after about 25 revolutions and maintained the amplitude in the zone of 25 – 30 mV throughout the remaining revolutions. When Cut#1 was loaded horizontally on top of Cut#4, the initial mixture vibration amplitude recorded was around 45 mV which was similar to the amplitude of the large size fraction of Cut#1. The vibration amplitude then decreased to around 25 mV after about 25 revolutions and maintained the amplitude in the zone of 20 – 25 mV throughout the remaining revolutions.

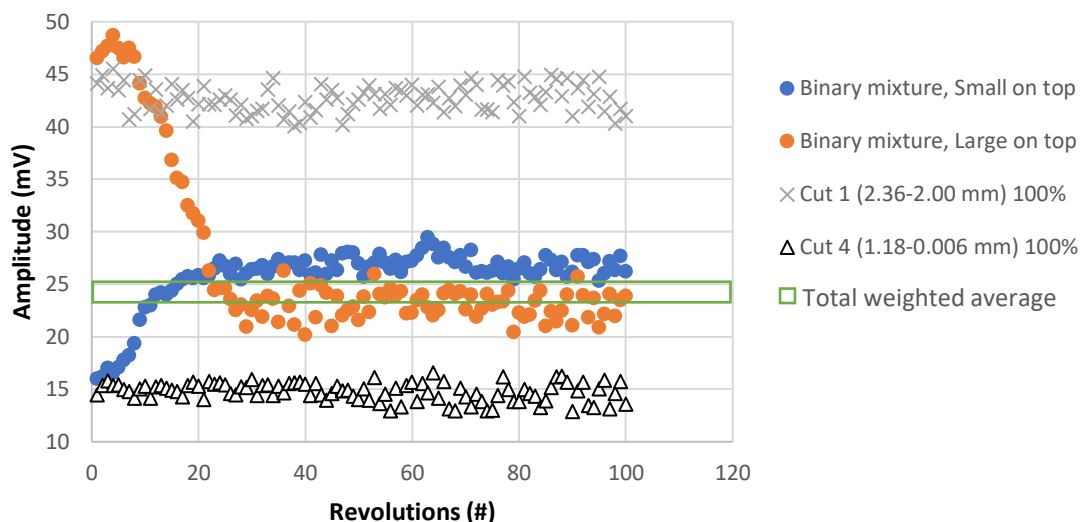


Figure 3.8: Acoustic profile of combined trials of Cut#1 (2.00 – 2.36 mm) and Cut#4 (0.006 – 1.18 mm)

Mixtures were in a 50-50% by mass ratio and were loaded horizontally in the V-blender

Figure 3.9 shows the vibration amplitude profiles of two very closely sized starch granule size fractions and their binary mixtures, Cut#2A and Cut#3. When Cut#3 was

loaded horizontally on top of Cut#2A, the initial mixture vibration amplitude was around 19 mV, similar to the amplitude of the small size fraction of Cut#3. The vibration amplitude then increased to around 28 mV after about 25 revolutions and maintained the amplitude in the zone of 24 – 29 mV throughout the remaining revolutions. When Cut#2A was loaded horizontally on top of Cut#3, the initial mixture vibration amplitude was around 31 mV, similar to the amplitude of the large size fraction of Cut#2A. The vibration amplitude then decreased to around 23 mV after about 30 revolutions and maintained the amplitude in the zone of 21 – 28 mV throughout the remaining revolutions.

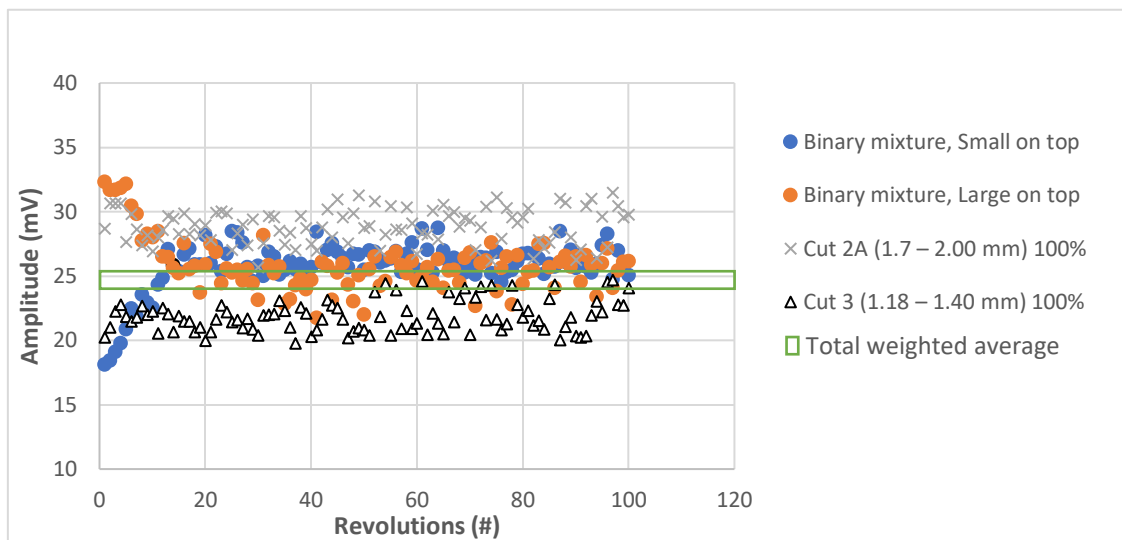


Figure 3.9: Acoustic profile of combined trials of Cut#2A (1.70 – 2.00 mm) and Cut#3 (1.18 – 1.40 mm)

Mixtures were in a 50-50% by mass ratio and were loaded horizontally in the V-blender

Figure 3.8 shows a large difference in starch granule size fraction cuts used. In this trial, Cut#1 and Cut#4 were used. Cut#1 has an average size of 2.18 mm and Cut#4 has an average size of 0.593 mm. By subtracting Cut#1 average size from Cut#4 average size, 1.587 mm will be the average size difference between the two cut sizes. Figure 3.9 shows a small difference in starch granules size fraction cuts used. In this trial, Cut#2A and Cut#3 were used. Cut#2A has an average size of 1.85 mm and Cut#3 has an average size of 1.29 mm. By subtracting Cut#2A average size from Cut#3 average size,

0.56 mm will be the average size difference between the two cut sizes. Table 3.1 shows the size range of each starch granule cut size and their average size values.

The weighted average amplitude was determined based on the percentage of small and large particles in the outer V-shell arm. This was done by sieving and weighing the particles in the outer V-shell arm after 100 revolutions. The percentages found in the outer V-shell arm along with the average amplitude recorded of each size fraction cut were then used to determine an approximate weighted average amplitude value. If the weighted average is 50-50% by mass ratio for each particle size, there will not be any segregation of particles seen and the recorded amplitude will be halfway between the amplitude of the two single-sized starch granules. However, in the trials conducted in this research, the weighted average was not 50-50% by mass ratio and segregation was observed with the composition of the system reflected the segregation of the combination mixtures used. If there is segregation, it is expected that the measured signal will plateau around the weighted average amplitude zone.

Stable mixtures were observed and identified in all trials for horizontal loadings. The minimum mixing needed for each mixture was calculated based on the average Standard Deviation (STD). The STD was calculated for the last 20 revolutions of the mixture while getting the average +1 and -1 of the STD. The first point to drop below the +1 STD or go above the -1 STD is set to be the minimum mixing in revolutions needed to reach a stable mixture as shown in the example in Figure 3.10 with the minimum mixing highlighted in an orange "X" shape for the binary mixture of Cut#2A and Cut#3. Table 3.4 shows the minimum mixing required for combination mixtures in the V-blender. Figure 3.11 shows the average minimum mixing for different mixtures loaded horizontally with different orders versus the size difference between different cuts. There was no significant trend observed with different size fraction binary mixtures with the loading order. Binary mixtures of Cut#1 and Cut#4 and Cut#2A and Cut#3 are the main trials reported with their profiles in this Chapter as they have the biggest and smallest size differences between the two cuts, respectively. Other trials were completed using different starch granule size combinations which showed similar results and their acoustic profiles are found in the Appendix section of this thesis

Table 3.4: Minimum mixing required to reach stable mixtures for different trials horizontally loaded in the V-blender and their loading order

Trial	Size cuts	Loading order	Loading configuration	Minimum mixing (revolutions)
I	Cut#1 and Cut#4	Cut#1 on top and Cut#4 on bottom	Horizontal loading	Trial 1: 27 Trial 2: 27 Trial 3: 25 Average: 26
II	Cut#1 and Cut#4	Cut#1 on bottom and Cut#4 on top	Horizontal loading	Trial 1: 24 Trial 2: 19 Trial 3: 23 Average: 22
III	Cut#1 and Cut#3	Cut#1 on top and Cut#3 on bottom	Horizontal loading	Trial 1: 29 Trial 2: 29 Trial 3: 28 Average: 29
IV	Cut#1 and Cut#3	Cut#1 on bottom and Cut#3 on top	Horizontal loading	Trial 1: 21 Trial 2: 17 Trial 3: 19 Average: 19
V	Cut#2A and Cut#4	Cut#2A on top and Cut#4 on bottom	Horizontal loading	Trial 1: 22 Trial 2: 18 Trial 3: 21 Average: 20
VI	Cut#2A and Cut#4	Cut#2A on bottom and Cut#4 on top	Horizontal loading	Trial 1: 15 Trial 2: 11 Trial 3: 14 Average: 13
VII	Cut#2B and Cut#4	Cut#2B on top and Cut#4 on bottom	Horizontal loading	Trial 1: 16 Trial 2: 16 Trial 3: 17 Average: 16
VIII	Cut#2B and Cut#4	Cut#2B on bottom and Cut#4 on top	Horizontal loading	Trial 1: 26 Trial 2: 23 Trial 3: 23 Average: 24
IX	Cut#2A and Cut#3	Cut#2A on top and Cut#3 on bottom	Horizontal loading	Trial 1: 14 Trial 2: 13 Trial 3: 12 Average: 13
X	Cut#2A and Cut#3	Cut#2A on bottom and Cut#3 on top	Horizontal loading	Trial 1: 17 Trial 2: 15 Trial 3: 17 Average: 16

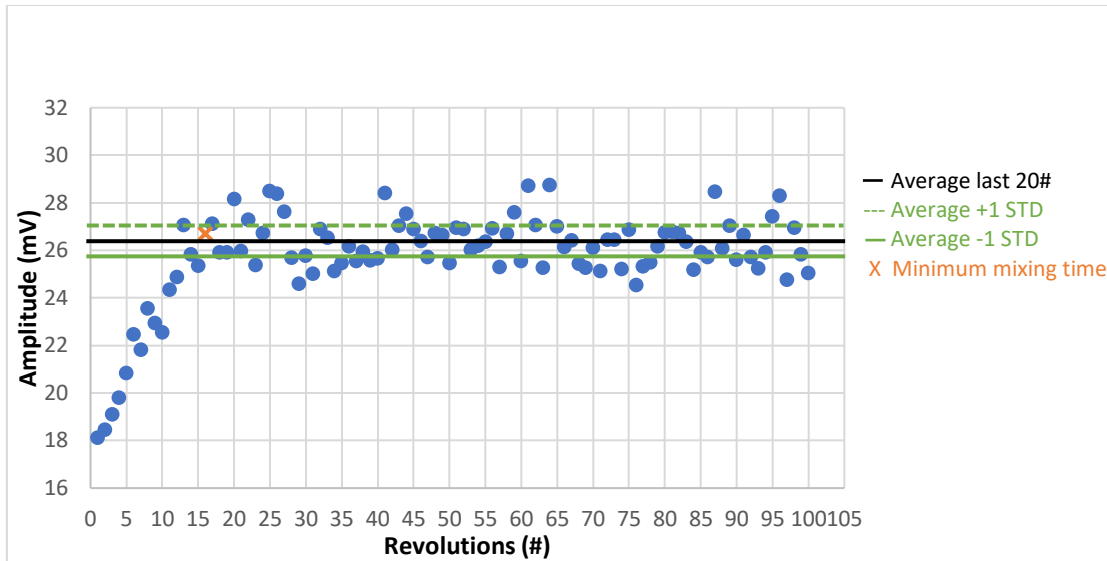


Figure 3.10: Calculation of the minimum mixing time needed to reach a stable mixture using +/- 1 STD

Calculations were based on the last 20 V-shell revolutions with Cut#2A and Cut#3 binary mixture used where Cut#3 was loaded on top

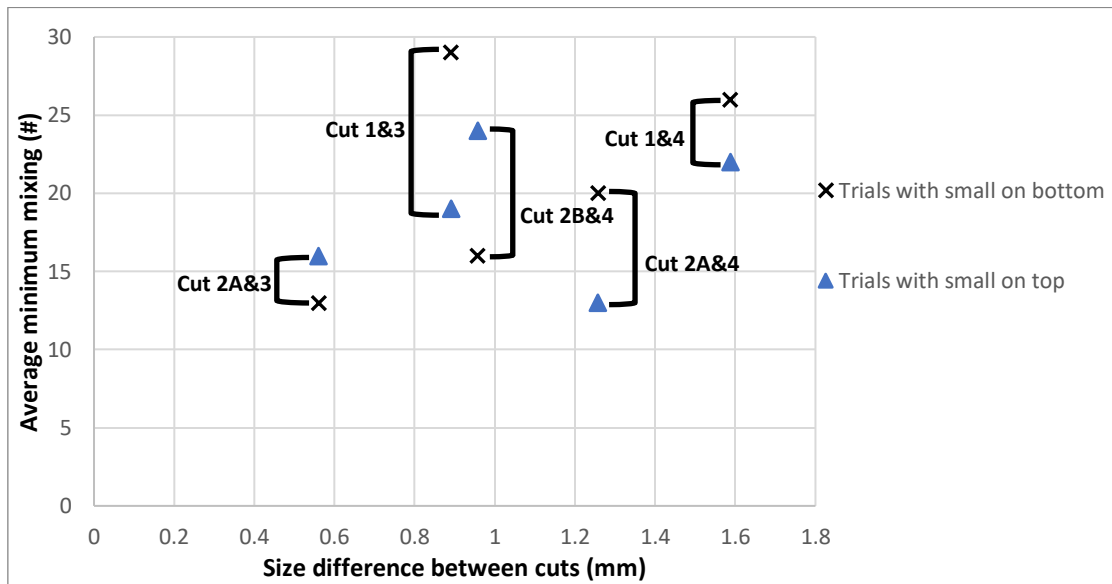


Figure 3.11: Average minimum mixing time in revolutions for horizontal loading trials vs size difference between cuts in millimeters

3.3.3 Vertical Loading Configuration

Starch granule size fraction cuts were vertically loaded into the V-blender and tumbled in a 50-50% at 25% fill level by mass ratio. Rotations of the V-shell allowed for mixing

of particles and segregation patterns were photographed. Larger differences in fraction sizes resulted in more segregation as observed with horizontal loading trials. The results were confirmed by photos and sieving data, indicating that segregation increased with larger differences in fraction size combination mixtures.

Figure 3.12 shows segregation levels every 10 revolutions between two size fraction combination mixtures having large differences in their diameter sizes, Cut#1(2.00 – 2.36 mm) and Cut#4 (0.006 – 1.18 mm). In Figure 3.12 column A, the larger dyed starch granules of Cut#1 were loaded in the inner arm of the V-shell and the smaller undyed starch granules of Cut#4 were loaded in the outer arm. The photos and sieving data confirm that the larger dyed granules segregated towards the inner arm of the V-shell, while smaller undyed granules segregated towards the outer arm. Figure 3.12 column B shows another trial with same size fraction combination mixtures but with opposite loading order, where larger dyed starch granules of Cut#1 were loaded in the outer arm of the V-shell and the smaller undyed starch granules of Cut#4 were loaded in the inner arm. Similar segregation patterns were observed, and the results were confirmed by visual observations and sieving data.

Figure 3.13 shows segregation levels every 10 revolutions of very close two-size fraction mixtures with small differences in their diameter sizes, Cut#2A (1.70 – 2.00 mm) and Cut#3 (1.18 – 1.40 mm). In Figure 3.13 column A, the larger dyed starch granules of Cut#2A were loaded in the inner arm of the V-shell and the smaller undyed starch granules of Cut#3 were loaded in the outer arm. Figure 3.13 column B shows another trial with same size fraction combination mixtures but with opposite loading order, where larger dyed starch granules of Cut#2A were loaded in the outer V-shell arm and the smaller undyed starch granules of Cut#3 were loaded in the inner arm. The photos, sieving data, and visual observations showed and confirmed that the segregation pattern developed for both trials was similar as seen with trials in Figure 3.12. The left-right segregation pattern was observed in all vertical loading trials which complemented and confirmed findings from horizontal loading trials. Vertical loading trials continued for 100 revolutions and showed that the left-right segregation pattern remained stable with no changes.

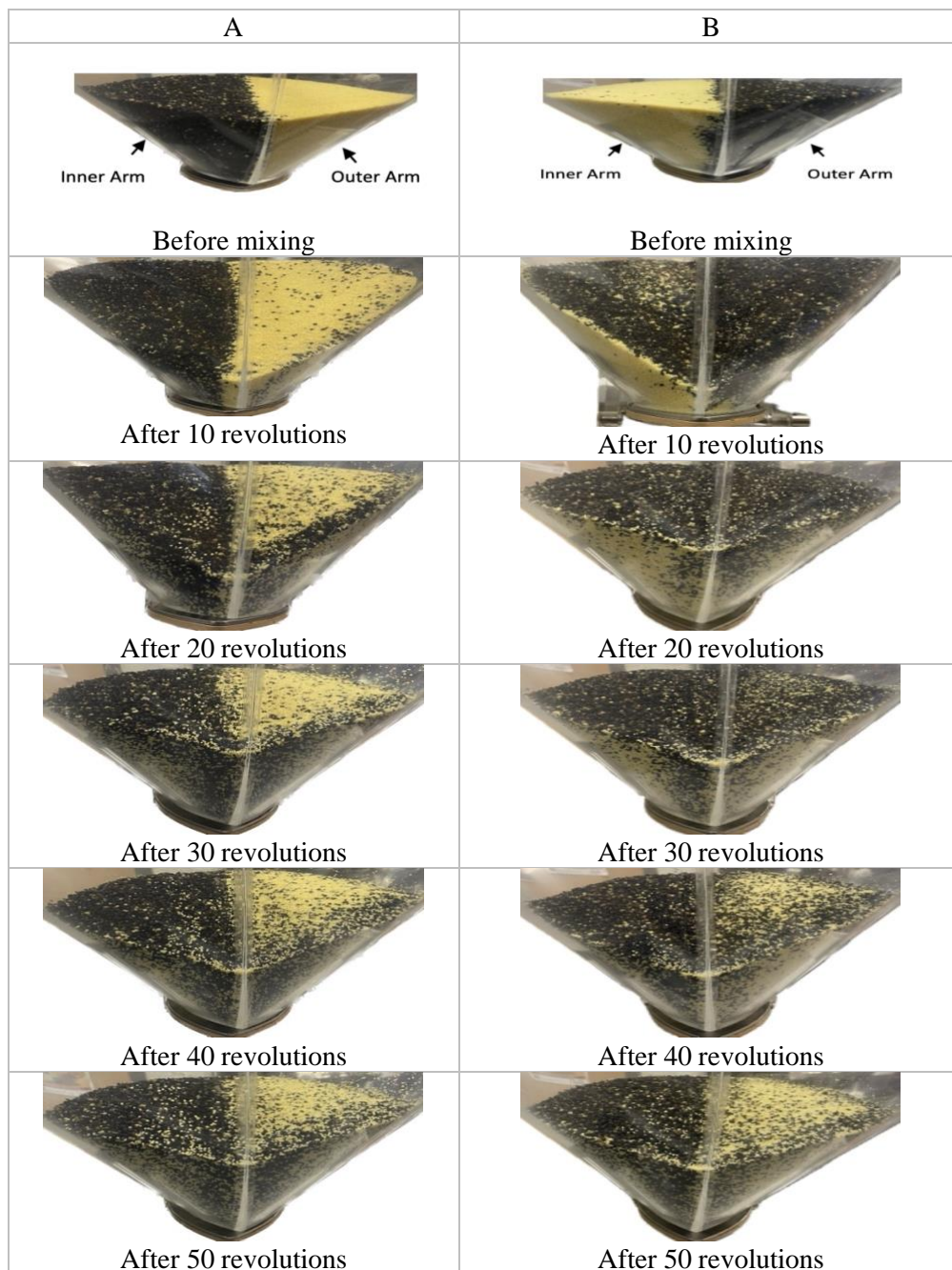


Figure 3.12: Visual observation of Cut#1 and Cut#4 binary mixtures vertically loaded in the V-blender

Mixtures were in a 50-50% by mass ratio, Column A: Cuts 1 and 4, where dyed Cut#1 (black) loaded in inner arm and undyed Cut#4 (yellow) in outer arm and Column B: Cuts 1 and 4, where dyed Cut#1 (black) loaded in outer arm and undyed Cut#4 (yellow) in inner arm

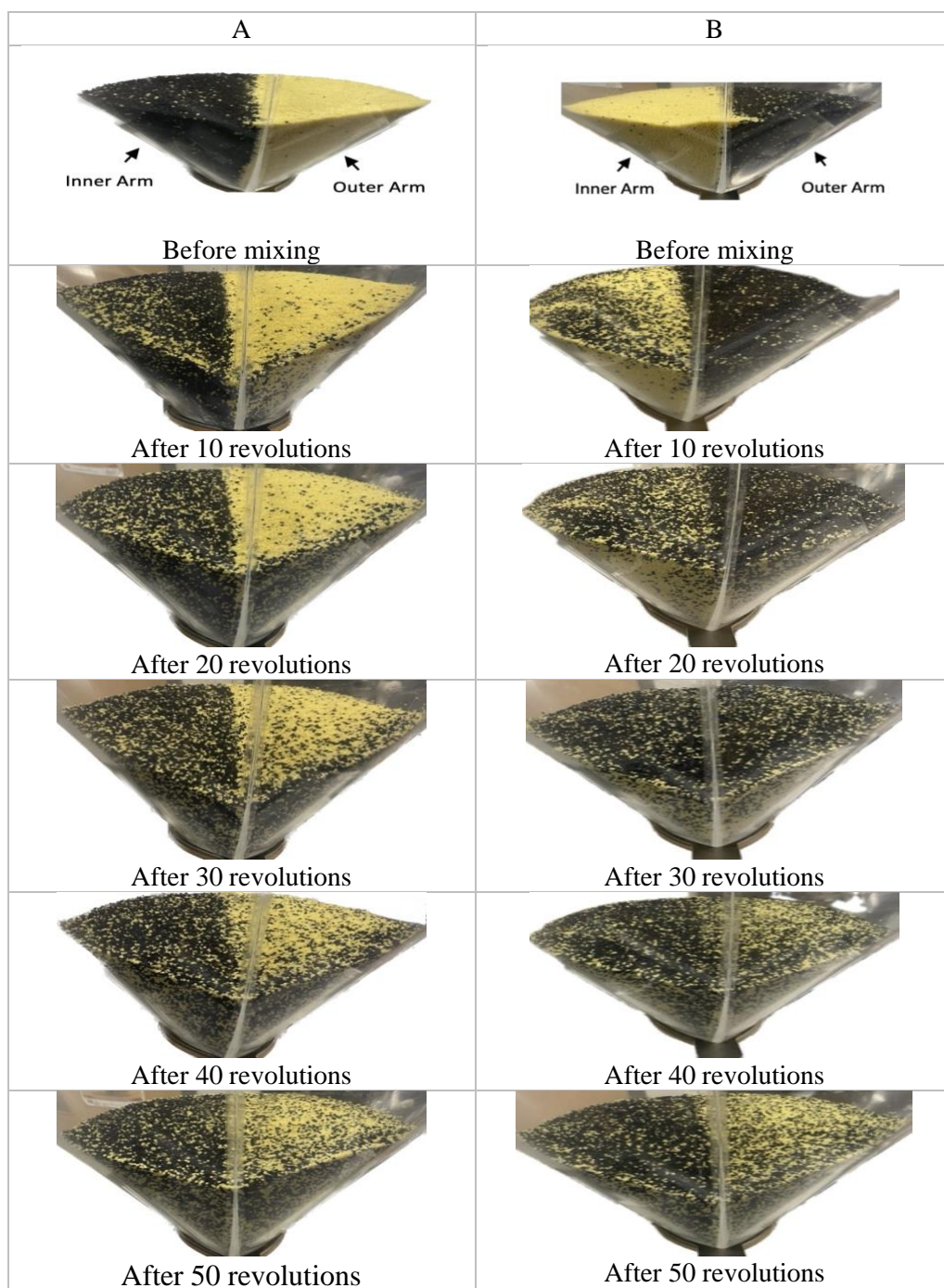


Figure 3.13: Visual observation of Cut#2A and Cut#3 binary mixtures vertically loaded in the V-blender

Mixtures were in a 50-50% by mass ratio, Column A: Cuts 2A and 3, where dyed Cut#2A (black) loaded in inner arm and undyed Cut#3 (yellow) in outer arm and Column B: Cuts 2A and 3, where dyed Cut#2A (black) loaded in outer arm and undyed Cut#3 (yellow) in inner arm

Sieving of the mixtures was completed for both V-shell arms using the same procedure performed as for horizontal loading trials. The sieving results confirmed the visual observations shown in Figures 3.12 and 3.13. Table 3.5 shows the sieving results for different starch granule mixtures when loaded in a vertical configuration pattern in the V-blender. Table 3.5 shows only sieving results for the trials conducted for the largest and smallest combination mixtures, Cut#1 and Cut#4 and Cut#2A and Cut#3 binary mixtures, respectively. All other sieving data for remaining size fraction combination mixtures are reported in the Appendix section of this thesis.

Table 3.5: Sieving data in the outer arm of the V-shell for different trials

Trial	Size cuts	Loading order	Loading configuration	Sieving results in outer arm (%)
A	Cut#1 and Cut#4	Cut#1 in inner arm and Cut#4 in outer arm	Vertical loading	Trial 1: Cut#4 (64), Cut#1 (36) Trial 2: Cut#4 (62), Cut#1 (38) Trial 3: Cut#4 (63), Cut#1 (37) Average: Cut#4 (63), Cut#1(37)
B	Cut#1 and Cut#4	Cut#1 in outer arm and Cut#4 in inner arm	Vertical loading	Trial 1: Cut#4 (67), Cut#1 (33) Trial 2: Cut#4 (64), Cut#1 (36) Trial 3: Cut#4 (63), Cut#1 (37) Average: Cut#4 (64), Cut#4 (36)
C	Cut#2A and Cut#3	Cut#2A in inner arm and Cut#3 in outer arm	Vertical loading	Trial 1: Cut#3 (59), Cut#2A (41) Trial 2: Cut#3 (58), Cut#2A (42) Trial 3: Cut#3 (58), Cut#2A (42) Average: Cut#3 (58), Cut#2A (42)
D	Cut#2A and Cut#3	Cut#2A in outer arm and Cut#3 in inner arm	Vertical loading	Trial 1: Cut#3 (58), Cut#2A (42) Trial 2: Cut#3 (59), Cut#2A (41) Trial 3: Cut#3 (61), Cut#2A (39) Average: Cut#3 (59), Cut#2A (41)

The vibration amplitude profiles of starch granule size fractions were recorded. All trials were conducted with 50-50% by mass ratio of binary mixtures of each size fraction and were loaded in a vertical configuration in the V-blender. Figure 3.14 shows the vibration amplitude profiles of the largest and the smallest starch granule size fractions of Cut#1 and Cut#4 with their binary mixtures, respectively. When Cut#1 was loaded in the inner arm and Cut#4 in the outer arm, the initial mixture vibration amplitude recorded was around 16 mV which was similar to the amplitude of the small size fraction of Cut#4. The vibration amplitude then increased to around 26 mV after

about 30 revolutions before decreasing to 25 mV at about 100 revolutions while maintaining the amplitude in the zone of 25 – 30 mV after reaching a stable mixture. When Cut#4 was loaded in the inner arm and Cut#1 in the outer arm, the initial mixture vibration amplitude recorded was around 46 mV which was similar to the amplitude of the large size fraction of Cut#1. The vibration amplitude then decreased to around 26 mV after about 35 revolutions before increasing to 29 mV at about 100 revolutions while maintaining the amplitude in the zone of 25 – 30 mV after reaching a stable mixture.

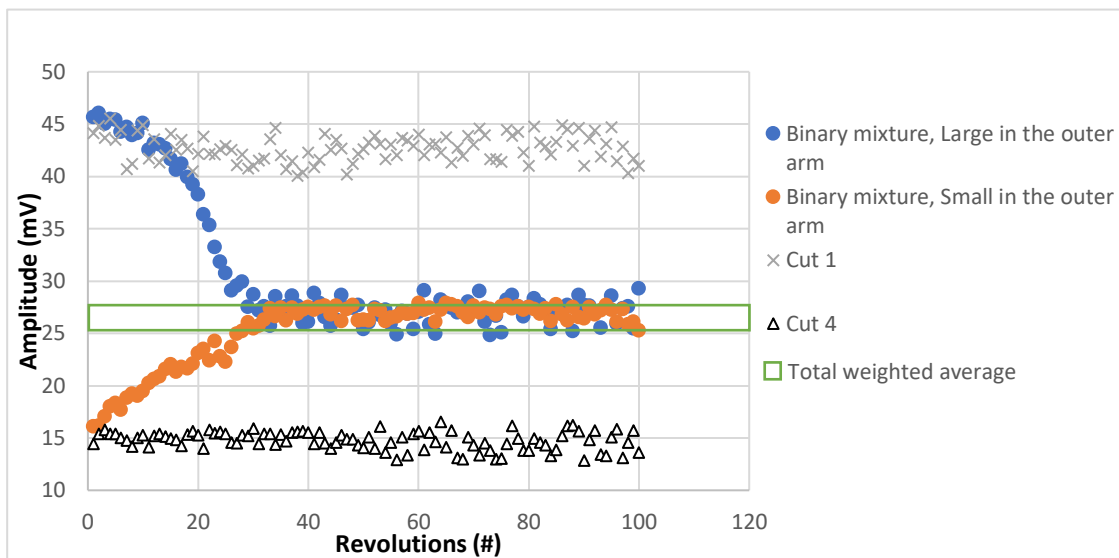


Figure 3.14: Acoustic profile of combined trials of Cut#1 (2.00 – 2.36 mm) and Cut#4 (0.006 – 1.18 mm)

Mixtures were in a 50-50% by mass ratio and were loaded vertically in the V-blender

Figure 3.15 shows the vibration amplitude profiles of two very closely sized starch granule size fractions and their binary mixtures, Cut#2A and Cut#3. When Cut#2A was loaded in the inner arm and Cut#3 in the outer arm, the initial mixture vibration amplitude was around 19 mV which was similar to the amplitude of the small size fraction of Cut#3. The vibration amplitude then increased to around 26 mV after about 40 revolutions before decreasing to 23 mV at about 100 revolutions while maintaining the amplitude in the zone of 20 – 27 after reaching a stable mixture. When Cut#3 was loaded in the inner arm and Cut#2A in the outer arm, the initial mixture vibration

amplitude was around 31 mV which was similar to the amplitude of the large size fraction of Cut#2A. The vibration amplitude then decreased to around 25 mV after about 35 revolutions before increasing to 28 mV at about 100 revolutions while maintaining the amplitude in the zone of 25 – 30 mV after reaching a stable mixture.

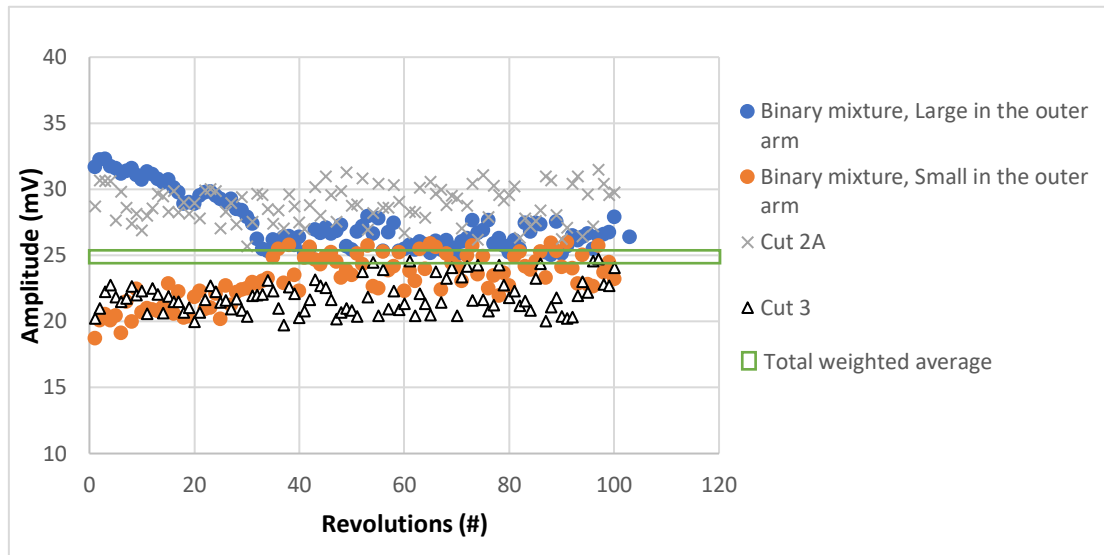


Figure 3.15: Acoustic profile of combined trials of Cut#2A (1.70 – 2.00 mm) and Cut#3 (1.18 – 1.40 mm)

Mixtures were a in 50-50% by mass ratio and were loaded vertically in the V-blender

The weighted average was determined based on the percentage of small and large particles in the outer V-shell arm of the V-blender after 100 revolutions. This was done using the same procedure performed for horizontal loading trials as well as identifying stable mixtures and the minimum mixing times for vertical loading trials. Table 3.6 shows the minimum mixing required for each size fraction mixture. Figure 3.16 shows the average minimum mixing for mixtures loaded vertically in the V-blender versus the size difference between different cuts. There is no significant trend observed with different size fraction binary mixtures as seen with horizontal loading trials. Binary mixtures of Cut#1 and Cut#4 and Cut#2A and Cut#3 are the main trials reported with their profiles as they have the biggest and smallest size differences between the two cuts, respectively. Other experimental trials were completed using different starch

granule size fraction mixtures with similar results observed. The acoustic vibration profiles for these trials are found in the Appendix section of this thesis.

Table 3.6: Minimum mixing required to reach stable mixtures for different trials vertically loaded in the V-blender and their loading order

Trial	Size cuts	Loading order	Loading configuration	Minimum mixing (revolutions)
A	Cut#1 and Cut#4	Cut#1 in inner arm and Cut#4 in outer arm	Vertical loading	Trial 1: 33 Trial 2: 34 Trial 3: 35 Average: 34
B	Cut#1 and Cut#4	Cut#1 in outer arm and Cut#4 in inner arm	Vertical loading	Trial 1: 29 Trial 2: 35 Trial 3: 30 Average: 31
C	Cut#1 and Cut#3	Cut#1 in inner arm and Cut#3 in outer arm	Vertical loading	Trial 1: 35 Trial 2: 37 Trial 3: 31 Average: 34
D	Cut#1 and Cut#3	Cut#1 in outer arm and Cut#3 in inner arm	Vertical loading	Trial 1: 33 Trial 2: 35 Trial 3: 32 Average: 33
E	Cut#2A and Cut#4	Cut#2A in inner arm and Cut#4 in outer arm	Vertical loading	Trial 1: 39 Trial 2: 37 Trial 3: 35 Average: 37
F	Cut#2A and Cut#4	Cut#2A in outer arm and Cut#4 in inner arm	Vertical loading	Trial 1: 41 Trial 2: 41 Trial 3: 40 Average: 41
G	Cut#2B and Cut#4	Cut#2B in inner arm and Cut#4 in outer arm	Vertical loading	Trial 1: 38 Trial 2: 36 Trial 3: 39 Average: 38
H	Cut#2B and Cut#4	Cut#2B in outer arm and Cut#4 in inner arm	Vertical loading	Trial 1: 32 Trial 2: 37 Trial 3: 33 Average: 34
I	Cut#2A and Cut#3	Cut#2A in inner arm and Cut#3 in outer arm	Vertical loading	Trial 1: 42 Trial 2: 39 Trial 3: 36 Average: 39
J	Cut#2A and Cut#3	Cut#2A in outer arm and Cut#3 in inner arm	Vertical loading	Trial 1: 34 Trial 2: 34 Trial 3: 33 Average: 34

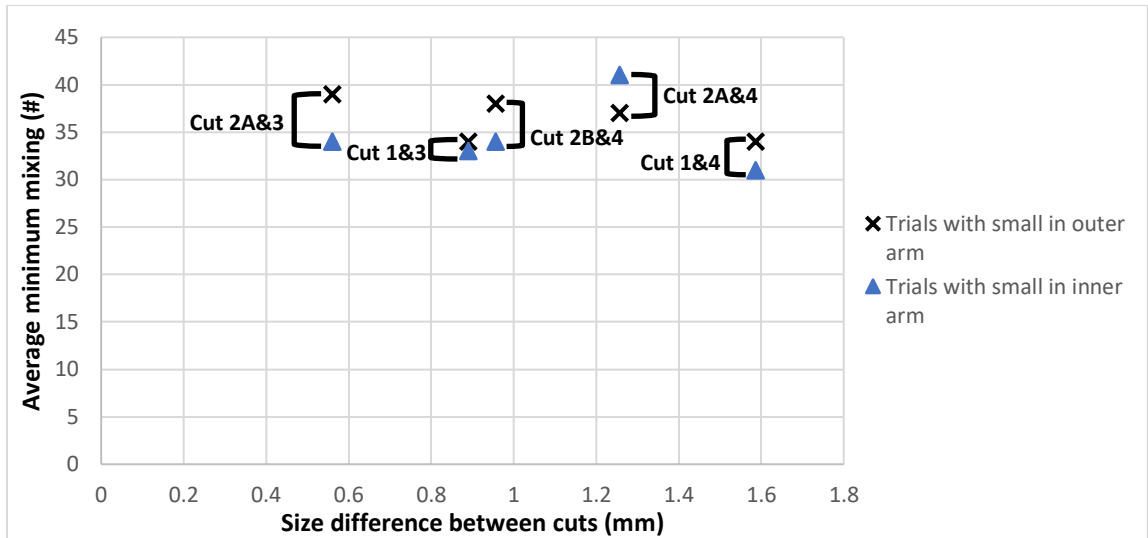


Figure 3.16: Average minimum mixing in revolutions for vertical loading trials vs size difference between cuts in millimeters

Figure 3.17 shows both horizontal and vertical loading trials for starch granules binary mixture of Cut#1 and Cut#4 plotted on the same graph and how the loading pattern affects the acoustic vibrations. The mixing profiles were similar for the different loading patterns. For both loadings, the amplitudes were initially similar to Cut#4 and then increased to a plateau of about 27 mV and remained constant around this value. The rate of increase varied with the loading pattern with the horizontal loading reaching the plateau faster than the vertical loading trial. Figure 3.18 also shows the trials for starch granules binary mixture of Cut#1 and Cut#4 but in opposite loadings. The mixing profiles were again similar for the different loading patterns. Both started at amplitudes similar to Cut#1 and then decreased to a plateau. The plateau values were slightly higher in the range of 25 – 30 mV for the vertical loading compared to a range of 20 -25 mV for the horizontal loading trial.

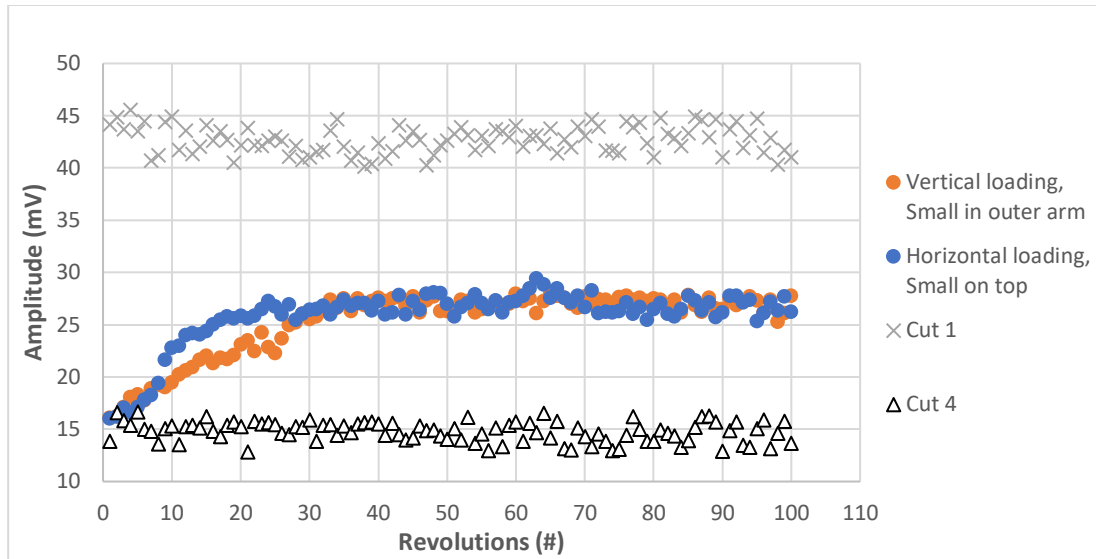


Figure 3.17: Horizontal versus vertical loadings of Cut#1 and Cut#4 binary mixture
 Mixtures were in a 50-50% ratio by mass at 25% fill level with Cut#4 loaded vertically in the outer arm and horizontally on top

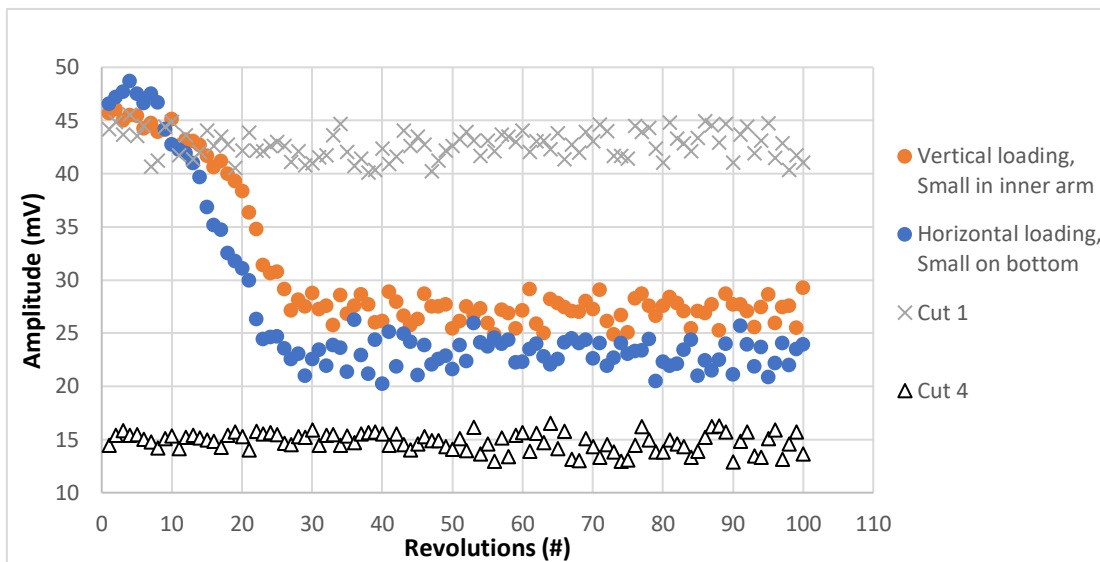


Figure 3.18: Vertical versus horizontal loadings of Cut#1 and Cut#4 binary mixture
 Mixtures were in a 50-50% ratio by mass at 25% fill level with Cut#4 loaded vertically in the inner arm and horizontally on bottom

Figure 3.19 shows both horizontal and vertical loading experimental trials for starch granules binary mixture of Cut#2A and Cut#3 plotted on the same graph. Those two cuts are very close in size and measured vibration amplitudes. Figure 3.19 shows the horizontal loading configuration when Cut#3 was loaded on top of Cut#2A while the vertical loading configuration was completed when Cut#3 was loaded in the outer arm and Cut#2A in the inner arm. Figure 3.20 shows another trial for the same starch granule size cuts but in opposite loadings. In the horizontal loading configuration, Cut#2A was loaded on top of Cut#3 while the vertical loading configuration was completed when Cut#2A was loaded in the outer arm and Cut#3 in the inner arm. For both loading patterns, the vibration amplitudes were initially similar to one of the individual sizes cut fractions of Cut#3 in Figure 3.19 and Cut#2A in Figure 3.20. The signals then changed and reached a plateau. As the differences in sizes are small and the range of vibration amplitudes is small as well, it is challenging to identify the minimum mixing times reliably and accurately, especially for the vertical loading trials. It appears that the horizontal loading may still reach a stable mixture with fewer revolutions of the V-shell.

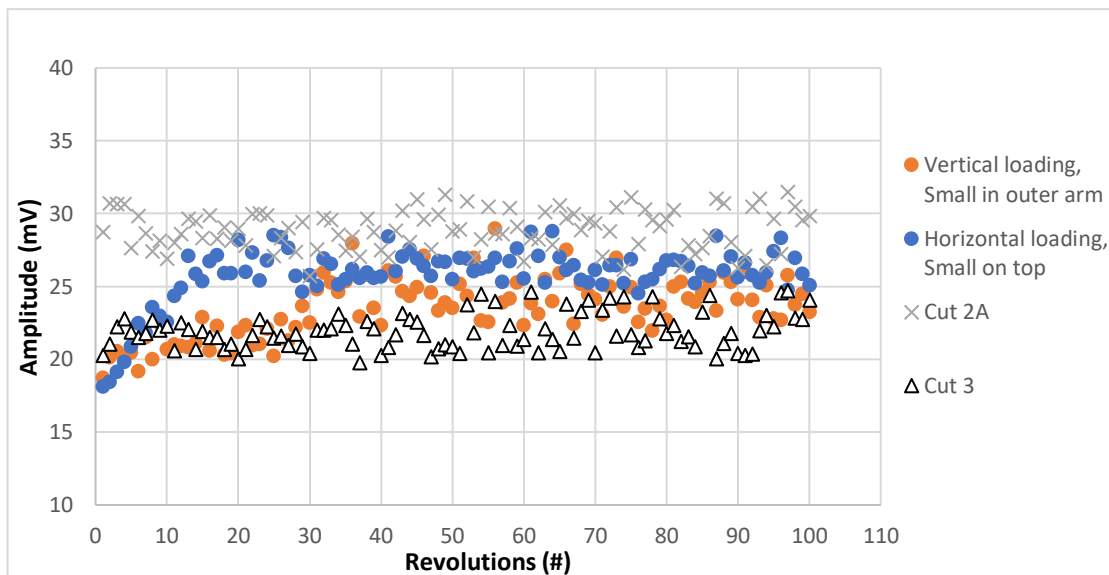


Figure 3.19: Horizontal versus vertical loadings of Cut#2A and Cut#3 binary mixture
 Mixtures were in a 50-50% ratio by mass at 25% fill level with Cut#3 loaded vertically in the outer arm and horizontally on top

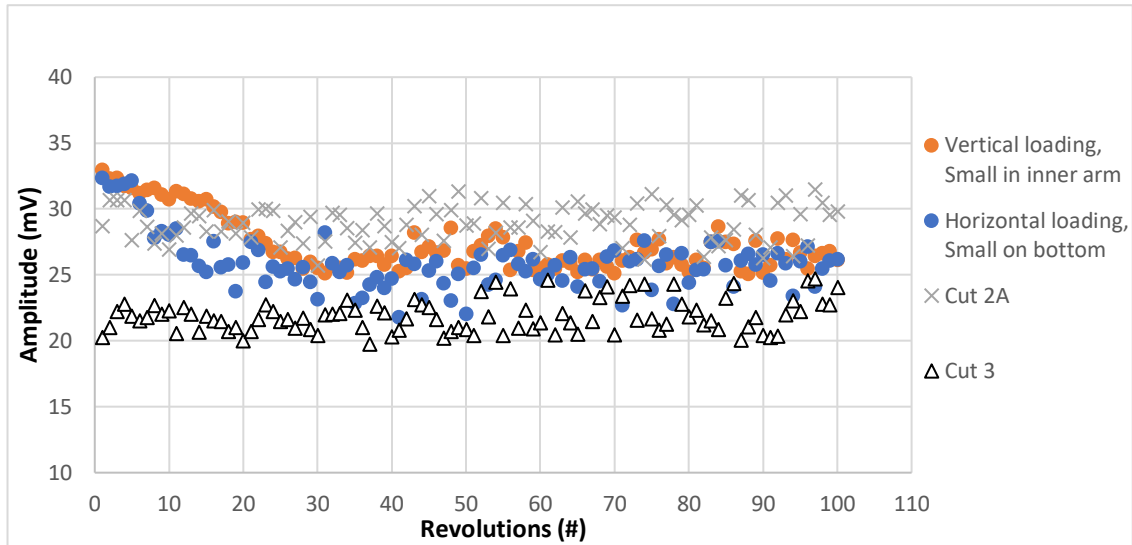


Figure 3.20: Vertical versus horizontal loadings of Cut#2A and Cut#3 binary mixture
 Mixtures were in a 50-50% ratio by mass at 25% fill level with Cut#3 loaded vertically in the inner arm and horizontally on bottom

It appears that mixtures used with horizontal loading configuration started to mix and reach stable mixtures faster than mixtures used with vertical loading with fewer revolutions of the V-shell as seen in Table 3.7. Also, Figure 3.21 shows a graph with the average minimum mixing time plotted versus the size difference between cuts for both horizontal and vertical loading configurations. There is no significant trend observed with different size fraction binary mixtures with the loading order. All vertical loading trials in blue needed more time to mix and reach stable mixtures compared to horizontal loading trials in black and the average minimum mixing in revolutions for vertical loading trials was higher than for horizontal loading trials.

Table 3.7: Vertical versus horizontal loading trials and their average minimum mixing in revolutions required to reach stable mixtures

Size fractions	Vertical loading order	Average minimum mixing for vertical loading	Horizontal loading order	Average minimum mixing for horizontal loading
Cut#1 and Cut#4	Cut#1 in inner arm	34	Cut#1 on top	26
Cut#1 and Cut#4	Cut#1 in outer arm	31	Cut#1 on bottom	22
Cut#1 and Cut#3	Cut#1 in inner arm	34	Cut#1 on top	29
Cut#1 and Cut#3	Cut#1 in outer arm	33	Cut#1 on bottom	19
Cut#2A and Cut#4	Cut#2A in inner arm	37	Cut#2A on top	20
Cut#2A and Cut#4	Cut#2A in outer arm	41	Cut#2A on bottom	13
Cut#2B and Cut#4	Cut#2B in inner arm	38	Cut#2B on top	16
Cut#2B and Cut#4	Cut#2B in outer arm	34	Cut#2B on bottom	24
Cut#2A and Cut#3	Cut#2A in inner arm	39	Cut#2A on top	13
Cut#2A and Cut#3	Cut#2A in outer arm	34	Cut#2A on bottom	16

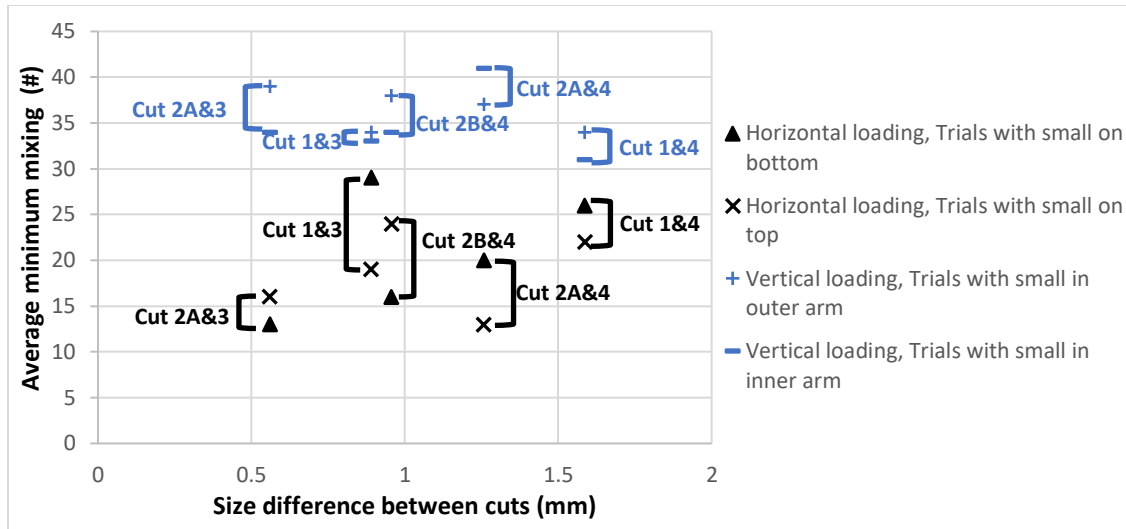


Figure 3.21: Average minimum mixing time in revolutions for horizontal and vertical loading trials vs size difference between cuts in millimeters

3.3.4 Intensifier Bar Addition

Trials with Cut#1 and Cut#4 binary mixture loaded horizontally in the V-shell were conducted with two intensifier bar additions (Figure 3.22). After 50 revolutions, the content of each arm was unloaded and sieved to measure any segregation developed. The results are provided in Table 3.8 along with the corresponding data provided from Table 3.3 for the trials without intensifier bar additions. Sieving of the mixtures was completed in the same procedure performed for horizontal and vertical loading trials. The sieving results shown in Table 3.8 suggest that the intensifier bar additions may decrease segregation development for the starch granules particles and tested conditions.

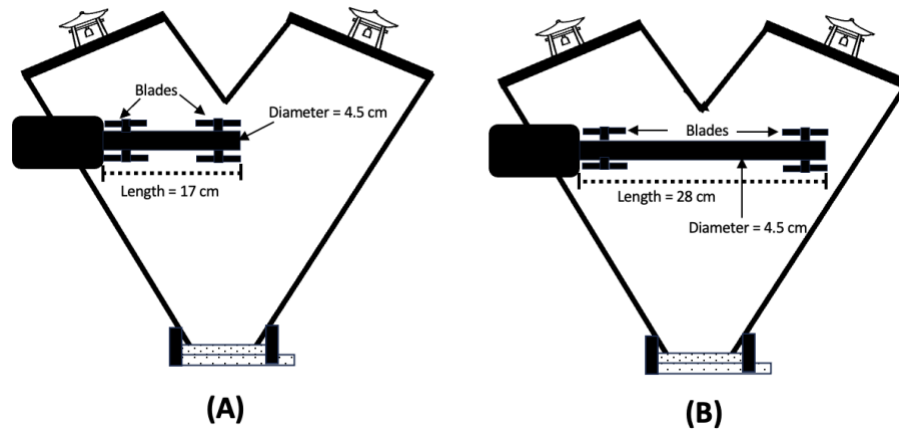


Figure 3.22: (A) Small and (B) large intensifier bar additions with their dimensions

Table 3.8: Sieving results of Cut#1 and Cut#4 binary mixture loaded horizontally in the V-blender with and without intensifier bar additions

Size cuts	Loading order	Intensifier bar	Sieving results in outer arm for trial 1 (%)	Sieving results in outer arm for trial 2 (%)	Sieving results in outer arm for trial 3 (%)	Average sieving results in outer arm (%)
Cut#1 and Cut#4	Cut#1 on top	Small bar	Cut#1: 39 Cut#4: 61	Cut#1: 40 Cut#4: 60	Cut#1: 38 Cut#4: 62	Cut#1: 39 Cut#4: 61
Cut#1 and Cut#4	Cut#4 on top	Small bar	Cut#1: 38 Cut#4: 62	Cut#1: 40 Cut#4: 60	Cut#1: 42 Cut#4: 58	Cut#1: 40 Cut#4: 60
Cut#1 and Cut#4	Cut#1 on top	Large bar	Cut#1: 42 Cut#4: 58	Cut#1: 40 Cut#4: 60	Cut#1: 40 Cut#4: 60	Cut#1: 41 Cut#4: 59
Cut#1 and Cut#4	Cut#4 on top	Large bar	Cut#1: 38 Cut#4: 62	Cut#1: 42 Cut#4: 58	Cut#1: 39 Cut#4: 61	Cut#1: 40 Cut#4: 60
Cut#1 and Cut#4	Cut#1 on top	None	Cut#1: 32 Cut#4: 68	Cut#1: 30 Cut#4: 70	Cut#1: 33 Cut#4: 67	Cut#1: 32 Cut#4: 68
Cut#1 and Cut#4	Cut#4 on top	None	Cut#1: 34 Cut#4: 66	Cut#1: 33 Cut#4: 67	Cut#1: 30 Cut#4: 70	Cut#1: 32 Cut#4: 68

3.4 Discussion

Particles in motion have kinetic energy when they collide with an object. Upon collision, some of the energy is retained by the particles while some energy is dissipated as stress waves. Stress waves are propagated from particle-particle and particle-wall collisions (29). In the V-blender, upon collision of the tested starch granules and glass beads with each other and with the V-shell, most of the energy was dissipated in the form of stress waves. Most of the energy dissipated as stress waves while other energy was retained by the particles. The stress waves were transmitted through the V-shell and the vibrations from these transmitted waves were measured using an accelerometer that was securely attached to the lid of the outer arm of the V-shell as shown in Figure 3.1-B.

The dissipated energy measured by the accelerometer depended on many factors. The dissipated energy is proportional to the kinetic energy of a particle upon collision and kinetic energy is dependent upon the mass and velocity of the particle. Figure 3.2 shows that the measured vibration amplitudes increased almost linearly with an increase in the mass of the glass beads. The largest measured vibration amplitudes also occurred with particles that had high velocities. These particles fell almost the entire height of the V-shell unimpeded before colliding with the V-shell lid and therefore had high velocities and kinetic energy. The measured vibration amplitudes from dissipated energy of starch granules collisions indicated the additional impact of particle shape (4). The measured amplitudes for the starch granules were lower (10 – 50 mV) than for the glass beads (150 – 450 mV). This was expected as the apparent density of the glass beads was close to twice the value of the starch granules (Table 3.1). Moreover, glass beads have higher recorded vibration amplitudes due to their uniform and spherical shape that retains more energy within the particles as well as glass beads have higher mass. More energy retained by the glass bead particles leads to more energy release in the system and more energy measured by the accelerometer as acoustic vibrations.

For the starch granules, however, there was a range of measured amplitudes for each size cut and an increasing slightly exponential trend was observed (Figure 3.3). Starch

granules were non-spherical with a measured sphericity of 0.70. Due to their irregular shape, starch granules may have spined and rolled during collision which would have resulted in less energy dissipated as stress waves to be measured by the accelerometer (79). The size distribution of starch granules led to a range of energies recorded at collision and therefore gives some fluctuations in amplitudes recorded (Figure 3.4). The properties of starch granules provided a range of measured vibration amplitudes for a given flow pattern within the V-shell. It is important to determine and identify the properties of the materials used as they can influence the recorded amplitude of acoustic emissions. These properties affect how particles respond to external forces and generate acoustic signals.

The dissipation of energy as particles collided with the V-shell walls depended on the angle of collision. Collisions with a surface normal to the particle trajectory allowed more dissipated energy as stress waves compared to collisions with an angled surface (31). Therefore, collisions with the V-shell lids dissipated more stress wave energy than collisions with the V-shell side walls. This difference was further enhanced by velocity; velocities of particles colliding with the lids could reach higher values compared to side collisions as possible unimpeded particle trajectories were longer. The vibration amplitudes measured by the accelerometer attached to the outer V-shell arm were affected by attenuation. The highest measured amplitudes were from direct particle collisions with the outer arm lid that is close to the accelerometer location as shown in Figure 3.1-B. Measured amplitudes from collisions with the wall of the V-shell arms were low due to the angle of collision and attenuation of the dissipated stress waves. Measured amplitudes from collisions with the bottom plate of the V-shell were very low due to the distance and attenuation through the rubber gasket attaching the plate to the V-shell (4).

“Left-right” segregation pattern was the main type of segregation seen to develop in the V-blender while mixing particles in this research. This pattern is characterized by the accumulation of higher amounts of the smaller particles in the outer V-shell arm and larger particles in the inner V-shell arm of the V-blender. This type of segregation is seen to develop while mixing particles of high inertia with other particles of low inertia.

As a result of inertia, particles with smaller size diameters tend to separate from particles with larger size diameters of the combined mixture. Particles that tend to have higher inertia will tend to follow a more straight-line trajectory, while particles with lower inertia will tend to follow a more curved trajectory. As a result, particles of different sizes may tend to separate into different regions in the V-blender, leading to uneven distribution and potential segregation. During mixing at initial rotations of the V-shell, the smaller particles with low inertia will tend to accumulate near the walls of the V-shell due to the friction, and the larger particles will accumulate near the base of the V-shell in the center due to the higher inertia. After some rotations, the opposite will happen with the larger and smaller particles switching places due to the force of inertia increasing leading to a decrease in the friction between the particles making the larger particles migrate near the walls of the V-shell and the smaller particles will accumulate at the center of the V-shell.

Dyed starch granules and a transparent acrylic V-shell allowed for visual observations of particle motion and identification of segregation. Figure 3.7 shows photos of the observations for two horizontal loadings, one with a large difference in the average size of the two components and the other one with a small size difference. For these and all other horizontal loading trials, left-right segregation pattern was observed by 50 revolutions and then remained stable for 50 more reaching 100 revolutions in total. Figures 3.12 and 3.13 also show that left-right segregation pattern also developed with vertical loading trials. This segregation of smaller particles in the outer arm of the V-shell even occurred when the smaller particles were loaded vertically into the inner V-shell arm. The extent of the segregation for both loading patterns was visually observed to be higher as the difference in size of the two components increased. The segregation did not appear to be significantly affected by the loading configuration; segregation was similar for both horizontal loading order and vertical loading sides. Visual observations, however, indicated that more revolutions of the V-shell were needed for the segregation pattern to develop with vertical loading compared to horizontal loading. Sieving of the particles in each of the V-shell arms after 100 revolutions confirmed the visually observed segregation. The sieving data for both horizontal and vertical loading

configurations were similar with minimal differences as shown in Table 3.3 for horizontal loading trials and Table 3.5 for vertical loading trials. For the large size difference between the two components of Cut#1 and Cut#4, 68% by mass of the smaller particles of Cut#4 segregated to the outer arm for horizontal loading for both loading orders when Cut#4 was loaded both on top and on bottom and 63% and 64% by mass of Cut#4 segregated to the outer arm for vertical loading trials when Cut#4 was loaded in the outer and inner arms, respectively. For the small size difference between the two components of Cut#2A and Cut#3, there was less segregation in the outer arm with 56% and 58% by mass of the smaller particles of Cut#3 when loaded horizontally on top and bottom respectively while segregation was seen with 58% and 59% by mass of Cut#3 when loaded vertically in the outer and inner arms, respectively. That is due to smaller size fractions having close size diameters making it challenging for particle separation in a mixture. Also, kinetic energy and forces such as rolling and sliding of particles are more noticeable with larger differences in particle size. Additionally, percolation effect was seen with mixtures with large differences in fraction size where smaller particles can roll and percolate through the interstitial spaces formed by larger particles, resulting in more separation of different-sized granules.

Experimental errors for the sieving can be present and variations of some data can be seen. Attrition of starch granules can be one of the factors for these variations. While starch granule particles rotate in the V-blender then sieved using the meshes, some particles may break and go down the holes of the mesh which eventually can result in incorrect particle size distribution in different meshes. Each mesh used has a size range that only allows specific particles with that size range to pass down through the holes. However, preliminary trials were conducted using a 100% by mass ratio of Cut#1 and the results showed that attrition was only 7% from the initial amount used.

In pharmaceutical production, segregation during tablet manufacturing must be avoided to ensure high product quality. Current sampling methods such as thief probes to identify segregation have challenges. Development of a method using passive acoustic emissions through vibration measurements to monitor powder mixing and identify segregation would provide significant manufacturing advantages. Figure 3.8 shows the

mixing profiles from the amplitudes for the horizontal loadings of two components with a large size difference, Cut#1 and Cut#4. Initially, the amplitudes were similar to those of the individual component that is loaded on the top. For the loading of the large component on the top, the amplitudes decreased as the V-shell was rotated until a plateau of 20 – 25 mV was reached. For the loading of the smaller component on the top, the amplitudes increased with the V-shell rotation until a plateau of 25 – 30 mV was reached. The horizontal mixing profiles reflected the flow pattern of particles within the tumbling V-shell and the measurement of the particle collisions with the lid on the outer V-shell arm.

As shown in the acoustic profiles of different binary mixtures of both horizontal loading (Figures 3.8 and 3.9) and vertical loading (Figures 3.14 and 3.15), the mixtures started out differently and the acoustic signals were different before the binary mixtures mixed and particles collided with each other and with V-shell walls. After the mixture plateaued around the weighted average, the acoustic signals recorded were very similar and the loading orders plateaued around similar regions. However, the binary mixtures were not identical and there will always be some variation between different binary mixtures even with the same size components. These variations can be in acoustic profiles generated, mixing speed, and reaching stable mixtures. This is because of the different loading order and configuration of the particles that contribute to some of the variations seen.

As shown in Figure 3.23-A, in the few initial rotations while the V-blender was rotating and mixing was happening, most of the particles on the top were the particles that collided with the V-shell lid and their energy was transmitted to the accelerometer and recorded before starting to trend towards the bottom particle's amplitude. After the initial few rotations and as the V-shell continued to rotate, the two components mixed such that particles collided with each other and with the V-shell. The measured vibration amplitudes either increased or decreased as the ratio of particles collided with the lid and their relative contributions to the measured amplitudes changed. Segregation eventually developed, and the amplitude value plateaued around the weighted average zone.

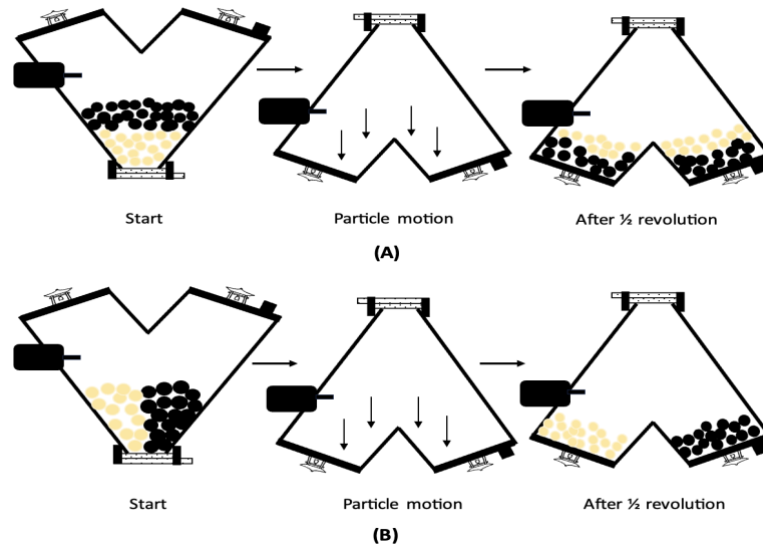


Figure 3.23: Schematic diagram for particle motion in the few initial rotations with (A) particles loaded horizontally and (B) particles loaded vertically in the V-blender

The vertical mixing profiles also reflected particle flow patterns and vibration measurements of particle collisions with the lid on the outer V-shell arm. As shown in Figure 3.14, for the vertical loadings of the two components with a large size difference, initially the measured average amplitudes corresponded to the amplitudes of the individual component loaded in the outer arm of the V-shell. For the first few revolutions of the V-shell, the particles that directly collided with the outer arm lid were the particles vertically loaded into the outer arm of the V-shell (Figure 3.23-B). As the particles mixed, the vibration amplitudes either increased or decreased as the ratio of particles colliding with the lids changed. The measured amplitude plateau of the vertical loading mixing profiles also identified segregation development.

The measured average amplitude of the stable mixture reflected the segregation of particles in the outer V-shell arm. For the combinations shown in Figure 3.8, an average of 68% by mass of the smaller particles segregated in the outer arm when the large component was loaded on top. The plateau of the vibration measurements reflected this: the plateau was near 23 – 25 mV range, closer to the measurements near 15 mV of the smaller particles. A uniform mixture with no segregation was expected to have an average measured amplitude of around 30 mV.

At around 20 revolutions, there is a high percolation potential that is associated with the horizontal loading order of smaller particles loaded on top of larger particles.

Percolation is seen when smaller particles fall through the gap spaces between larger particles (4). At the start of the mixing process when smaller particles are loaded on top of larger particles, percolation is seen to be high. When the V-shell tumbles and reaches its upright position, the smaller particles percolate through the larger particles, which then flow reaching the V-shell's bottom plate. When larger particles are loaded on top of smaller particles, percolation would only occur when the V-shell is in its inverted position. The mixture is separated into each arm when the V-shell reaches an inverted position and the smaller particle over larger particle areas would decrease the frequency of percolation to develop. The time required to reach a stable mixture is affected by the different flow of particles, particle characteristics, loading configuration, and order.

The mixing profiles shown in Figures 3.8 and 3.14 were for a binary mixture of components with a large size difference: Cut#1 had a range of 2.00 – 2.36 mm particle diameter with an average diameter of 2.18 mm and Cut#4 had a range of 0.006 – 1.18 mm with an average particle diameter of 0.59 mm (Table 3.1). As shown in Figure 3.3, there was a large difference of about 28 mV in measured average amplitudes between these two components. This large difference allowed for distinct mixing profiles with relatively easily identified transitions and plateaus reflecting stable mixtures. Mixing profiles for components with a small size difference are shown in Figures 3.9 and 3.15. The components were Cut#2A with a size diameter range of 1.70 – 2.00 mm and an average diameter of 1.85 mm and Cut#3 with a size range of 1.18 – 1.40 mm and an average diameter of 1.29 mm. Moreover, Cut#2A and Cut#3 binary mixture had an average size difference of 0.56 mm between the two size components (Table 3.1). The average amplitudes from these particles were 29 and 22 mV with an average difference in measured amplitudes between these two components of only 7 mV. These individual ranges were close and similar but did not overlap. The -1/+1 STD for the average vibration amplitudes recorded for Cut#2A and Cut#3 were about 6 mV and 9 mV, respectively. Considering the average amplitudes and STD values, the amplitudes were below 10 mV difference between the two components. However, these similar ranges

resulted in full profiles that relatively overlap with transitions and plateaus reflecting stable mixtures that were challenging to identify.

The very narrow diameter difference between Cut#2A and Cut#3 binary mixture along with the small amplitude difference makes the segregation and separation of starch granules particles while mixing in the V-blender a not easy and smooth process to happen as well as stable mixtures were seen to be challenging to reach and identify. Also, this can be due to the starch granules with close size differences may follow similar trajectories during mixing in the V-blender leading to fewer variations in the acoustic signals recorded. This can result in similar acoustic signals making it difficult to distinguish between the two size components. This can lead to overlapping acoustic profiles. Moreover, large particles have higher kinetic energy and may dominate the acoustic signals, overshadowing contributions from smaller particles. The measured vibrations of the mixture reaching a plateau can be seen, but it appears that detecting segregation and indicating a precise stable mixture appears not to be very distinct and challenging to determine for mixtures with very close size and amplitude differences. However, it was still possible to identify a stable mixture. It is hypothesized that very close size fraction mixtures with recorded amplitude and particle size differences less than 10 mV and 1.00 mm respectively appear not to be accurately and reliably monitored using passive acoustic emissions as a monitoring process analytical technology.

The amplitude and diameter difference between binary mixtures of Cut#2A and Cut#3 and Cut#2B and Cut#4 were less than 10 mV and 1.00 mm, respectively. That is why those mixture components show relative overlapping in their acoustic profiles and estimating stable mixtures was challenging to determine. This is also can be confirmed by acoustic profiles for larger size fraction components with amplitude and particle size differences of more than 10 mV and 1.00 mm, respectively. The acoustic profiles for these binary mixtures show no overlapping between loading orders and segregation was seen with stable mixtures that were relatively easily identified as shown in Figure 3.6 for Cut#1 and Cut#4 binary mixtures and the remaining acoustic profiles of binary

mixtures of Cut#1 and Cut#3 and Cut#2A and Cut#4 found in the Appendix section of this thesis.

The mixing profiles from the measured vibration amplitudes showed a transition to a plateau. This transition corresponded to the minimum number of V-shell revolutions required to reach a stable mixture. Figure 3.10 illustrates the procedure used to estimate this minimum mixing time in revolutions. A defined procedure helped to reduce visual bias estimates, especially for mixtures of components with small size differences. Figures 3.11 and 3.16 summarize the estimates for the horizontal and vertical loading trials, respectively. The minimum mixing time did not vary significantly as the size difference between the components changed. However, as shown in Figure 3.21, the required minimum number of revolutions to reach a stable mixture was higher for the vertical loadings than for the horizontal loadings.

The weighted average was determined based on the percentage of small and large particles in the outer V-shell arm after 100 revolutions. Sieving and weighing the particles in the outer arm was completed to get the percentage of large and small particles. The percentages found in the outer V-shell arm along with the average amplitude recorded of each size fraction were then used to determine an approximate weighted average value. For example, the weighted average was calculated for one trial as shown in Figure 3.8 for binary mixture of Cut#1 and Cut#4 as: (32%) of Cut#1 was found in the outer V-shell arm that was multiplied by (42.5 mV) which is Cut#1 average amplitude then summed up to Cut#4 percentage found in the outer arm (68%) that was multiplied by (15 mV) which is Cut#4 average amplitude to give the result as follows:

“(0.32 × 42.5) + (0.68 × 15) = 23.8 mV”. Figure 3.3 and Table 3.3 show the amplitude recorded for starch granule cuts and sieving results in the outer V-shell arm. This was done in triplicate for every combination mixture and plotted as an average on the graph. The weighted average matches the acoustic profiles for the combination mixtures and the zone was seen around where the mixture amplitudes for different loading orders plateaued.

The mixing rate depends on the particle flow patterns as the V-shell rotates. All the tested granules were confirmed to exhibit good flowability (4). Therefore, the minimum mixing time did not vary significantly with changes in the particle sizes. Particle motion within a V-shell occurs primarily in the vertical direction as shown schematically in Figure 3.24. Horizontal particle motion primarily occurs for only a small fraction of the particles moving across the axis of symmetry into the other arm of the V-shell as the V-shell rotates into the upright position. In this position, all of the particles flow into the restricted space at the bottom of the V-shell. For horizontal loadings, the particles were already distributed across the V-shell arms and mixing was only required vertically. For vertical loadings, horizontal particle motion was also required for mixing. As this particle motion was slower, minimum mixing times were slower for vertical loadings than for horizontal loadings. Cameron and Briens (2019) also showed that mixing of magnesium stearate into granules occurred faster when the lubricant was added across both arms compared to loading only into one arm (30).

Acoustics emission monitoring of mixing is dependent on differences in measured vibrations between the particles to be mixed. The mixing profiles were therefore easier to identify for the particles with a larger size difference and challenging for those close in size. This is also reflected in the reliability of identifying a minimum mixing time. To implement acoustic emission monitoring in powder mixing and segregation, it is recommended that the vibration amplitudes of each component are distinct as well as differences in diameter size are not similar.

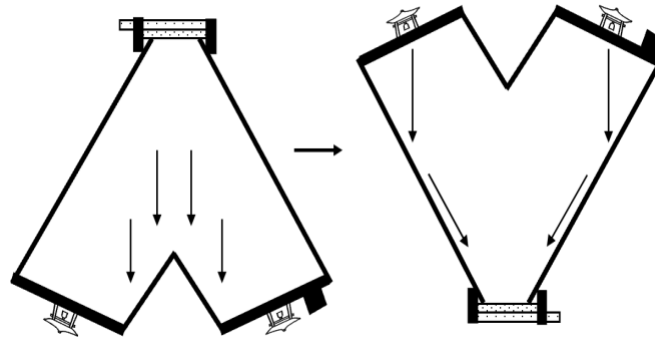


Figure 3.24: Schematic diagram for particle motion in the vertical direction of mixing in the V-blender

The “V” shape of the V-blender promotes the flow of particles as the blender rotates. This cascading motion allows for mixing by facilitating the movement of particles from the top to the bottom of the V-blender in a vertical direction as shown in Figure 3.24. Horizontal loading configuration where the particles were loaded in a pattern as shown in Figure 3.23-A where one size cut is loaded on top and the other one on bottom works in favour of how the V-blender operates and tumbles with mainly vertical mixing happening. Rotations then occurred where normally the V-blender tumbles and cascading motion works in a vertical direction, therefore enhancing the mixing process and mixtures can mix and reach stable mixture faster. Conversely, in vertical loading configuration, the particles are loaded in a pattern where one component is loaded in the outer arm and the other component in the inner arm of the V-shell (Figure 3.23-B). In this loading pattern, the rotation of the V-shell with mainly vertical mixing happening does not allow for faster mixing due to the nature of the V-blender operation and how it rotates which results in slower mixing time.

Stable mixtures were observed and identified in all trials for both horizontal and vertical loading configurations. A stable mixture is generally defined as the combination of substances that remain without changing their properties over a certain time under defined conditions. The minimum mixing time in revolutions was calculated based on the average, +1, and -1 STD for the last 20 revolutions of the V-shell. The first point to drop below the +1 STD or go above the -1 STD was set to be the minimum mixing time in revolutions needed to reach a stable mixture. Another way

was used to identify the minimum mixing time by getting the STD for the last 50 revolutions of the V-shell, but it resulted in a wider range of points across the acoustic profile for combination mixtures that led to less accurate estimations of stable mixtures as seen in Figure 3.25 with a minimum mixing time of 11 revolutions compared to a more accurate estimation in Figure 3.10 with a minimum mixing time of 17 revolutions for the same binary mixture of Cut#2A and Cut#3. Table 3.7 shows the average minimum mixing time in revolutions required for each size fraction mixture combination for both horizontal and vertical loading configurations.

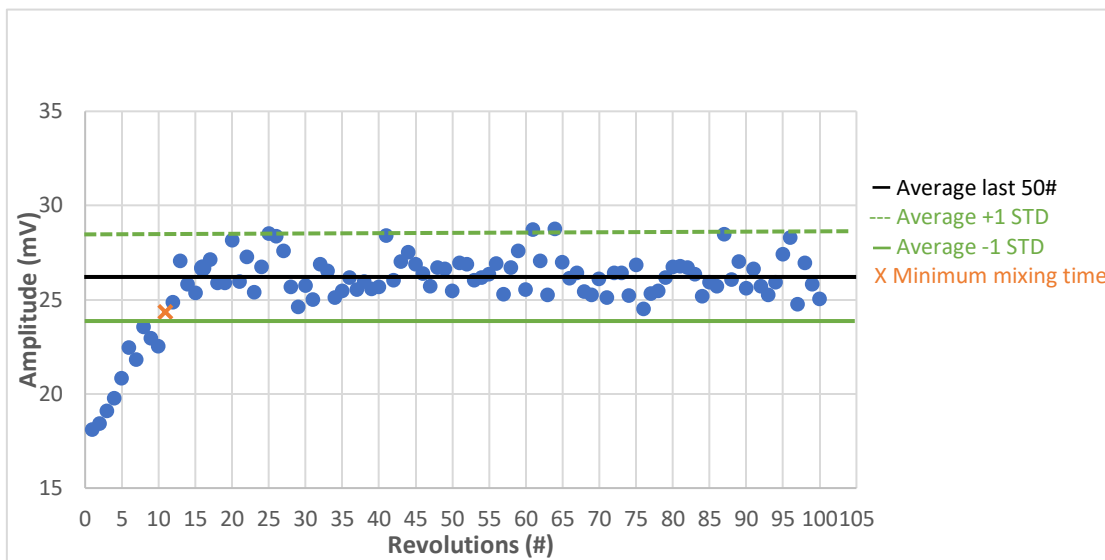


Figure 3.25: Estimation of minimum mixing time required in revolutions to reach a stable mixture for binary mixture of Cut#2A and Cut#3 using +/- 1 STD

Calculations of the minimum mixing time were based on the last 50 rotations of the V-shell

During rotation of the V-shell, segregation of particles that flow well, but have different sizes is primarily due to a trajectory segregation mechanism. As the V-shell rotates into an inverted position, the particles fall vertically into the inner and outer arms of the V-shell. The particles followed different trajectories based on their size with the smaller particles followed a curved flow path into the arms while the larger particles due to their higher inertia followed a more rectilinear trajectory and many collided near the joint and inner arms before flowing along the arms to impact the lids as shown in Figure 3.26-A.

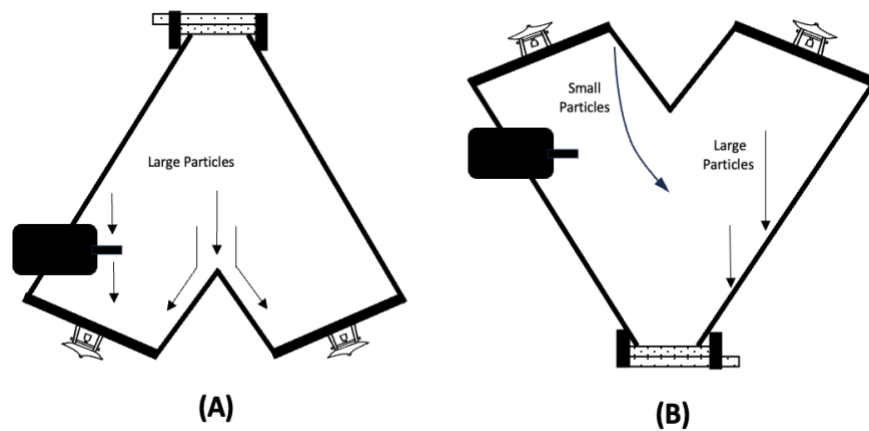


Figure 3.26: Schematic diagram showing particle trajectories based on size when (A) V-shell was inverted and (B) V-shell was in an upright position

Following inversion, only a small number of particles fall reaching nearly the full height of the V-shell to collide directly with the lids. Consequently, particles tend to accumulate along the inner arms and on the top of the lids, leading to increased collisions between particles rather than direct contact with the V-shell lids or walls. As the V-shell continues to rotate, particles flow across the lids to the outer walls and slide towards the bottom of the V-shell. The particles continue to slide, predominantly colliding with the lower walls and accumulating on the bottom plate. When the V-shell was rotated into an upright position, trajectory segregation forced the larger particles toward the outer walls while the small particles followed a more curvilinear flow toward the center of the V-shell as shown in Figure 3.26-B.

As the V-shell rotates from an inverted position back to its upright position, there are further different observed particle motions and measured vibration profiles. The particles flow along the outer wall arms towards the base of the V-shell. The particle velocities and energies are low as the particles continuously collide with each other and with the V-shell walls. The vibrations reaching the accelerometer on the lid have low amplitudes due to a combination of the low energies and tilted collisions with the walls and these energies decrease through the walls to the lid. The particles then fall towards the base of the V-shell and collide with the bottom plate and surrounding walls near the base of the V-shell. Recorded vibrations by the accelerometer are very low in amplitude

due to significant attenuation as the bottom plate is separate and attached through a rubber gasket and lock.

Percolation segregation occurs when smaller particles move downwards or percolate through the voids between the larger particles. When the V-shell was in the inverted position, the smaller particles percolated through the larger particles in each arm of the V-shell. Followed by percolation of the smaller particles near the center of the V-shell through the larger particles when the V-shell rotated back into an upright position reaching the V-shell base. Percolation segregation was more difficult to observe through the transparent acrylic V-shell and appeared to be not as significant relative to trajectory segregation. Trajectory segregation is the main driving force for left-right segregation pattern development. Trajectory and percolation mechanisms segregated the smaller particles towards the center of the V-shell and the larger particles towards the V-shell walls. This was partially observed for the particles with a large size difference. The primary segregation, however, was left-right with smaller particles segregated to the outer arm and larger particles to the inner arm. Therefore, there must have been another influence on the particle motion within the V-shell.

Figure 3.27-A shows the support arm protruding into the inner arm for rotating the V-shell. It is hypothesized that this support arm enhanced trajectory differences of the particles to promote the observed left-right segregation pattern of more larger particles in the inner V-shell arm. The support arm interfered with the motion of the particles as the particles fell vertically through the V-shell and as the particles flowed along the outer wall of the inner arm. During V-blender rotations, particles in the inner arm may collide with the projecting arm support. Because of the large inertia of the particles and the tendency to follow a straight-line flow pattern, larger particles would potentially collide more frequently with the arm support when compared to smaller particles. These collisions decrease the kinetic energy of the particles and therefore the particles are even more likely to travel in a straight-line pattern rather than in a curved pattern as shown in Figure 3.27-B. After many revolutions of the V-blender, the larger particles will start to accumulate in the inner arm leading to left-right segregation development.

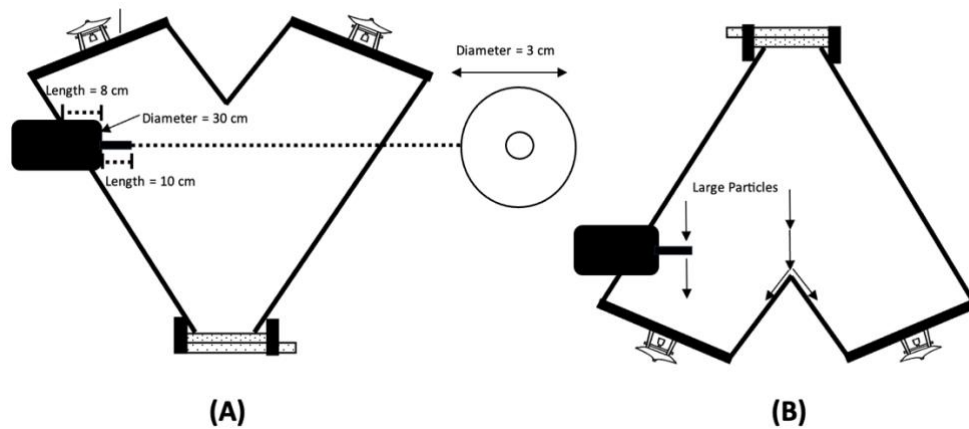


Figure 3.27: (A) Schematic diagram of the support arm protruding into the inner V-shell arm and (B) trajectory segregation of larger particles flow path inside the V-blender

To test the hypothesis that the support arm influenced left-right segregation development by interfering with vertical particle flow, two intensifier bars were added to the V-shell inner arm. One intensifier bar protruded 17 cm into the V-shell (Figure 3.22-A) while the other one protruded 28 cm (Figure 3.22-B). Therefore, the shorter intensifier bar spanned only one V-shell arm while the longer intensifier bar spanned both V-shell arms. The sieving results from these trials are provided in Table 3.8 and showed that the intensifier bars decreased left-right segregation slightly. The decrease in the percentages for both the small and larger particles in the outer arm was not very significant and the sieving results were close to the trials completed without the added intensifier bars as shown in Table 3.3. This means that the suggested hypothesis is not completely valid, and it appears that other factors are contributing to the left-right segregation development due to trajectory mechanism and the little support arm that projects slightly into the inner V-shell arm has an insignificant impact on left-right segregation development. Trials to test the hypothesis that the support arm interfered with flow along the wall were not developed and conducted. It is recommended that these trials be included in future work.

It is hypothesized that the reason for left-right segregation pattern development may be due to the centrifugal forces generated while the V-blender is rotating and how it may exert an influence on particle movement. These forces act radially outward from the

center of rotation, pushing particles toward the outer regions of the blender. With smaller particles being lighter and more susceptible to these forces, smaller particles tend to segregate towards the outer arm by the effect of these forces compared to the larger and heavier particles that end up with more amount in the inner arm. This is due to smaller particles having less resistance to the centrifugal forces, making them more easily pushed toward the outer arm of the V-shell. Also, the V-blender geometry and design with its sloping walls and angled arms, may contribute to the development of left-right segregation. The geometric configuration of the V-blender combined with its rotational motion, creates conditions that favor the development of left-right segregation during mixing.

3.5 Conclusions

Horizontal and vertical loading configurations were used with starch granules in the V-blender and the minimum mixing time in revolutions and stable mixtures was determined for each combination mixture. Horizontal loading configuration in the V-blender showed more promising results in terms of monitoring the mixing and segregation of starch granule particles. When compared to vertical loading configuration, horizontal loading configuration resulted in faster mixing of combination mixtures and stable mixtures were reached in fewer time or revolutions. Left-right segregation pattern was observed with both horizontal and vertical loading trials with smaller particles seen to segregate in the outer arm and the larger particles in the inner arm of the V-shell even with adding external intensifier bars attached to the inner arm of the V-shell.

Passive acoustic emissions are a potential PAT method for inline monitoring of multi-component powder mixtures. Passive acoustic emissions provide reliable particle flow process information that will allow for improved inline control and monitoring of mixing and segregation. Acoustics is a reliable method to be used in the pharmaceutical industry to investigate and monitor powder mixing and segregation. It has a lot of advantages such as its ease of use, low cost, inline monitoring, non-invasiveness, and non-destructiveness, and it does not require any further equipment modifications like other PATs. Passive acoustic emissions have some disadvantages such as the large

volume of data produced and the need for processing and space for storage. To implement acoustic emission monitoring in powder mixing and segregation, it is recommended that the vibration amplitudes of each component are distinct as well as differences in diameter size are not similar. It is also recommended to use particles of diameter size and amplitude differences of more than 1 mm and 10 mV, respectively. Also, a horizontal loading configuration of particles is recommended rather than a vertical loading configuration. This allows for better monitoring and identification of powder mixing and segregation. This research supports the potential of passive acoustic emissions in monitoring pharmaceutical powder mixing and segregation development.

3.6 References

1. G. Léonard, F. Bertrand, J. Chaouki, and P. M. Gosselin, “An experimental investigation of effusivity as an indicator of powder blend uniformity,” *Powder Technology*, vol. 181, no. 2, pp. 149–159, Feb. 2008, doi: <https://doi.org/10.1016/j.powtec.2006.12.007>.
2. N. Debotton and A. Dahan, “Applications of Polymers as Pharmaceutical Excipients in Solid Oral Dosage Forms,” *Medicinal Research Reviews*, vol. 37, no. 1, pp. 52–97, Aug. 2016, doi: <https://doi.org/10.1002/med.21403>.
3. J. Bridgwater, “Mixing of powders and granular materials by mechanical means—A perspective,” *Particuology*, vol. 10, no. 4, pp. 397–427, Aug. 2012, doi: <https://doi.org/10.1016/j.partic.2012.06.002>.
4. K. Wilson and L. Briens, “Investigation of passive acoustic emissions during powder mixing in a V-blender,” *Powder Technology*, vol. 408, pp. 117754–117754, Aug. 2022, doi: <https://doi.org/10.1016/j.powtec.2022.117754>.
5. Basel Alchikh-Sulaiman, Meysam Alian, Farhad Ein-Mozaffari, A. Lohi, and S. R. Upreti, “Using the discrete element method to assess the mixing of polydisperse solid particles in a rotary drum,” *Particuology*, vol. 25, pp. 133–142, Apr. 2016, doi: <https://doi.org/10.1016/j.partic.2015.05.006>.
6. K. Wilson, “Application of Passive Acoustic Emissions for Inline Monitoring of Segregation Prone Mixtures in a V-Blender.” Aug. 2022.
7. H. Buschmann, “Fundamentals of Early Clinical Drug Development: From Synthesis Design to Formulation. Edited by A. F. Abdel-Magid and Stéphane Caron.,” *ChemMedChem*, vol. 2, no. 4, pp. 561–562, Apr. 2007, doi: <https://doi.org/10.1002/cmdc.200700037>.
8. G. T. McInnes, M. J. Asbury, L. E. Ramsay, J. R. Shelton, and I. R. Harrison, “Effect of micronization on the bioavailability and pharmacologic activity of spironolactone,” *Journal of Clinical Pharmacology*, vol. 22, no. 8–9, pp. 410–417, 1982, doi: <https://doi.org/10.1002/j.1552-4604.1982.tb02694.x>.
9. Center for Drug Evaluation and Research, “Q8(R2) Pharmaceutical Development,” U.S. Food and Drug Administration, 2019.

- <https://www.fda.gov/regulatory-information/search-fda-guidance-documents/q8r2-pharmaceutical-development>
10. “Guidance for Industry Q8(R2) Pharmaceutical Development,” 2009. Available: <https://www.fda.gov/media/71535/download>.
 11. J. Tewari, R. M. Strong, and P. Boulas, “At-line determination of pharmaceuticals small molecule’s blending end point using chemometric modeling combined with Fourier transform near infrared spectroscopy,” vol. 173, pp. 886–891, Feb. 2017, doi: <https://doi.org/10.1016/j.saa.2016.10.013>.
 12. A. S. El-Hagrasy and J. K. Drennen, “A Process Analytical Technology approach to near-infrared process control of pharmaceutical powder blending. Part III: Quantitative near-infrared calibration for prediction of blend homogeneity and characterization of powder mixing kinetics,” *Journal of Pharmaceutical Sciences*, vol. 95, no. 2, pp. 422–434, Feb. 2006, doi: <https://doi.org/10.1002/jps.20465>.
 13. Y. Sulub, M. Konigsberger, and J. Cheney, “Blend uniformity end-point determination using near-infrared spectroscopy and multivariate calibration,” *Journal of Pharmaceutical and Biomedical Analysis*, vol. 55, no. 3, pp. 429–434, Jun. 2011, doi: <https://doi.org/10.1016/j.jpba.2011.02.017>.
 14. Joaquim Jaumot, Benoît Igne, C. A. Anderson, J. K. Drennen, and Anna de Juan, “Blending process modeling and control by multivariate curve resolution,” *Talanta*, vol. 117, pp. 492–504, Dec. 2013, doi: <https://doi.org/10.1016/j.talanta.2013.09.037>.
 15. R. Besseling et al., “An efficient, maintenance free and approved method for spectroscopic control and monitoring of blend uniformity: The moving F-test,” *Journal of Pharmaceutical and Biomedical Analysis*, vol. 114, pp. 471–481, Oct. 2015, doi: <https://doi.org/10.1016/j.jpba.2015.06.019>.
 16. Wee Beng Lee, E. Widjaja, P. Wan, and Lai Wah Chan, “Near infrared spectroscopy for rapid and in-line detection of particle size distribution variability in lactose during mixing,” *International Journal of Pharmaceutics*, vol. 566, pp. 454–462, Jul. 2019, doi: <https://doi.org/10.1016/j.ijpharm.2019.06.002>.

17. M. Blanco, "Monitoring powder blending in pharmaceutical processes by use of near infrared spectroscopy," *Talanta*, vol. 56, no. 1, pp. 203–212, Jan. 2002, doi: [https://doi.org/10.1016/s0039-9140\(01\)00559-8](https://doi.org/10.1016/s0039-9140(01)00559-8).
18. D. M. Koller et al., "Continuous quantitative monitoring of powder mixing dynamics by near-infrared spectroscopy," *Powder Technology*, vol. 205, no. 1–3, pp. 87–96, Jan. 2011, doi: <https://doi.org/10.1016/j.powtec.2010.08.070>.
19. M. Blanco, J. Coello, H. Iturriaga, S. Maspoch, and C. de, "Effect of Data Preprocessing Methods in Near-Infrared Diffuse Reflectance Spectroscopy for the Determination of the Active Compound in a Pharmaceutical Preparation," vol. 51, no. 2, pp. 240–246, Feb. 1997, doi: <https://doi.org/10.1366/0003702971939947>.
20. P. A. Hailey, P. Doherty, P. Tapsell, T. Oliver, and P. K. Aldridge, "Automated system for the on-line monitoring of powder blending processes using near-infrared spectroscopy part I. System development and control," *Journal of Pharmaceutical and Biomedical Analysis*, vol. 14, no. 5, pp. 551–559, Mar. 1996, doi: [https://doi.org/10.1016/0731-7085\(95\)01674-0](https://doi.org/10.1016/0731-7085(95)01674-0).
21. J. Rantanen, "Process analytical applications of Raman spectroscopy," *Journal of Pharmacy and Pharmacology*, vol. 59, no. 2, pp. 171–177, Feb. 2007, doi: <https://doi.org/10.1211/jpp.59.2.0004>.
22. J Michael Hollas, *Modern spectroscopy*. Hoboken, New Jersey: Wiley, 2013.
23. Smith and G. Dent, *Modern Raman spectroscopy : a practical approach*. Hoboken, Nj Wiley, Ewen 2019.
24. G. Walker, S. E. J. Bell, M. Vann, D. S. Jones, and G. Andrews, "Fluidised bed characterisation using Raman spectroscopy: Applications to pharmaceutical processing," *Chemical Engineering Science*, vol. 62, no. 14, pp. 3832–3838, Jul. 2007, doi: <https://doi.org/10.1016/j.ces.2007.04.017>.
25. H. Wikström, S. Romero-Torres, S. Wongweragiat, J. A. S. Williams, E. R. Grant, and L. S. Taylor, "On-Line Content Uniformity Determination of Tablets Using Low-Resolution Raman Spectroscopy," *Applied Spectroscopy*, vol. 60, no. 6, pp. 672–681, Jun. 2006, doi: <https://doi.org/10.1366/000370206777670684>.
26. T. R. M. De Beer et al., "Raman spectroscopy as a process analytical technology (PAT) tool for the in-line monitoring and understanding of a powder blending

- process,” *Journal of Pharmaceutical and Biomedical Analysis*, vol. 48, no. 3, pp. 772–779, Nov. 2008, doi: <https://doi.org/10.1016/j.jpba.2008.07.023>.
27. D. Riolo et al., “Raman spectroscopy as a PAT for pharmaceutical blending: Advantages and disadvantages,” *Journal of Pharmaceutical and Biomedical Analysis*, vol. 149, pp. 329–334, Feb. 2018, doi: <https://doi.org/10.1016/j.jpba.2017.11.030>.
 28. A. Crouter and L. Briens, “The effect of granule moisture on passive acoustic emissions in a V-blender,” *Powder Technology*, vol. 299, pp. 226–234, Oct. 2016, doi: <https://doi.org/10.1016/j.powtec.2016.05.037>.
 29. A. Cameron and L. Briens, “Monitoring lubricant addition in pharmaceutical tablet manufacturing through passive vibration measurements in a V-blender,” *Powder Technology*, vol. 364, pp. 708–718, Mar. 2020, doi: <https://doi.org/10.1016/j.powtec.2020.02.018>.
 30. A. Cameron and L. Briens, “An Investigation of Magnesium Stearate Mixing Performance in a V-Blender Through Passive Vibration Measurements,” *AAPS PharmSciTech*, vol. 20, no. 5, May 2019, doi: <https://doi.org/10.1208/s12249-019-1402-3>.
 31. A. Cameron and L. Briens, “Monitoring Magnesium Stearate Blending in a V-Blender Through Passive Vibration Measurements,” *AAPS PharmSciTech*, vol. 20, no. 7, Jul. 2019, doi: <https://doi.org/10.1208/s12249-019-1469-x>.
 32. P. Allan, L. J. Bellamy, A. Nordon, and D. Littlejohn, “Non-invasive monitoring of the mixing of pharmaceutical powders by broadband acoustic emission,” *The Analyst*, vol. 135, no. 3, p. 518, 2010, doi: <https://doi.org/10.1039/b922446g>.
 33. P. Tily, S. Porada, C. Scruby, and S. Lidington, “Monitoring of mixing processes using acoustic emission.” *Fluid Mixing III*, Institution of Chemical Engineers, Rugby 75-94, 1988.
 34. P. Allan, L. J. Bellamy, A. Nordon, D. Littlejohn, J. Andrews, and P. Dallin, “In situ monitoring of powder blending by non-invasive Raman spectrometry with wide area illumination,” *Journal of Pharmaceutical and Biomedical Analysis*, vol. 76, pp. 28–35, Mar. 2013, doi: <https://doi.org/10.1016/j.jpba.2012.12.003>

35. C.-Y. Yang and X.-Y. Fu, "Development and validation of a material-labeling method for powder process characterization using X-ray computed tomography," vol. 146, no. 1–2, pp. 10–19, Aug. 2004, doi: <https://doi.org/10.1016/j.powtec.2004.06.011>.
36. A. W. Chester, J. A. Kowalski, M. E. Coles, E. L. Muegge, F. J. Muzzio, and D. Brone, "Mixing dynamics in catalyst impregnation in double-cone blenders," *Powder Technology*, vol. 102, no. 1, pp. 85–94, Apr. 1999, doi: [https://doi.org/10.1016/S0032-5910\(98\)00193-4](https://doi.org/10.1016/S0032-5910(98)00193-4).
37. R. Liu et al., "Visualization and quantitative profiling of mixing and segregation of granules using synchrotron radiation X-ray microtomography and three dimensional reconstruction," *International Journal of Pharmaceutics*, vol. 445, no. 1–2, pp. 125–133, Mar. 2013, doi: <https://doi.org/10.1016/j.ijpharm.2013.02.010>.
38. A. Bulent Koc, Hasan Silleli, Caner Koc, and M. Ali Dayioglu, "Monitoring of Dry Powder Mixing With Real-Time Image Processing," *Journal of Applied Sciences*, vol. 7, no. 8, pp. 1218–1223, Aug. 2007, doi: <https://doi.org/10.3923/jas.2007.1218.1223>.
39. A.-L. Le Coënt, A. Rivoire, S. Briançon, and J. Lieto, "An original image-processing technique for obtaining the mixing time: The box-counting with erosions method," *Powder Technology*, vol. 152, no. 1–3, pp. 62–71, Apr. 2005, doi: <https://doi.org/10.1016/j.powtec.2005.01.025>.
40. C.-C. Chen and C.-K. Yu, "Two-dimensional image characterization of powder mixing and its effects on the solid-state reactions," *Materials Chemistry and Physics*, vol. 85, no. 1, pp. 227–237, May 2004, doi: <https://doi.org/10.1016/j.matchemphys.2004.01.024>.
41. X. Liu, C. Zhang, and J. Zhan, "Quantitative comparison of image analysis methods for particle mixing in rotary drums," *Powder Technology*, vol. 282, pp. 32–36, Sep. 2015, doi: <https://doi.org/10.1016/j.powtec.2014.08.076>.
42. A. Realpe and C. Velázquez, "Image processing and analysis for determination of concentrations of powder mixtures," *Powder Technology*, vol. 134, no. 3, pp. 193–200, Sep. 2003, doi: [https://doi.org/10.1016/s0032-5910\(03\)00138-4](https://doi.org/10.1016/s0032-5910(03)00138-4).

43. Chawki Ammarcha, Cendrine Gatamel, Jean-Louis Dirion, M. Cabassud, and Henri Berthiaux, "Continuous powder mixing of segregating mixtures under steady and unsteady state regimes: Homogeneity assessment by real-time on-line image analysis," *Powder Technology*, vol. 315, pp. 39–52, Jun. 2017, doi: <https://doi.org/10.1016/j.powtec.2017.02.010>.
44. Björn Daumann, A. Fath, H. Anlauf, and H. Nirschl, "Determination of the mixing time in a discontinuous powder mixer by using image analysis," *Chemical Engineering Science*, vol. 64, no. 10, pp. 2320–2331, May 2009, doi: <https://doi.org/10.1016/j.ces.2009.01.032>.
45. H. Berthiaux, V. Mosorov, L. Tomczak, C. Gatamel, and J. F. Demeyre, "Principal component analysis for characterising homogeneity in powder mixing using image processing techniques," *Chemical Engineering and Processing: Process Intensification*, vol. 45, no. 5, pp. 397–403, May 2006, doi: <https://doi.org/10.1016/j.cep.2005.10.005>.
46. M. Nakagawa, S. A. Altobelli, Arvind Caprihan, E. Fukushima, and Euh Duck Jeong, "Non-invasive measurements of granular flows by magnetic resonance imaging," vol. 16, no. 1, pp. 54–60, Jan. 1993, doi: <https://doi.org/10.1007/bf00188507>.
47. T. Kawaguchi, K. Tsutsumi, and Y. Tsuji, "MRI Measurement of Granular Motion in a Rotating Drum," *Particle & Particle Systems Characterization*, vol. 23, no. 3–4, pp. 266–271, Oct. 2006, doi: <https://doi.org/10.1002/ppsc.200601065>.
48. K. M. Hill, A. Caprihan, and J. Kakalios, "Bulk Segregation in Rotated Granular Material Measured by Magnetic Resonance Imaging," *Physical Review Letters*, vol. 78, no. 1, pp. 50–53, Jan. 1997, doi: <https://doi.org/10.1103/physrevlett.78.50>.
49. M. Bruneau and T. Scelo, *Fundamentals of Acoustics*. New York, NY: John Wiley & Sons, 2013.
50. J. Boyd and J. Varley, "The uses of passive measurement of acoustic emissions from chemical engineering processes," *Chemical Engineering Science*, vol. 56, no. 5, pp. 1749–1767, Mar. 2001, doi: [https://doi.org/10.1016/s0009-2509\(00\)00540-6](https://doi.org/10.1016/s0009-2509(00)00540-6).
51. M. P. Whitaker et al., "Application of acoustic emission to the monitoring and end point determination of a high shear granulation process," *International Journal of*

- Pharmaceutics, vol. 205, no. 1–2, pp. 79–91, Sep. 2000, doi:
[https://doi.org/10.1016/s0378-5173\(00\)00479-8](https://doi.org/10.1016/s0378-5173(00)00479-8).
52. E. M. Hansuld, L. Briens, A. Sayani, and Joe, “The effect of process parameters on audible acoustic emissions from high-shear granulation,” *Drug Development and Industrial Pharmacy*, vol. 39, no. 2, pp. 331–341, May 2012, doi:
<https://doi.org/10.3109/03639045.2012.681055>.
53. E. M. Hansuld, L. Briens, A. Sayani, and J. A. B. McCann, “An investigation of the relationship between acoustic emissions and particle size,” *Powder Technology*, vol. 219, pp. 111–117, Mar. 2012, doi:
<https://doi.org/10.1016/j.powtec.2011.12.025>.
54. E. M. Hansuld, L. Briens, Joe A.B. McCann, and A. Sayani, “Audible acoustics in high-shear wet granulation: Application of frequency filtering,” *International Journal of Pharmaceutics*, vol. 378, no. 1–2, pp. 37–44, Aug. 2009, doi:
<https://doi.org/10.1016/j.ijpharm.2009.05.042>.
55. E. M. Hansuld, L. Briens, A. Sayani, and J. A. B. McCann, “Monitoring quality attributes for high-shear wet granulation with audible acoustic emissions,” *Powder Technology*, vol. 215–216, pp. 117–123, Jan. 2012, doi:
<https://doi.org/10.1016/j.powtec.2011.09.034>.
56. M. K. Papp, C. P. Pujara, and R. Pinal, “Monitoring of High-shear Granulation using Acoustic Emission: Predicting Granule Properties,” *Journal of Pharmaceutical Innovation*, vol. 3, no. 2, pp. 113–122, May 2008, doi:
<https://doi.org/10.1007/s12247-008-9030-6>.
57. L. Briens, D. Daniher, and A. Tallevi, “Monitoring high-shear granulation using sound and vibration measurements,” *International Journal of Pharmaceutics*, vol. 331, no. 1, pp. 54–60, Feb. 2007, doi:
<https://doi.org/10.1016/j.ijpharm.2006.09.012>.
58. J. F. Gamble, A. B. Dennis, and M. Toby, “Monitoring and end-point prediction of a small scale wet granulation process using acoustic emission,” *Pharmaceutical Development and Technology*, vol. 14, no. 3, pp. 299–304, Jun. 2009, doi:
<https://doi.org/10.1080/10837450802603618>.

59. D. Daniher, L. Briens, and A. Tallevi, “End-point detection in high-shear granulation using sound and vibration signal analysis,” *Powder Technology*, vol. 181, no. 2, pp. 130–136, Feb. 2008, doi: <https://doi.org/10.1016/j.powtec.2006.12.003>.
60. D. Vervloet, J. Nijenhuis, and J. R. van Ommen, “Monitoring a lab-scale fluidized bed dryer: A comparison between pressure transducers, passive acoustic emissions and vibration measurements,” *Powder Technology*, vol. 197, no. 1–2, pp. 36–48, Jan. 2010, doi: <https://doi.org/10.1016/j.powtec.2009.08.015>.
61. L. Briens, R. Smith, and C. Briens, “Monitoring of a rotary dryer using acoustic emissions,” *Powder Technology*, vol. 181, no. 2, pp. 115–120, Feb. 2008, doi: <https://doi.org/10.1016/j.powtec.2006.12.004>.
62. E. Serris, L. Perier-Camby, G. Thomas, M. Desfontaines, and G. Fantozzi, “Acoustic emission of pharmaceutical powders during compaction,” *Powder Technology*, vol. 128, no. 2–3, pp. 296–299, Dec. 2002, doi: [https://doi.org/10.1016/s0032-5910\(02\)00174-2](https://doi.org/10.1016/s0032-5910(02)00174-2).
63. J. Whiting, A. Springer, and F. Sciammarella, “Real-time acoustic emission monitoring of powder mass flow rate for directed energy deposition,” *Additive Manufacturing*, vol. 23, pp. 312–318, Oct. 2018, doi: <https://doi.org/10.1016/j.addma.2018.08.015>.
64. K. Albion, L. Briens, C. Briens, and F. Berruti, “Modelling of oversized material flow through a horizontal hydrotransport slurry pipe to optimize its acoustic detection,” *Powder Technology*, vol. 194, no. 1–2, pp. 18–32, Aug. 2009, doi: <https://doi.org/10.1016/j.powtec.2009.03.017>.
65. R. Hou, A. Hunt, and R. A. Williams, “Acoustic monitoring of pipeline flows: particulate slurries,” *Powder Technology*, vol. 106, no. 1–2, pp. 30–36, Nov. 1999, doi: [https://doi.org/10.1016/s0032-5910\(99\)00051-0](https://doi.org/10.1016/s0032-5910(99)00051-0).
66. K. Albion, L. Briens, Cédric Briens, Franco Berruti, and G. Book, “Flow regime determination in upward inclined pneumatic transport of particulates using non-intrusive acoustic probes,” *Chemical Engineering and Processing - Process Intensification*, vol. 46, no. 6, pp. 520–531, Jun. 2007, doi: <https://doi.org/10.1016/j.cep.2006.06.012>.

67. K. Albion, L. Briens, C. Briens, and F. Berruti, "Flow regime determination in horizontal pneumatic transport of fine powders using non-intrusive acoustic probes," *Powder Technology*, vol. 172, no. 3, pp. 157–166, Mar. 2007, doi: <https://doi.org/10.1016/j.powtec.2006.10.040>.
68. K. Albion, L. Briens, C. Briens, and F. Berruti, "Detection of the breakage of pharmaceutical tablets in pneumatic transport," *International Journal of Pharmaceutics*, vol. 322, no. 1–2, pp. 119–129, Sep. 2006, doi: <https://doi.org/10.1016/j.ijpharm.2006.05.039>.
69. S. Oka, A. Sahay, W. Meng, and F. Muzzio, "Diminished segregation in continuous powder mixing," *Powder Technology*, vol. 309, pp. 79–88, Mar. 2017, doi: <https://doi.org/10.1016/j.powtec.2016.11.038>.
70. A. Alexander, F. J. Muzzio, and T. Shinbrot, "Segregation patterns in V-blenders," *Chemical Engineering Science*, vol. 58, no. 2, pp. 487–496, Jan. 2003, doi: [https://doi.org/10.1016/s0009-2509\(02\)00530-4](https://doi.org/10.1016/s0009-2509(02)00530-4).
71. A. Alexander, T. Shinbrot, B. Johnson, and F. J. Muzzio, "V-blender segregation patterns for free-flowing materials: effects of blender capacity and fill level," *International Journal of Pharmaceutics*, vol. 269, no. 1, pp. 19–28, Jan. 2004, doi: [https://doi.org/10.1016/s0378-5173\(03\)00296-5](https://doi.org/10.1016/s0378-5173(03)00296-5).
72. R. Hogg, "Mixing and Segregation in Powders: Evaluation, Mechanisms and Processes," *KONA Powder and Particle Journal*, vol. 27, no. 0, pp. 3–17, 2009, doi: <https://doi.org/10.14356/kona.2009005>.
73. S. Oka and F. J. Muzzio, "Continuous powder mixing and lubrication," Elsevier eBooks, pp. 59–92, Jan. 2022, doi: <https://doi.org/10.1016/b978-0-12-813479-5.00013-6>.
74. Misiti, Michel, Yves Misiti, Georges Oppenheim, and Jean-Michel Poggi. "Wavelet toolbox for use with Matlab, the MathWorks," Natick, MA. 1996.
75. B.-M. Block and Paolo Mercorelli, "Conceptual understanding of complex components and Nyquist-Shannon sampling theorem: A design based research in Engineering," Mar. 2015, doi: <https://doi.org/10.1109/educon.2015.7096011>.
76. E. Por, M. Van Kooten, and V. Sarkovic, "Nyquist-Shannon sampling theorem 1 Theory 1.1 The Nyquist-Shannon sampling theorem," 2019.

77. A. Crouter and L. Briens, "Passive acoustic emissions from particulates in a V-blender," *Drug Development and Industrial Pharmacy*, vol. 41, no. 11, pp. 1809–1818, Feb. 2015, doi: <https://doi.org/10.3109/03639045.2015.1009913>.
78. I. Daubechies, "The wavelet transform, time-frequency localization and signal analysis," *IEEE Transactions on Information Theory*, vol. 36, no. 5, pp. 961–1005, 1990, doi: <https://doi.org/10.1109/18.57199>.
79. K. Wilson and L. Briens, "Passive acoustic emissions application to a segregation prone mixture in a V-blender," *Powder Technology*, vol. 428, pp. 118827–118827, Oct. 2023, doi: <https://doi.org/10.1016/j.powtec.2023.118827>.

Chapter 4

4 Effect of Fill Level on Powder Mixing and Segregation in a V-blender Using Passive Acoustic Emissions

4.1 Introduction

Most of the pharmaceutical formulations are produced in the form of solid dosage forms. Tablets and capsules are the most common formulations and approximately account for around 80% of all pharmaceuticals produced in the form of solid doses (1). The reason capsules and tablets account for that high percentage is due to their convenient route for drug administration because of their ease of transport, use, cost-effectiveness, and stability (1,2,3). The pharmaceutical tablet manufacturing process consists of several batch steps and each step must be monitored and controlled to ensure quality standards are met. Most of the pharmaceutical tablet manufacturing is done offline using different batch processes. Process analytical technologies (PATs) are recommended techniques to improve pharmaceutical efficiency, stability, and quality of products produced to monitor product quality better and improve process understanding (4,5).

Powder mixing in the pharmaceutical industry is considered one of the very important processes. The active pharmaceutical ingredient (API) is added with excipients, and all ingredients are mixed until the required mixture is reached. If insufficient mixing occurs, it may result in poor product quality and rejection of the batch. That is why it is crucial to monitor and control powder mixing in the pharmaceutical industry (7,8). In pharmaceutical manufacturing, optimal mixing of powders must be reached which is crucial in establishing content uniformity. Powder mixing depends on powder properties and behavior inside a mixer which are important factors to monitor and control powder mixing. However, powder mixing is not fully understood, and the processes are not clear and defined. Many factors can affect powder mixing such as particle density, size, shape, and flowability. Moreover, mixer type and geometry can

interfere with and affect powder mixing. Mixing is considered an art rather than science (6,9).

The production of pharmaceutical solid dosage is still often done batch-wise. Following each batch mixing step, samples are extracted and examined offline to verify the uniformity and consistency of the blend. This ensures that the final product will have all the desired properties (10). PATs refer to techniques utilized in pharmaceutical manufacturing to design, analyze, and regulate processes in pharmaceutical manufacturing. These methods involve the measurement of critical process parameters that influence the quality attributes of the API in a specified dosage form (4). There are many methods and techniques used to measure and monitor the process parameters for mixing including image analysis, magnetic nuclear resonance imaging, near-infrared spectroscopy, and passive acoustic emissions.

These PATs are intended to replace the offline methods currently being used in the pharmaceutical industry. One of the major offline methods used in the industry is thief probes to determine mixture quality and homogeneity. Samples are extracted using thief probes at regular time intervals and analyzed. Thief probes can produce inaccurate and unreliable results. Preliminary studies included research for several PATs in pharmaceutical powder mixing with most of the research done on the application of PATs focused on near-infrared (NIR) spectroscopy (23,24).

Passive Acoustic Emissions (PAE) are the study of vibrations and sound waves that are generated by a source, transmitted through a medium, and received by a receiver as a form of wave energy (11,12). Within the V-blender, energy is generated in the form of stress waves because of interactions between particles and the V-shell during powder mixing (13). The energy released as stress waves are recorded as vibrations. An accelerometer, affixed to the lid of the outer arm of the V-shell records this energy as vibrations. The recorded vibrations due to particle collision are dependent on various factors including particle characteristics and mixer design. Larger particles usually have more kinetic energy and upon collisions, they release more energy that leads to increased vibrations in the form of stress waves recorded by the accelerometer.

PAE is under exploration across different industries to gain insights into the physicochemical changes that happen during a process. PAE is being investigated in the pharmaceutical industry in monitoring powder mixing and few studies have been completed. Previous research into PAE determined preliminary connections and data for particle motion and behaviors inside the V-blender and provided guidelines for extracting the data needed from the recorded vibrations. Also, previous studies identified preliminary connections between the different motion phases of particles within the V-shell and the emissions as well as provided guidelines for extracting information from the recorded vibrations. Particle collisions with the outer arm V-shell lid where the accelerometer is attached provided the most important and reliable information regarding the particle properties and their flow within the V-shell from the recorded vibrations. Additionally, preliminary studies have focused on monitoring the mixing of some particle components with uniform and regular properties with limited loading configurations (13-18). Mixing can occur between particles having different properties and hence it is crucial to develop methods that can be applied to industrial conditions and setup.

Segregation or de-mixing refers to the presence of areas within a mixture where particles with similar properties are seen to accumulate. In the pharmaceutical industry, mixing of powders can lead to segregation when particles with different physical characteristics, such as shape, flowability, size, and density are used in the mixture. These differences in physical characteristics should be accounted for to prevent the occurrence of segregation development. Segregation can be seen when particles separate due to variations in physical characteristics, affecting the homogeneity and uniformity of the mixture (19). Several factors influence the possibility of segregation development. Differences in particle properties can increase the chances of segregation. The more the difference in particle properties, the more segregation development can be developed (19,20).

Preliminary studies discussed segregation development patterns and how the physical properties of the particles, fill level, and process parameters can influence the segregation pattern. It was found in the literature that fill level and rotational speed has

a significant impact on segregation pattern development in the V-blender. Four major different segregation patterns are seen to develop in the V-blender while mixing based on rotation speed and fill level of the blender. The four segregation patterns are “Small-out”, “Stripes”, “Inverse stripes”, and “Left-right” patterns. (20,21). The literature also discussed the effect of other factors on particle mixing and segregation. Mixing rates and uniformity were compared while changing some process parameters such as fill level. It was found that mixing rates were more efficient when the fill levels were low compared to a high fill level, which resulted in an improvement in the mixing performance of the mixtures (21,23). Cameron and Briens (2019) tested the effect of fill level on particles coated with magnesium stearate lubricant and found that the optimum fill level to promote effective mixing was 21–23% by volume and higher fill levels resulted in less efficient mixing.

Left-right segregation pattern is the main type of segregation seen to develop in the V-blender because of the trajectory segregation mechanism. Trajectory segregation can be seen to develop when mixing powders of high and low inertia. Differences in inertia result in distinct behaviors in particle movement in the V-blender. Smaller particles tend to move away and separate from larger particles. Particles with higher inertia follow a more linear trajectory, while those with lower inertia tend to follow a curved path (19,20,21,25). In a V-blender, trajectory segregation can be further enhanced by collisions with the V-shell joint along the flow path. Segregation is a phenomenon that can be seen during particle mixing in a V-blender, primarily through trajectory and percolation mechanisms. These segregation types become more apparent with particles characterized by high flowability, exposure to a curving flow field, and a range of sizes. However, the starch granules used in this research are not spherical and have irregular shapes of different diameter size ranges with a spherical value of 0.70, but they have good flowability due to the low avalanche times below 4.8 seconds.

Acoustics offers numerous advantages in comparison to alternative techniques used for monitoring powder mixing and segregation in the pharmaceutical industry. PAE monitoring is non-invasive, cost-effective, non-destructive, requires no modification to equipment, and can be integrated as an in-line monitoring method. Previous research

has focused on monitoring the mixing of a specific number of particles with uniform properties and with limited loading configurations and orders. Moreover, changes in process parameters were not widely applied to monitor their effect on powder mixing and segregation (13-18). The main aim of this research was to further explore and investigate the potential of PAE in monitoring mixing and segregation while adjusting the V-blender fill level and evaluating the effect of fill level on mixing and segregation. Monitoring powder mixing and identifying segregation to prevent its development are critical processes in the industry and can result in higher quality control and assurance standards as well as enhance good manufacturing practices in the industry. This can be achieved by developing real-time and in-line monitoring methods using PAE.

4.2 Materials and Methods

4.2.1 Materials

Starch granules were the particles used in the experimental trials completed in this research. The starch granules used had irregular shapes with a range of different sizes. Using various meshes with different sizes, the starch granules were sieved into five distinct size fraction cuts. Only Cut#1 and Cut#4 were used. Cut#1 has the biggest size fraction with a diameter range of 2.00 – 2.36 mm and Cut#4 has the smallest size fraction with a diameter range of 0.006 – 1.18 mm. Iodine solution was used to dye Cut#1, allowing for visual observation of any segregation that may develop.

Preliminary testing indicated that the iodine solution used had no substantial effect on the other characteristics of the starch granules. Wilson and Briens (2022) measured the apparent density of the starch granules through estimation by volume displacement measurements using 4°C distilled water and photos of the starch granules were taken and examined with Image Pro software to estimate the circularity of the granules.

Image Pro defines circularity as $\frac{Perimeter^2}{4p*Area}$, with a perfectly circular particle having a value of 1.00 (6). Starch granules experimental trials were measured in duplicates with average values reported. Table 4.1 shows the characteristics of the particles used for this study.

Table 4.1: Summary of particles used and their characteristics

Particle	Size (mm)	Apparent density (g/cm ³)	Sphericity (-)
Starch granules Cut#1	2.00 – 2.36	1.3	0.70
Starch granules Cut#4	0.006 – 1.18	1.3	0.70

4.2.2 Equipment

A Patterson-Kelly V-blender with a fixed rotation speed of 25 rotations per minute (rpm) was used in all the experimental trials completed in this research. A 16-quart (15.1 liter) transparent acrylic V-shell was used. The V-shell was filled by starch granule particles corresponding to different percentages ranging from 5% to 75% ratio by mass. The V-shell of the blender has inner and outer arms with two lids attached to them and a bottom plate. Figure 4.1 shows a schematic diagram of the V-blender with all of its properties.

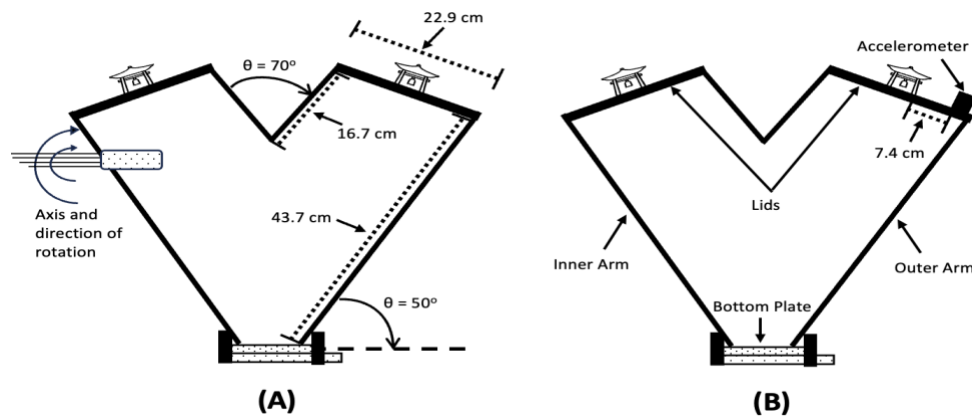


Figure 4.1: (A) Schematic diagram for the V-blender and its properties and (B) schematic diagram showing accelerometer location

PCB Piezotronics Accelerometer of model 353B3 combined with an ICP signal conditioner of model 480E0 were used to measure the vibrations generated from PAE. The accelerometer combined with the signal conditioner was attached to the lower front center of the outer arm of the V-shell at a radial position of $r/R = 0.74$. Figure 4.1-B shows the location of the accelerometer. Labview with a National Instruments DAQ-

6036E card was used to record the vibrations from PAE. The vibrations were recorded at an acquisition frequency of 40,000 Hz. The acquisition frequency of 40,000 Hz was used to exceed the Nyquist frequency of the signal of interest. The Nyquist Shannon Sampling Theorem states that to accurately construct a signal, the sampling frequency must be at least twice the highest frequency present in the signal. In the case of audio signals, where the human hearing range is up to 20,000 Hz, a common choice is to use a sampling frequency of at least 40,000 Hz to make sure that all audible frequencies were sufficiently captured and to avoid aliasing and as well to ensure that the signal preserves the original characteristics of the analog signal (26,27).

Daubechies wavelet filter in Matlab was used to filter the measurements recorded. Daubechies wavelet filter was used to remove the oscillation motion generated due to the V-shell to focus mostly on the vibrations generated from the particle collision inside the V-shell. Noise generated from the rotations of the V-blender can affect the wavelets recorded due to particle collision and interaction with other particles or with the V-shell.

4.2.3 Experimental Trials

Experimental trials were completed using starch granule size fractions of Cut#1 and Cut#4 as shown in Table 4.1. Starch granule particles were loaded in the V-blender while changing the V-blender fill levels. The mixture combinations were loaded horizontally in the V-blender and tumbled. Rotations of mixtures were completed with varying fill levels allowing for mixing and segregation. Mixing for individual size fraction cuts and mixture combinations was observed and any segregation developed was photographed. All starch granules experimental trials were conducted in duplicates for reproducibility and confirmation of the results.

4.2.3.1 Fill Level for Individual Size Fractions

Vibration measurements were recorded for individual starch granule sizes of Cut#1 and Cut#4. The starch granules were loaded in the 16-quart transparent acrylic V-shell with varying fill level percentages from 5% to 75% of the V-shell at intervals of 5% by mass ratio. The height of the starch granules in the V-shell relative to the V-shell geometry

was measured for each loading. An accelerometer was attached to the outer arm lid of the V-shell as indicated in Figure 4.1-B to record the vibrations generated upon V-blender rotations. The vibrations were measured and recorded over 50 revolutions of the V-shell. After the vibrations were measured, the measurements were filtered and analyzed using Matlab.

4.2.3.2 Fill Level for Mixture Combinations

Vibration measurements were recorded for binary mixtures of starch granules from Cut#1 and Cut#4 in a 50-50% ratio based on mass. Cut#1 and Cut#4 size fractions were loaded in the V-shell with varying fill level percentages from 10% to 70% at intervals of 10%. Cut#1 was dyed using iodine solution to observe any segregation pattern that may develop while mixing. The size fraction of starch granules was loaded in a horizontal loading configuration in the V-shell. Particles were loaded in a horizontal configuration to obtain a symmetrical top-bottom loading pattern for the geometry of the V-blender shells. An accelerometer was attached to the outer arm lid of the V-shell as indicated in Figure 4.1-B. The vibrations were measured and recorded over 50 revolutions of the V-shell. After the vibrations were measured, the measurements were filtered and analyzed using Matlab.

While the V-blender was tumbling and rotating, the V-shell was stopped at 50 revolutions to take photos and sieve the mixture inside. Sieving of the mixture was done for both inner and outer V-shell arms using meshes based on the size mixture. This was performed to observe the extent of segregation developed and quantify the amount of smaller and larger particles found in each arm of the V-shell. Photos of the dyed starch granules mixture allowed for visual observations of any segregation pattern development and monitored the mixing stage. The sieving data allowed for confirmation of mixing and segregation to be observed in each arm of the V-shell. In the sieving analysis, the V-shell was stopped while inverted and both the inner and outer arms were unloaded separately after 50 revolutions. Each arm emptied contained a mixture which was then sieved to determine the percentage composition by weight of each component.

4.3 Results

4.3.1 Fill Level for Individual Size Fractions

Starch granules were loaded in the V-blender and tumbled at different fill levels. Size fractions of Cut#1 and Cut#4 were used, and rotations were completed at varying fill-level percentages. Trials were conducted in duplicate, and the average values were reported. Vibration amplitudes were recorded throughout 50 rotations. Figure 4.2 shows the average vibration amplitudes recorded in the V-blender for the individual size fractions of Cut#1 and Cut#4 at different fill level percentages from 5% to 75% at intervals of 5%. The fill level and amount of loaded materials inside the V-shell affected the recorded vibration amplitudes for both starch granule individual cuts. The average vibration amplitude did not show a consistent and significant trend with the fill level of the material.

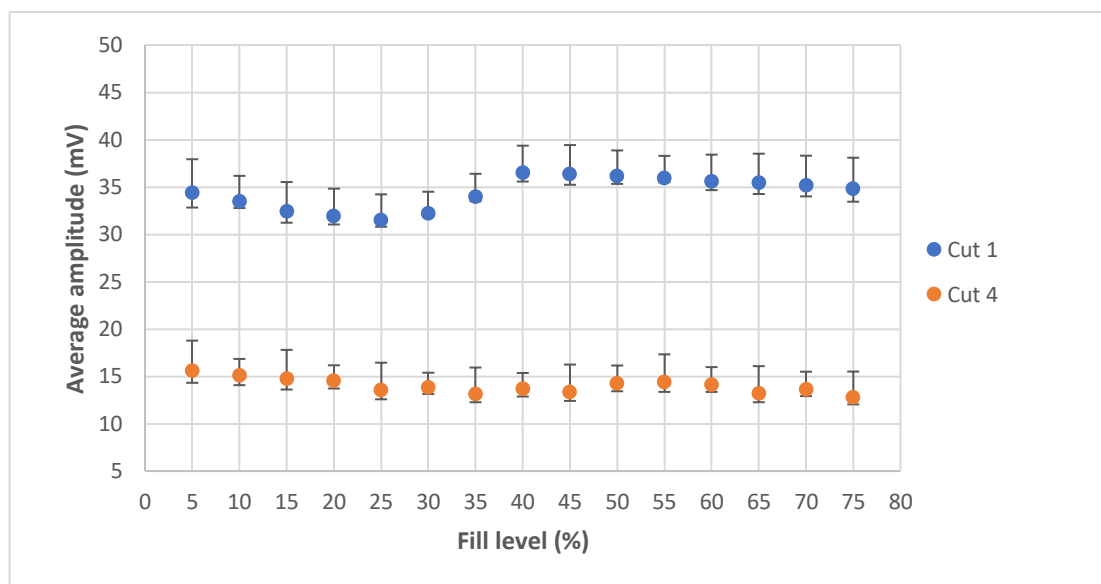


Figure 4.2: Average vibration amplitudes of individual Cut#1 and Cut#4 at different fill levels with vertical error bars representing +/- 1 STD values

4.3.2 Fill Level for Mixture Combinations

Starch granule size fractions were used in a 50-50% composition by mass ratio and the mixture combinations were loaded horizontally in the V-blender and tumbled. Cut#1 and Cut#4 binary mixture were used, and rotations of the binary mixture were

completed and allowed for mixing and segregation patterns were photographed. Figure 4.3 shows the extent of segregation between Cut#1 and Cut#4 after 50 revolutions with varying fill levels from 10% to 70%. There is a large difference in size fraction cuts used, the larger size fraction Cut#1 (2.00 – 2.36 mm) was mixed with the smaller size fraction Cut#4 (0.006 – 1.18 mm). Cut#1 was dyed using iodine solution and loaded on top of the smaller undyed Cut#4. Cut#4 segregated towards the outer arm and Cut#1 segregated towards the inner arm of the V-shell. Visual observations of the starch granule mixtures show that a left-right segregation pattern was developed for the low fill levels.

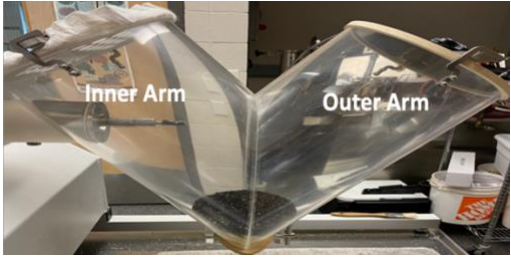
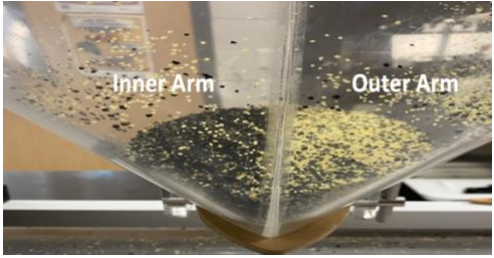

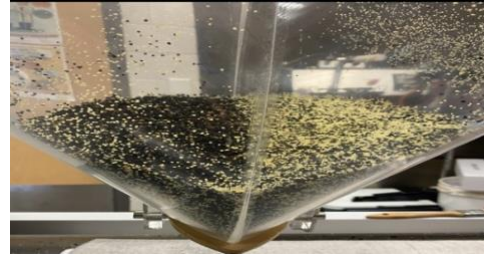
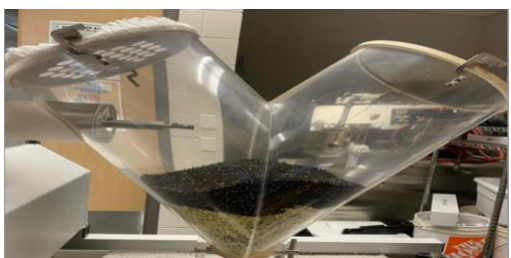
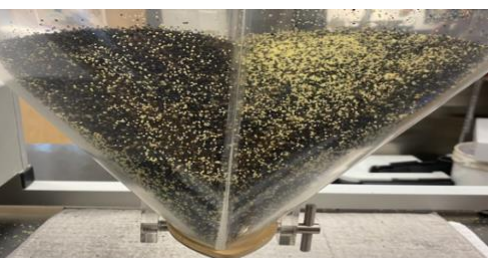


Fill Level (%)	Before mixing	After 50 revolutions
10	 A V-blender with a 10% fill level. The mixture is undyed Cut#4 (yellow) at the bottom. The inner and outer arms are labeled. The mixture is not yet mixed.	 A V-blender with a 10% fill level after 50 revolutions. The mixture is now a binary mixture of dyed Cut#1 (black) and undyed Cut#4 (yellow), showing some mixing.
30	 A V-blender with a 30% fill level. The mixture is undyed Cut#4 (yellow) at the bottom. The inner and outer arms are labeled. The mixture is not yet mixed.	 A V-blender with a 30% fill level after 50 revolutions. The mixture is now a binary mixture of dyed Cut#1 (black) and undyed Cut#4 (yellow), showing more mixing.
50	 A V-blender with a 50% fill level. The mixture is undyed Cut#4 (yellow) at the bottom. The inner and outer arms are labeled. The mixture is not yet mixed.	 A V-blender with a 50% fill level after 50 revolutions. The mixture is now a binary mixture of dyed Cut#1 (black) and undyed Cut#4 (yellow), showing significant mixing.
70	 A V-blender with a 70% fill level. The mixture is undyed Cut#4 (yellow) at the bottom. The inner and outer arms are labeled. The mixture is not yet mixed.	 A V-blender with a 70% fill level after 50 revolutions. The mixture is now a binary mixture of dyed Cut#1 (black) and undyed Cut#4 (yellow), showing extensive mixing.

Figure 4.3: Visual observation of Cut#1 and Cut#4 binary mixture at varying fill levels in the V-blender

Mixtures were in a 50-50% by mass ratio at 25% fill level with dyed Cut#1 (black) loaded horizontally on top of undyed Cut#4 (yellow)

Sieving of the mixture was completed for both V-shell arms at varying fill level percentages from 10% to 70% using meshes based on mixture size fraction. Sieving was performed with the same procedures for horizontal and vertical loading trials in Chapter 3 of this thesis. The sieving results confirmed the visual observations shown in Figure 4.3. Table 4.2 shows the sieving which are then visualized in Figure 4.4. By increasing the fill level of the V-shell, the segregation development was seen to decrease and mixing efficiency was also decreased.

Table 4.2: Sieving results of Cut#1 and Cut#4 binary mixture in the outer arm of the V-shell at different fill levels

Size cuts	Loading order	Loading configuration	Fill level (%)	Sieving results in outer arm for trial 1 (%)	Sieving results in outer arm for trial 2 (%)	Average sieving results in outer arm (%)
Cut#1 and Cut#4	Cut#1 on top	Horizontal	10	Cut#1: 25 Cut#4: 75	Cut#1: 27 Cut#4: 73	Cut#1: 26 Cut#4: 74
Cut#1 and Cut#4	Cut#1 on top	Horizontal	20	Cut#1: 35 Cut#4: 65	Cut#1: 33 Cut#4: 67	Cut#1: 34 Cut#4: 66
Cut#1 and Cut#4	Cut#1 on top	Horizontal	30	Cut#1: 36 Cut#4: 64	Cut#1: 37 Cut#4: 63	Cut#1: 36.5 Cut#4: 63.5
Cut#1 and Cut#4	Cut#1 on top	Horizontal	40	Cut#1: 37 Cut#4: 63	Cut#1: 39 Cut#4: 61	Cut#1: 38 Cut#4: 62
Cut#1 and Cut#4	Cut#1 on top	Horizontal	50	Cut#1: 39 Cut#4: 61	Cut#1: 42 Cut#4: 58	Cut#1: 40.5 Cut#4: 59.5
Cut#1 and Cut#4	Cut#1 on top	Horizontal	60	Cut#1: 49 Cut#4: 51	Cut#1: 47 Cut#4: 53	Cut#1: 48 Cut#4: 52
Cut#1 and Cut#4	Cut#1 on top	Horizontal	70	Cut#1: 50 Cut#4: 50	Cut#1: 49 Cut#4: 51	Cut#1: 49.5 Cut#4: 50.5
Cut#1 and Cut#4	Cut#4 on top	Horizontal	10	Cut#1: 30 Cut#4: 70	Cut#1: 31 Cut#4: 69	Cut#1: 30.5 Cut#4: 69.5
Cut#1 and Cut#4	Cut#4 on top	Horizontal	20	Cut#1: 33 Cut#4: 67	Cut#1: 33 Cut#4: 67	Cut#1: 33 Cut#4: 67
Cut#1 and Cut#4	Cut#4 on top	Horizontal	30	Cut#1: 34 Cut#4: 66	Cut#1: 35 Cut#4: 65	Cut#1: 34.5 Cut#4: 65.5
Cut#1 and Cut#4	Cut#4 on top	Horizontal	40	Cut#1: 35 Cut#4: 65	Cut#1: 37 Cut#4: 63	Cut#1: 36 Cut#4: 64
Cut#1 and Cut#4	Cut#4 on top	Horizontal	50	Cut#1: 39 Cut#4: 61	Cut#1: 41 Cut#4: 59	Cut#1: 40 Cut#4: 60
Cut#1 and Cut#4	Cut#4 on top	Horizontal	60	Cut#1: 47 Cut#4: 53	Cut#1: 48 Cut#4: 52	Cut#1: 47.5 Cut#4: 52.5
Cut#1 and Cut#4	Cut#4 on top	Horizontal	70	Cut#1: 49 Cut#4: 51	Cut#1: 50 Cut#4: 50	Cut#1: 50 Cut#4: 50

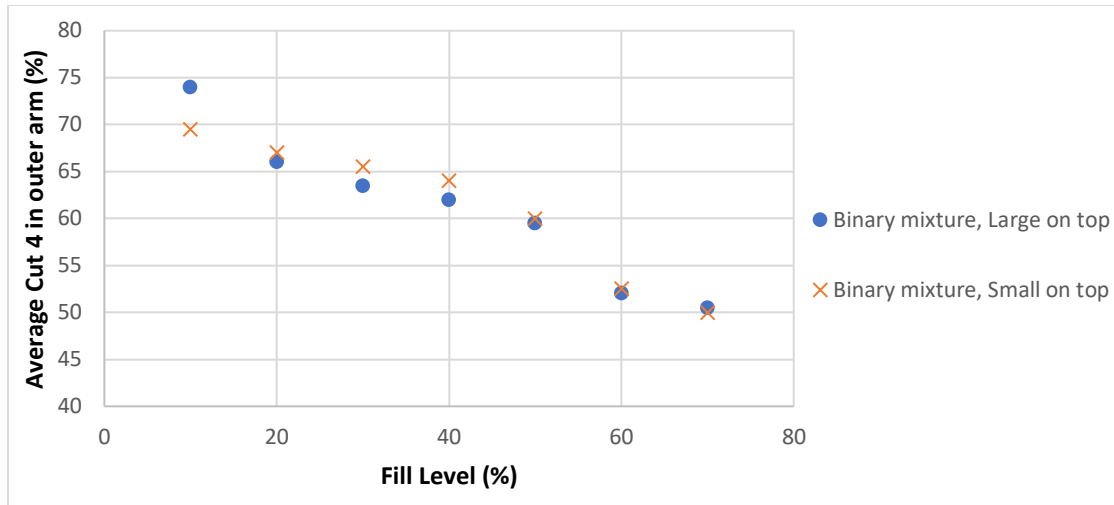


Figure 4.4: Effect of fill level on sieving of Cut#4 in the outer arm of the V-shell with trendlines and R^2 and P-values

The vibration amplitude profiles of Cut#1 and Cut#4 binary mixture were recorded. Experimental trials were conducted with 50-50% by mass ratio of binary mixtures of each size fraction and were loaded in a horizontal configuration in the V-blender. Figure 4.5 shows the vibration amplitude profile of Cut#1 and Cut#4 binary mixture at 10% fill level. When Cut#1 was loaded on top of Cut#4, the initial mixture vibration amplitude recorded was around 40 mV which was similar to the amplitude of the large size fraction of Cut#1. The vibration amplitude then decreased to around 20 mV after about 20 revolutions while maintaining the amplitude in the zone of 18 – 25 mV. When Cut#4 was loaded on top of Cut#1, the initial mixture vibration amplitude recorded was around 17 mV which was similar to the amplitude of the small size fraction of Cut#4. The vibration amplitude then increased to around 25 mV after about 20 revolutions while maintaining the amplitude in the zone of 20 – 27 mV.

The weighted average was determined based on the percentage of small and large particles in the outer V-shell by sieving and weighing the particles after 50 revolutions. This was done using the same procedure as mentioned in trials of Chapter 3 of this thesis. The percentages found in the outer V-shell arm along with the average amplitude recorded of each size fraction were then used to determine an approximate weighted average value. The weighted average was calculated in duplicates to account

for reproducibility and confirm the results therefore the weighted average was calculated twice and displayed on the graph as a zone that corresponds to two trials completed.

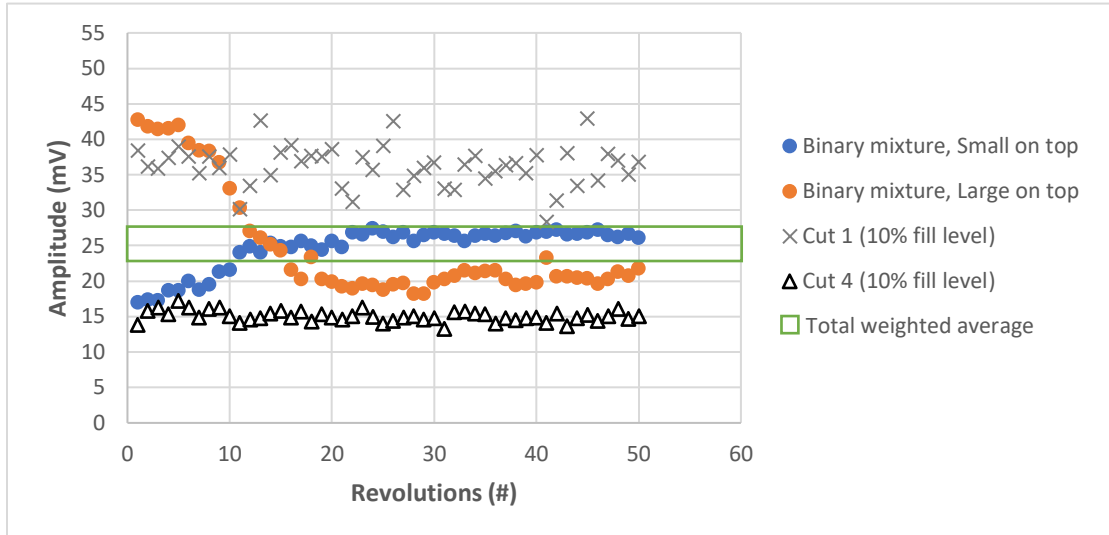


Figure 4.5: Acoustic profile of combined trials of Cut#1 (2.00 – 2.36 mm) and Cut#4 (0.006 – 1.18 mm) at 10% fill level

Mixtures were in a 50-50% by mass ratio and were loaded horizontally in the V-blender

Figure 4.6 shows the vibration amplitude profiles of Cut#1 and Cut#4 binary mixture at 30% fill level. When Cut#1 was loaded on top of Cut#4, the initial mixture vibration amplitude recorded was around 38 mV. The vibration amplitude then decreased to around 25 mV after about 20 revolutions while maintaining the amplitude in the zone of 24 – 30 mV. When Cut#4 was loaded on top of Cut#1, the initial mixture vibration amplitude recorded was around 15 mV. The vibration amplitude then increased to around 28 mV after about 25 revolutions while maintaining the amplitude in the zone of 24 – 30 mV.

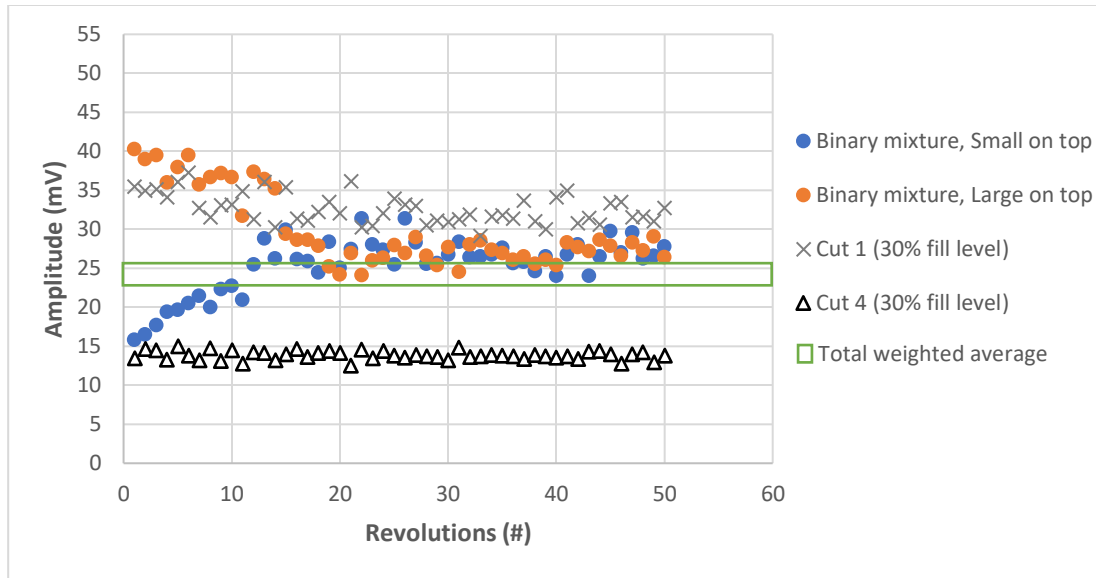


Figure 4.6: Acoustic profile of combined trials of Cut#1 (2.00 – 2.36 mm) and Cut#4 (0.006 – 1.18 mm) at 30% fill level

Mixtures were in a 50-50% by mass ratio and were loaded horizontally in the V-blender

Figure 4.7 shows the vibration amplitude profiles of Cut#1 and Cut#4 binary mixture at 70% fill level. When Cut#1 was loaded on top of Cut#4, the initial mixture vibration amplitude recorded was around 47 mV. The vibration amplitude then decreased to around 37 mV after about 20 revolutions while maintaining the amplitude in the zone of 35– 50 mV. When Cut#4 was loaded on top of Cut#1, the initial mixture vibration amplitude recorded was around 17 mV. The vibration amplitude then increased to around 39 mV after about 20 revolutions while maintaining the amplitude in the zone of 35 – 45 mV.

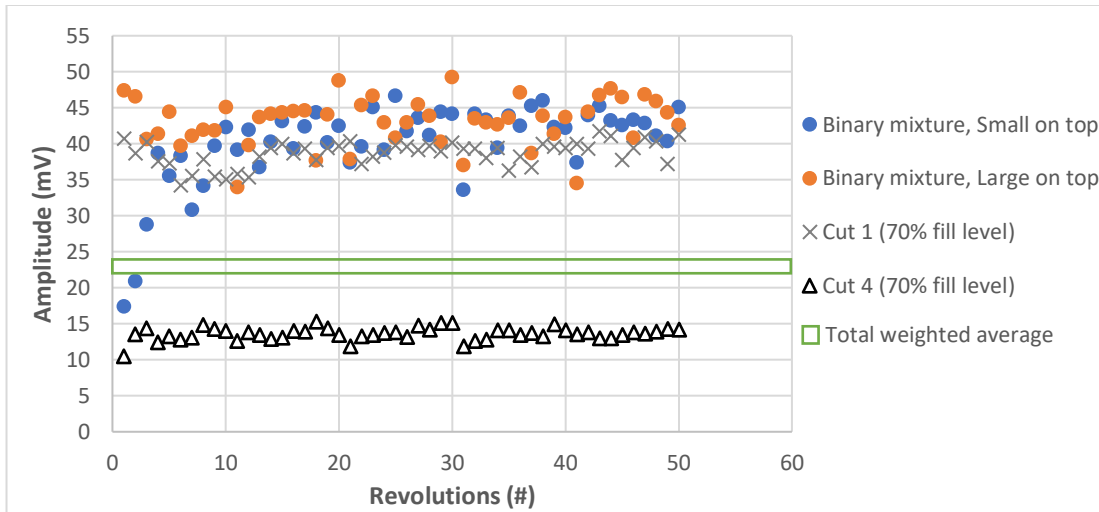


Figure 4.7: Acoustic profile of combined trials of Cut#1 (2.00 – 2.36 mm) and Cut#4 (0.006 – 1.18 mm) at 70% fill level

Mixtures were in a 50-50% by mass ratio and were loaded horizontally in the V-blender

The sieving results combined with individual particle size cut average amplitudes allowed a mixture amplitude to be estimated. For low fill levels (Figure 4.5), the measured and estimated amplitudes were similar. As the fill level increased, the measured mixture amplitudes were higher than the estimated values (Figures 4.6 and 4.7).

4.4 Discussion

Particle collisions with other particles or with the shell walls result in the propagation of some kinetic energy in the form of stress waves while other energy is retained by the particles (14). Upon collision of the tested starch granules with each other and with the V-shell, most of the energy was either retained by the particle or dissipated mainly as stress waves. The energy dissipated as stress waves were propagated and measured using an accelerometer securely attached to the outer arm of the V-shell as seen in Figure 4.1-B. In the V-blender, while starch granules were colliding with each other and with the V-shell wall, less energy was retained by the starch granule particles and less energy was dissipated as stress waves. That is due to the non-spherical and irregular shape of the starch granules. Due to their shape, starch granules may have

rotated and rolled during collision which would have resulted in less dissipated energy as stress waves that were recorded by the accelerometer (17).

The dissipated energy is proportional to the kinetic energy of the particles upon collision and the kinetic energy is dependent on the mass and velocity of the particles. Particles with high velocity fell almost the entire height of the V-shell unimpeded before colliding with the V-shell lid and therefore had high kinetic energy and velocities. The dissipation of energy because of particle collision with the V-shell depended on the angle of collision. Collision with a surface normal to the particle trajectory allowed more energy dissipation as stress waves. In contrast, collisions with an angled surface resulted in less energy dissipation as stress waves (15). Therefore, collisions with the lids of the V-shell resulted in more stress waves dissipation than collisions with the V-shell side walls. These dissipations were further enhanced by the velocity of the particles where the velocity of the particles colliding with the lids could reach higher values when compared to particles colliding with the side walls due to unimpeded particle trajectories being longer with particles colliding with the V-shell lids.

The flow pattern of particles was reflected as the result of the horizontal mixing profiles of the particles within the V-shell rotations and the recorded vibrations due to particle collisions with each other and with the V-shell lids and walls. In the first initial revolutions, most of the starch granule particles collided with the lids of the V-shell were the particles that were loaded on top of the bed. As the V-shell continued to rotate, the two components loaded in the V-shell started to mix with both components directly collided with the V-shell lids. Then the measured vibration amplitudes were either increased or decreased as the ratio of the particles colliding with the V-shell lids and their relative contributions to the measured amplitudes changed.

The mixing rate depends on the flow of particles in the V-shell while it rotates. The motion and flow of the particles in the V-shell occur mainly in the vertical direction. Horizontal particle motion occurs only for a small portion of the starch granule particles moving across the axis of symmetry into the V-shell's other arm as the V-shell

rotates into an upright position. Vertical particle movement is the main motion that dominates while rotation of the V-shell due to the V-shell geometry and how it operates. When the V-shell reaches an upright position, all of the particles flow into the restricted space at the bottom of the V-shell. For horizontal loading of particles in the V-shell, the particles were already distributed across the V-shell arms and mixing was only required in a vertical movement.

Increasing the fill level in the V-shell of the V-blender increased the mass of particles loaded in the V-shell and simultaneously reduced the available height for particle movement. More particles will result in more collisions between the particles with each other and with the V-shell walls but collisions with less kinetic energy. That is due to the velocity of an individual particle will be lower as the distance that a particle will fall unimpeded before collision with another particle or with the V-shell walls is shorter because of increasing the fill level in the V-shell. This change in collision dynamics affects the mixing process and can influence the resulting mixture's homogeneity and uniformity. Additionally, by increasing the fill level the flow of the particles inside the blender will change as there are more particles present and less available space for movement and interaction between particles with each other and with the V-shell walls. This change in particle flow can affect the overall mixing behavior and the pattern of measured acoustic emissions generated during mixing. Due to the presence of factors such as collision dynamics, particle flow, and acoustic emissions, acquiring a clear and consistent trend with fill level can be complex. The relationship between fill level and mixing efficiency and segregation may not follow a straightforward pattern and the trend observed can be hard to analyze clearly as seen in Figure 4.2 with individual size components and Figures 4.5, 4.6, and 4.7 with binary mixtures at different fill level percentages in the V-shell.

Figure 4.3 shows the fill level percentages of particles loaded in the V-blender and the available height relative to the V-shell before mixing. Upon increasing the fill level of the V-shell, the height of the V-shell was reduced due to the addition of more starch granule particles and consequently more particle mass. The high fill level of particle mass significantly restricted particle movement and interaction inside the V-shell. The

distance from the top of the bed of particles resting at the bottom of the V-shell to the top lid decreased from 43 cm to 27 cm as the fill level in the V-shell was increased from 10% to 70% by mass ratio. The change in the height of the V-shell resulted in a decrease in the ability of the particles to move and interact with each other and with the V-shell walls. Also, this change in the V-shell height reflected the decrease in distances that a particle could fall unimpeded within the V-shell before collision with another particle or with the V-shell walls. Shorter unimpeded distances reduced the potential of a particle reaching its maximum velocity or momentum before a collision. Therefore, starch granule particles would have low velocities and low kinetic energies.

At low fill levels, the probability that the starch granules will fall the height of the V-shell unimpeded as it is inverted before collision with the lid is high. A relatively high kinetic energy is reached and dissipated into stress waves with measured high amplitudes at low fill levels. As the fill level increased, the total mass of starch granules colliding with the lid increased but collision with less kinetic energy as the velocity of the individual particle is lower due to the small distance that is available for the particles before collision. The kinetic energy of a starch granule upon collision with the lid begins to decrease with corresponding lower dissipated measured stress wave energy. With more addition of starch granules and increasing in the fill level of the V-shell, a starch granule will collide with many other starch granules before its collision with the lid and consequently, the kinetic energy at collision and the amplitude of stress waves recorded by the accelerometer continue to decrease. The vibration amplitudes measured by the accelerometer attached to the outer V-shell arm will be affected by attenuation due to decreasing the kinetic energy and velocities of the starch granule particles. The acoustic emissions reflect mainly the impact of particles with the V-shell surfaces and the amplitude of the emission is associated with the particle momentum (25).

The flow of particles in the V-shell upon inversion can be classified into three main parts. The first part is associated with the flow of particles while the V-shell is inverted which is named Feature#1. The second part is associated with the flow of particles along the V-shell arms of the outer side which is named Feature#2. The third part is

associated with the flow of particles reaching the V-shell base which is named Feature#3. Feature#1 showed the most information about particle properties and behaviour inside the V-blender (26). Feature#1 had three sub-features. The first sub-feature is when the particles collide with the inner arms of the V-shell and then flow along the arms toward the V-shell lids. The second sub-feature is when collisions happen with the V-shell lids and between particles accumulating in the upper V-shell arms. The third sub-feature is seen when the particles accumulating in the upper V-shell arms flow across the lids toward the V-shell outer arms. All these three events are not distinct, but they overlap in duration (17). Wilson and Briens (2022) explained more about particle movement and behavior inside the V-blender and named the three sub-features: Feature#1a, Feature#1b, and Feature#1c.

Figure 4.8 shows the filtered raw acoustic signals for low and high fill levels of 10% and 70% by mass ratio in the V-shell, respectively. As the fill level increases, the characteristic groupings of vibrations change. At a very high fill level of 70% of the V-shell mass capacity, the filtered signals were seen to change in characteristics intensity and groupings (Figure 4.8-B). The second and third groupings were seen to merge at 70% fill level. With the merge of the second and third groupings, the flow of particles along the V-shell arms of the outer side and the flow of particles reaching the V-shell base were seen to happen simultaneously with no distinct time observed for each particle movement and flow across the V-shell. These changes can be due to the large masses of particles that resulted in overlapping of the sliding of particles along the side of the V-shell and falling and impacting particles at the bottom side of the V-shell. Also, it can be due to the restricted movement of particles in the V-shell which led to less energy dissipated as stress waves that resulted in particles with lesser velocities and kinetic energy and less energy travelled across the V-shell and recorded by the accelerometer.

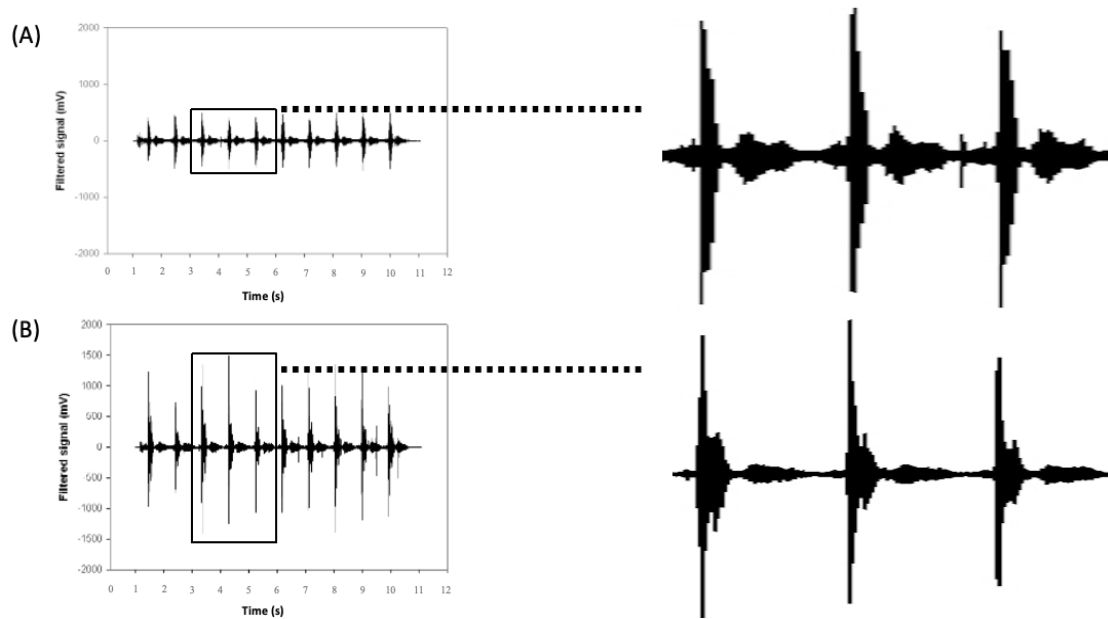


Figure 4.8: Filtered raw signals of binary mixtures of Cut#1 and Cut#4 at (A) 10% and (B) 70% fill levels by mass ratio of the V-shell

Visual observations showed that a left-right segregation pattern was seen to develop with the binary mixture of Cut#1 and Cut#4 after 20 revolutions and was fully developed at 50 revolutions at low fill levels (Figure 4.3). Furthermore, visual observation and sieving data showed that by increasing the fill level, the blend uniformity and segregation were affected and minimized, and less mixing can be seen to be happening between particles. At 70% fill level by mass ratio, left-right segregation development was negligible, and this can be supported by the sieving results shown in Table 4.3 with the larger component of Cut#1 seen in the outer arm with a 50% and the smaller component of Cut#4 with a 50%. This indicates inefficient mixing and no segregation development with the two components having equal percentages in each V-shell arm. This can be due to the restriction of particle movements and interactions at high percentages of fill levels of 70% that can hinder the mixing process leading to inefficient mixing between starch granule particles. Additionally, at low fill levels, more space was available in the V-shell for the movement of particles. While the V-blender tumbles, the particles collide with each other and with V-shell walls, and with the available space in the V-shell at 10% fill level, vertical mixing was seen to happen as well as lateral mixing and movements that

allowed for starch granules mixing. These mixing mechanisms enhanced the mixing process and blend uniformity of the mixture. Vertical mixing in addition to lateral mixing can be seen at low fill levels due to the presence of space allowing for more particle movements and interaction, therefore enhancing mixing efficiency. Left-right segregation was seen to develop also at low fill levels of the V-shell. As the fill level increased, there was no space for lateral mixing which minimized the left-right segregation development as seen with a higher fill level of 70%. The sieving changes seen in percentages of larger and smaller particles in the V-shell outer arm were majorly observed between 10% – 20% and 50% – 60% fill levels, especially between 50% – 60% fill levels which aligns with the visual observation in Figure 4.3.

4.5 Conclusion

Different V-shell fill levels were used with starch granules individual cuts and binary mixtures and were loaded horizontally in the V-blender to evaluate the effect of varying fill levels on mixing and segregation. At a very low fill level of 10% by mass ratio, left-right segregation was seen to develop with segregation of small particles in the outer arm and large particles in the inner arm of the V-shell. By increasing the fill level, the mixing and segregation were seen to change. At a high fill level of 70%, the mixing efficiency was decreased as well as left-right segregation was significantly decreased with no segregation seen to develop. At low fill level, there was more space available in the V-shell for particles which allowed for vertical and lateral mixing and movements. These mixing mechanisms resulted in more particle interactions and efficient mixing allowing for collisions between particles. By increasing the fill level, less space was available for lateral mixing which affected the mixing and segregation development. The sieving data confirmed the visual observations. The data from the trials conducted in this research suggests that there is indeed an effect of fill level on vibration amplitudes in the V-blender. However, the relationship between the fill level and mixing efficiency and segregation is complex. This highlights the need for further research to fully understand the underlying factors influencing mixing behavior at different fill levels. This research further supports the potential of passive acoustic emissions in monitoring powder mixing and segregation.

4.6 References

1. G. Léonard, F. Bertrand, J. Chaouki, and P. M. Gosselin, “An experimental investigation of effusivity as an indicator of powder blend uniformity,” *Powder Technology*, vol. 181, no. 2, pp. 149–159, Feb. 2008, doi: <https://doi.org/10.1016/j.powtec.2006.12.007>.
2. Debotton and A. Dahan, “Applications of Polymers as Pharmaceutical Excipients in Solid Oral Dosage Forms,” *Medicinal Research Reviews*, vol. 37, no. 1, pp. 52–97, Aug. 2016, doi: <https://doi.org/10.1002/med.21403>.
3. Center for Drug Evaluation and Research, “Q8(R2) Pharmaceutical Development,” U.S. Food and Drug Administration, 2019. <https://www.fda.gov/regulatory-information/search-fda-guidance-documents/q8r2-pharmaceutical-development>.
4. “Guidance for Industry Q8(R2) Pharmaceutical Development,” 2009. Available: <https://www.fda.gov/media/71535/download>.
5. J. Bridgwater, “Mixing of powders and granular materials by mechanical means—A perspective,” *Particuology*, vol. 10, no. 4, pp. 397–427, Aug. 2012, doi: <https://doi.org/10.1016/j.partic.2012.06.002>.
6. F. J. Muzzio, P. Robinson, C. Wightman, and Dean Brone, “Sampling practices in powder blending,” *International Journal of Pharmaceutics*, vol. 155, no. 2, pp. 153–178, Sep. 1997, doi: [https://doi.org/10.1016/s0378-5173\(97\)04865-5](https://doi.org/10.1016/s0378-5173(97)04865-5).
7. H. Berthiaux, K. Marikh, and C. Gatumel, “Continuous mixing of powder mixtures with pharmaceutical process constraints,” *Chemical Engineering and Processing: Process Intensification*, vol. 47, no. 12, pp. 2315–2322, Nov. 2008, doi: <https://doi.org/10.1016/j.cep.2008.01.009>.
8. N. Harnby, “An engineering view of pharmaceutical powder mixing,” *Pharmaceutical Science & Technology Today*, vol. 3, no. 9, pp. 303–309, Sep. 2000, doi: [https://doi.org/10.1016/s1461-5347\(00\)00283-2](https://doi.org/10.1016/s1461-5347(00)00283-2).
9. M. Asachi, E. Nourafkan, and A. Hassanpour, “A review of current techniques for the evaluation of powder mixing,” *Advanced Powder Technology*, vol. 29, no. 7, pp. 1525–1549, Jul. 2018, doi: <https://doi.org/10.1016/j.appt.2018.03.031>.

10. Fabien Anselmet and Pierre-Olivier Mattei, *Acoustics, aeroacoustics and vibrations*. London: Iste ; Wiley, 2016.
11. M. Bruneau and T. Scelo, *Fundamentals of Acoustics*. New York, NY: John Wiley & Sons, 2013.
12. A. Crouter and L. Briens, "The effect of granule moisture on passive acoustic emissions in a V-blender," *Powder Technology*, vol. 299, pp. 226–234, Oct. 2016, doi: <https://doi.org/10.1016/j.powtec.2016.05.037>
13. A. Cameron and L. Briens, "Monitoring lubricant addition in pharmaceutical tablet manufacturing through passive vibration measurements in a V-blender," *Powder Technology*, vol. 364, pp. 708–718, Mar. 2020, doi: <https://doi.org/10.1016/j.powtec.2020.02.018>.
14. A. Cameron and L. Briens, "An Investigation of Magnesium Stearate Mixing Performance in a V-Blender Through Passive Vibration Measurements," *AAPS PharmSciTech*, vol. 20, no. 5, May 2019, doi: <https://doi.org/10.1208/s12249-019-1402-3>.
15. A. Cameron and L. Briens, "Monitoring Magnesium Stearate Blending in a V-Blender Through Passive Vibration Measurements," *AAPS PharmSciTech*, vol. 20, no. 7, Jul. 2019, doi: <https://doi.org/10.1208/s12249-019-1469-x>.
16. K. Wilson and L. Briens, "Passive acoustic emissions application to a segregation prone mixture in a V-blender," *Powder Technology*, vol. 428, pp. 118827–118827, Oct. 2023, doi: <https://doi.org/10.1016/j.powtec.2023.118827>.
17. K. Wilson and L. Briens, "Investigation of passive acoustic emissions during powder mixing in a V-blender," *Powder Technology*, vol. 408, pp. 117754–117754, Aug. 2022, doi: <https://doi.org/10.1016/j.powtec.2022.117754>.
18. S. Oka, A. Sahay, W. Meng, and F. Muzzio, "Diminished segregation in continuous powder mixing," *Powder Technology*, vol. 309, pp. 79–88, Mar. 2017, doi: <https://doi.org/10.1016/j.powtec.2016.11.038>.
19. A. Alexander, F. J. Muzzio, and T. Shinbrot, "Segregation patterns in V-blenders," *Chemical Engineering Science*, vol. 58, no. 2, pp. 487–496, Jan. 2003, doi: [https://doi.org/10.1016/s0009-2509\(02\)00530-4](https://doi.org/10.1016/s0009-2509(02)00530-4).

20. A. Alexander, T. Shinbrot, B. Johnson, and F. J. Muzzio, "V-blender segregation patterns for free-flowing materials: effects of blender capacity and fill level," *International Journal of Pharmaceutics*, vol. 269, no. 1, pp. 19–28, Jan. 2004, doi: [https://doi.org/10.1016/s0378-5173\(03\)00296-5](https://doi.org/10.1016/s0378-5173(03)00296-5).
21. A. Mehrotra and F. J. Muzzio, "Comparing mixing performance of uniaxial and biaxial bin blenders," *Powder Technology*, vol. 196, no. 1, pp. 1–7, Nov. 2009, doi: <https://doi.org/10.1016/j.powtec.2009.06.008>.
22. J. Tewari, R. M. Strong, and P. Boulas, "At-line determination of pharmaceuticals small molecule's blending end point using chemometric modeling combined with Fourier transform near infrared spectroscopy," vol. 173, pp. 886–891, Feb. 2017, doi: <https://doi.org/10.1016/j.saa.2016.10.013>.
23. Wee Beng Lee, E. Widjaja, P. Wan, and Lai Wah Chan, "Near infrared spectroscopy for rapid and in-line detection of particle size distribution variability in lactose during mixing," *International Journal of Pharmaceutics*, vol. 566, pp. 454–462, Jul. 2019, doi: <https://doi.org/10.1016/j.ijpharm.2019.06.002>.
24. R. Hogg, "Mixing and Segregation in Powders: Evaluation, Mechanisms and Processes," *KONA Powder and Particle Journal*, vol. 27, no. 0, pp. 3–17, 2009, doi: <https://doi.org/10.14356/kona.2009005>.
25. R. Hou, A. Hunt, and R. A. Williams, "Acoustic monitoring of pipeline flows: particulate slurries," *Powder Technology*, vol. 106, no. 1–2, pp. 30–36, Nov. 1999, doi: [https://doi.org/10.1016/s0032-5910\(99\)00051-0](https://doi.org/10.1016/s0032-5910(99)00051-0).
26. A. Crouter and L. Briens, "Passive acoustic emissions from particulates in a V-blender," *Drug Development and Industrial Pharmacy*, vol. 41, no. 11, pp. 1809–1818, Feb. 2015, doi: <https://doi.org/10.3109/03639045.2015.1009913>.
27. E. Por, M. Van Kooten, and V. Sarkovic, "Nyquist-Shannon sampling theorem 1 Theory 1.1 The Nyquist-Shannon sampling theorem," 2019.

Chapter 5

5 Conclusion

5.1 General Discussion and Conclusions

Powder mixing is a particularly important process in the pharmaceutical manufacture of tablets and capsules. Tablets and capsules account for approximately 80% of all available pharmaceutical formulations as solid dosage forms (1). Powder mixing is required at different points through the process of tablet and capsule production due to the use of multistage batch processes. The process of powder mixing must be done very carefully to ensure that the Active Pharmaceutical Ingredient (API) is well mixed along with the other excipients and additives used. If the mixing processes were done incorrectly, the produced tablets may have an incorrect amount of API and physical characteristics (1,2).

Different monitoring methods and techniques are required to control and monitor powder mixing in pharmaceutical production. Effective inline monitoring is crucial, especially with particles with large differences in physical properties like particle size, density, and flowability which can lead to segregation development. Segregation can affect the final product quality which can lead to batch rejection. (3-5). Optimal powder mixing depends on powder behavior and characteristics which are considered important factors needed to be able to understand and control the mixing process. However, due to a poor understanding of powder mixing, it is still not a clear and efficient process. That is due to the presence of many factors that can influence and interfere with powder mixing. Powder mixing still requires more research to further understand the process and develop methods to better monitor it.

Currently, the pharmaceutical industry uses offline methods for powder monitoring and control with samples required to be withdrawn from different areas of the mixture bed. After the samples are withdrawn, they are tested with destructive testing methods which are invasive, expensive, and inefficient methods (4). Process Analytical Technologies (PATs) are potential methods that can be used to monitor mixing in

pharmaceutical production. PATs provide mechanisms to maintain high-quality standards and improve processes (7). Some PATs are currently in development, and some are used in the industry, but most of these PATs require expensive alteration in equipment to function as needed or have some limitations for the processes involved. Passive acoustic emissions (PAE) provide a potential inline monitoring method for powder mixing and segregation that is effective, non-invasive, non-destructive, and has a comparatively low cost.

Preliminary studies identified the best location for the sensor and extraction of information from the emissions using the amplitude of the measured vibrations as well as observing particle movements and behaviors inside the V-blender. Moreover, some studies focused on the connections between particle motion and passive acoustic emissions from a V-blender and identified methods to best extract relevant process information as well as apply passive acoustic emissions in detecting segregation (8-13). The objective of the current research was to further investigate and apply PAE in monitoring powder mixing and segregation with different loading configurations and orders. An additional objective was to monitor mixing and segregation while changing fill levels of the V-shell of the V-blender. An accelerometer was attached to the lid of the outer V-shell arm to allow for the measurement of PAE while mixing. Starch granules and glass beads with a similar density to those commonly used pharmaceutical granules were used in five different size cuts of starch granules and three diameter sizes of glass beads.

Experimental trials were completed using starch granules and glass beads to understand the connection between particle motion and measured vibrations. Moreover, starch granule trials were conducted by loading the starch granules into the V-shell in two configurations, horizontally and vertically with different loading orders. In Chapter 3 trials, the rotation rate of the V-shell and the fill level were kept consistent at 25 rpm and 25% fill level by mass ratio, respectively. Left-right segregation pattern was developed with all trials of horizontal and vertical loading even with intensifier bar additions. The PAE amplitudes recorded were initially similar to that of the particle loaded on top in case of horizontal loading and the outer arm in case of vertical loading

before starting to trend towards the bottom and inner arm particle's amplitude and reaching a plateau. The plateau amplitude was representative of the weighted average amplitude area based on the particle composition in the outer V-shell arm. Stable mixtures were identified in all trials according to the minimum mixing time needed. From these trials, it was concluded that horizontal loading trials resulted in faster mixing and stable mixtures were reached in fewer revolutions compared to vertical loading trials. In Chapter 4 trials, the rotation rate of the V-shell was kept consistent, but the fill level was changed with low and high fill levels ranging from 5% to 75% by mass ratio at 5% and 10% intervals. The results showed that at low fill levels, the mixing efficiency was high, and left-right segregation was seen to develop while at high fill levels, the mixing efficiency was low, and blend uniformity was reduced as well as segregation was negligible with no left-right segregation development during mixing.

This research demonstrated the ability of PAE to monitor powder mixing and allowed for the identification of segregation during mixing. The findings of this thesis support the potential use of PAE as a process analytical technology for monitoring multi-component powder mixtures. PAE provides reliable particle flow process information that will allow for improved inline control and monitoring of mixing and segregation. However, PAE has some limitations in monitoring powder mixing and segregation when used with particles with close diameter and amplitude differences.

5.2 Future Work and Recommendations

Current research should be expanded upon to further develop and improve the application of PAE for monitoring powder mixing and segregation. The research conducted in this thesis has been completed using offline analysis of the signals. Additional studies should establish techniques and approaches to apply PAE for inline and real-time monitoring. Moreover, other research is required to help commercially implement PAE for monitoring powder mixing and segregation on an industrial scale. The pharmaceutical industry is still uncertain about adopting new technologies even when supported and approved by governing groups such as the Food and Drug Administration (FDA). Having large amounts of supporting studies and research can

reveal the advantages of PAE and increase the possibility of this technology being implemented by the pharmaceutical industry for monitoring powder mixing and segregation.

Monitoring powder mixing and segregation using PAE still requires more future development. In this research, the process conditions selected resulted in a left-right segregation pattern; consequent research should be performed to assess the effectiveness of PAE for identifying other segregation patterns as well as changing the process parameters used. By further exploring these applications, a greater number of potential future industrial applications can be identified. Generally, PAE provide an effective method for monitoring powder mixing. By using this method in industry, process quality, safety, control, and monitoring can be achieved while helping to detect and take actions to mitigate segregation development during mixing that results in improved product quality.

5.3 References

1. G. Léonard, F. Bertrand, J. Chaouki, and P. M. Gosselin, “An experimental investigation of effusivity as an indicator of powder blend uniformity,” *Powder Technology*, vol. 181, no. 2, pp. 149–159, Feb. 2008, doi: <https://doi.org/10.1016/j.powtec.2006.12.007>.
2. Muzzio, F. J, C. L Goodridge, A Alexander, P Arratia, H Yang, O Sudah, and G Mergen. 2003. “Sampling and Characterization of Pharmaceutical Powders and Granular Blends.” *International Journal of Pharmaceutics* 250 (1): 51–64. [https://doi.org/10.1016/S0378-5173\(02\)00481-7](https://doi.org/10.1016/S0378-5173(02)00481-7). A. Alexander, F. J. Muzzio, and T. Shinbrot, “Segregation patterns in V-blenders,” *Chemical Engineering Science*, vol. 58, no. 2, pp. 487–496, Jan. 2003, doi: [https://doi.org/10.1016/s0009-2509\(02\)00530-4](https://doi.org/10.1016/s0009-2509(02)00530-4).
3. S. Oka, A. Sahay, W. Meng, and F. Muzzio, “Diminished segregation in continuous powder mixing,” *Powder Technology*, vol. 309, pp. 79–88, Mar. 2017, doi: <https://doi.org/10.1016/j.powtec.2016.11.038>.
4. M. Asachi, E. Nourafkan, and A. Hassanpour, “A review of current techniques for the evaluation of powder mixing,” *Advanced Powder Technology*, vol. 29, no. 7, pp. 1525–1549, Jul. 2018, doi: <https://doi.org/10.1016/j.appt.2018.03.031>.
5. J. Bridgwater, “Mixing of powders and granular materials by mechanical means—A perspective,” *Particuology*, vol. 10, no. 4, pp. 397–427, Aug. 2012, doi: <https://doi.org/10.1016/j.partic.2012.06.002>.
6. Center for Drug Evaluation and Research, “Q8(R2) Pharmaceutical Development,” U.S. Food and Drug Administration, 2019. <https://www.fda.gov/regulatory-information/search-fda-guidance-documents/q8r2-pharmaceutical-development>
7. A. Crouter and L. Briens, “The effect of granule moisture on passive acoustic emissions in a V-blender,” *Powder Technology*, vol. 299, pp. 226–234, Oct. 2016, doi: <https://doi.org/10.1016/j.powtec.2016.05.037>
8. A. Cameron and L. Briens, “Monitoring lubricant addition in pharmaceutical tablet manufacturing through passive vibration measurements in a V-blender,” *Powder*

- Technology, vol. 364, pp. 708–718, Mar. 2020, doi: <https://doi.org/10.1016/j.powtec.2020.02.018>.
9. A. Cameron and L. Briens, “An Investigation of Magnesium Stearate Mixing Performance in a V-Blender Through Passive Vibration Measurements,” *AAPS PharmSciTech*, vol. 20, no. 5, May 2019, doi: <https://doi.org/10.1208/s12249-019-1402-3>.
 10. A. Cameron and L. Briens, “Monitoring Magnesium Stearate Blending in a V-Blender Through Passive Vibration Measurements,” *AAPS PharmSciTech*, vol. 20, no. 7, Jul. 2019, doi: <https://doi.org/10.1208/s12249-019-1469-x>.
 11. K. Wilson and L. Briens, “Investigation of passive acoustic emissions during powder mixing in a V-blender,” *Powder Technology*, vol. 408, pp. 117754–117754, Aug. 2022, doi: <https://doi.org/10.1016/j.powtec.2022.117754>.
 12. K. Wilson and L. Briens, “Passive acoustic emissions application to a segregation prone mixture in a V-blender,” *Powder Technology*, vol. 428, pp. 118827–118827, Oct. 2023, doi: <https://doi.org/10.1016/j.powtec.2023.118827>.
 13. “An Investigation of Magnesium Stearate Mixing Performance in a V-Blender Through Passive Vibration Measurements,” *AAPS PharmSciTech*, vol. 20, no. 5, May 2019, doi: <https://doi.org/10.1208/s12249-019-1402-3>.
 14. A. Cameron and L. Briens, “Monitoring Magnesium Stearate Blending in a V-Blender Through Passive Vibration Measurements,” *AAPS PharmSciTech*, vol. 20, no. 7, Jul. 2019, doi: <https://doi.org/10.1208/s12249-019-1469-x>.
 15. K. Wilson and L. Briens, “Investigation of passive acoustic emissions during powder mixing in a V-blender,” *Powder Technology*, vol. 408, pp. 117754–117754, Aug. 2022, doi: <https://doi.org/10.1016/j.powtec.2022.117754>.
 16. K. Wilson, “Application of Passive Acoustic Emissions for Inline Monitoring of Segregation Prone Mixtures in a V-Blender.” Aug. 2022.

Appendices

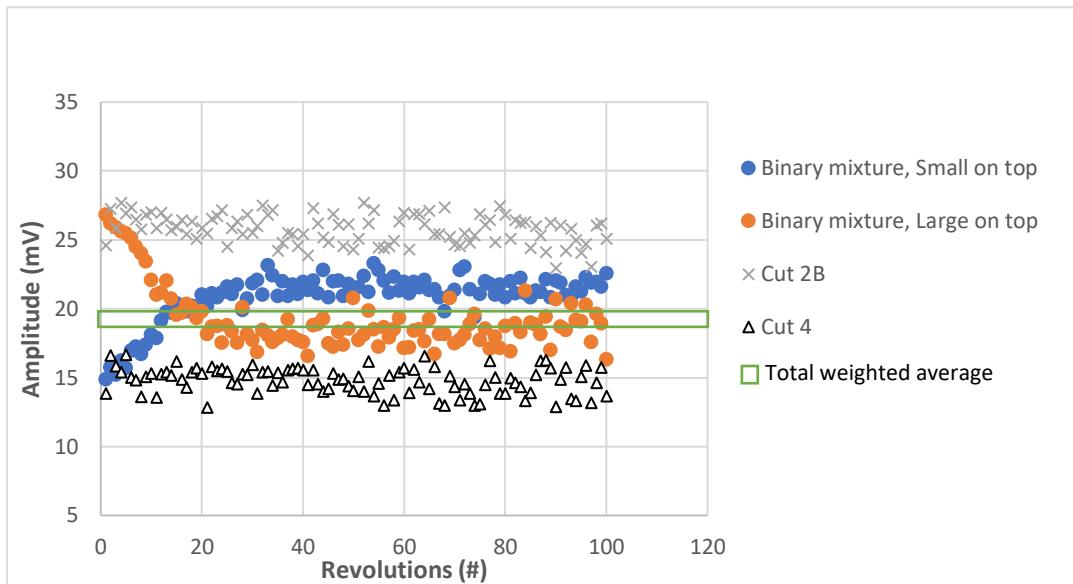
Appendix A: Sieving data for different horizontal loading trials in the outer arm of the V-shell

Trial	Size cuts	Loading order	Loading configuration	Sieving results in outer arm (%)
I	Cut#1 and Cut#4	Cut#1 on top and Cut#4 on bottom	Horizontal	Trial 1: Cut#4 (68), Cut#1 (32) Trial 2: Cut#4 (70), Cut#1 (30) Trial 3: Cut#4 (67), Cut#1 (33) Average: Cut#4 (68), Cut#1 (32)
II	Cut#1 and Cut#4	Cut#1 on bottom and Cut#4 on top	Horizontal	Trial 1: Cut#4 (66), Cut#1 (34) Trial 2: Cut#4 (67), Cut#1 (33) Trial 3: Cut#4 (70), Cut#1 (30) Average: Cut#4 (68), Cut#1 (32)
III	Cut#1 and Cut#3	Cut#1 on top and Cut#3 on bottom	Horizontal	Trial 1: Cut#3 (64), Cut#1 (36) Trial 2: Cut#3 (65), Cut#1 (35) Trial 3: Cut#3 (61), Cut#1 (39) Average: Cut#3 (63), Cut#1 (37)
IV	Cut#1 and Cut#3	Cut#1 on bottom and Cut#3 on top	Horizontal	Trial 1: Cut#3 (63), Cut#1 (37) Trial 2: Cut#3 (63), Cut#1 (37) Trial 3: Cut#3 (62), Cut#1 (38) Average: Cut#3 (63), Cut#1 (37)
V	Cut#2A and Cut#4	Cut#2A on top and Cut#4 on bottom	Horizontal	Trial 1: Cut#2A (60), Cut#4 (40) Trial 2: Cut#2A (62), Cut#4 (38) Trial 3: Cut#2A (61), Cut#4 (39) Average: Cut#2A (61), Cut#4 (39)
VI	Cut#2A and Cut#4	Cut#2A on bottom and Cut#4 on top	Horizontal	Trial 1: Cut#2A (58), Cut#4 (42) Trial 2: Cut#2A (62), Cut#4 (38) Trial 3: Cut#2A (61), Cut#4 (39) Average: Cut#2A (60), Cut#4 (40)
VII	Cut#2A and Cut#3	Cut#2A on top and Cut#3 on bottom	Horizontal	Trial 1: Cut#3 (55), Cut#2A (45) Trial 2: Cut#3 (61), Cut#2A (39) Trial 3: Cut#3 (58), Cut#2A (42) Average: Cut#3 (58), Cut#2A (42)
VIII	Cut#2A and Cut#3	Cut#2A on bottom and Cut#3 on top	Horizontal	Trial 1: Cut#3 (53), Cut#2A (47) Trial 2: Cut#3 (57), Cut#2A (43) Trial 3: Cut#3 (57), Cut#2A (43) Average: Cut#3 (56), Cut#2A (44)
IX	Cut#2B and Cut#4	Cut#2B on top and Cut#4 on bottom	Horizontal	Trial 1: Cut#2B (61), Cut#4 (39) Trial 2: Cut#2B (62), Cut#4 (38) Trial 3: Cut#2B (59), Cut#4 (41) Average: Cut#2B (61), Cut#4 (39)
X	Cut#2B and Cut#4	Cut#2B at bottom and Cut#4 on top	Horizontal	Trial 1: Cut#2B (56), Cut#4 (44) Trial 2: Cut#2B (61), Cut#4 (39) Trial 3: Cut#2B (63), Cut#4 (37) Average: Cut#2B (60), Cut#4 (40)

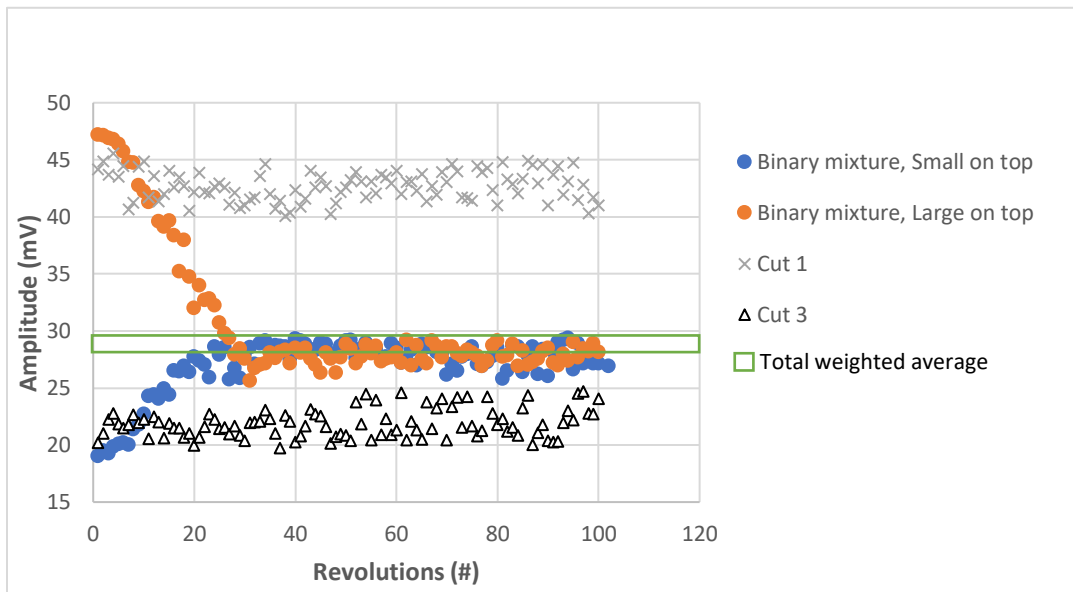
Appendix B: Sieving data for different vertical loading trials in the outer arm of the V-shell

Trial	Size cuts	Loading order	Loading configuration	Sieving results in outer arm (%)
A	Cut#1 and Cut#4	Cut#1 in inner arm and Cut#4 in outer arm	Vertical	Trial 1: Cut#4 (64), Cut#1 (36) Trial 2: Cut#4 (62), Cut#1 (38) Trial 3: Cut#4 (63), Cut#1 (37) Average: Cut#4 (63), Cut#1(37)
B	Cut#1 and Cut#4	Cut#1 in outer arm and Cut#4 in inner arm	Vertical	Trial 1: Cut#4 (67), Cut#1 (33) Trial 2: Cut#4 (64), Cut#1 (34) Trial 3: Cut#4 (63), Cut#1 (37) Average: Cut#4 (65), Cut#4 (35)
C	Cut#1 and Cut#3	Cut#1 in inner arm and Cut#3 in outer arm	Vertical	Trial 1: Cut#3 (63), Cut#1 (37) Trial 2: Cut#3 (67), Cut#1 (33) Trial 3: Cut#3 (66), Cut#1 (34) Average: Cut#4 (65), Cut#1 (35)
D	Cut#1 and Cut#3	Cut#1 in outer arm and Cut#3 in inner arm	Vertical	Trial 1: Cut#3 (62), Cut#1 (38) Trial 2: Cut#3 (65), Cut#1 (35) Trial 3: Cut#3 (66), Cut#1 (34) Average: Cut#4 (64), Cut#1 (36)
E	Cut#2A and Cut#4	Cut#2A in inner arm and cut#4 in outer arm	Vertical	Trial 1: Cut#4 (62), Cut#2A (38) Trial 2: Cut#4 (63), Cut#2A(37) Trial 3: Cut#4 (64), Cut#2A(36) Average: Cut#4 (63), Cut#2A(37)
F	Cut#2A and Cut#4	Cut#2A in outer arm and Cut#4 in inner arm	Vertical	Trial 1: Cut#4 (65), Cut#2A (35) Trial 2: Cut#4 (61), Cut#2A(39) Trial 3: Cut#4 (62), Cut#2A(38) Average: Cut#4 (63), Cut#2A(37)
G	Cut#2A and Cut#3	Cut#2A in inner arm and Cut#3 in outer arm	Vertical	Trial 1: Cut#3 (58), Cut#2A (42) Trial 2: Cut#3 (59), Cut#2A (41) Trial 3: Cut#3 (58), Cut#2A (42) Average: Cut#3 (58), Cut#2A (42)
H	Cut#2A and Cut#3	Cut#2A in outer arm and Cut#3 in inner arm	Vertical	Trial 1: Cut#3 (61), Cut#2A (39) Trial 2: Cut#3 (58), Cut#2A (42) Trial 3: Cut#3 (59), Cut#2A (41) Average: Cut#3 (59), Cut#2A (41)
I	Cut#2B and Cut#4	Cut#2B in inner arm and Cut#4 in outer arm	Vertical	Trial 1: Cut#4 (61), Cut#2B (39) Trial 2: Cut#4 (61), Cut#2B (39) Trial 3: Cut#4 (62), Cut#2B (38) Average: Cut#4 (61), Cut#2B (39)
G	Cut#2B and Cut#4	Cut#2B in outer arm and Cut#4 in inner arm	Vertical	Trial 1: Cut#4 (61), Cut#2B (39) Trial 2: Cut#4 (60), Cut#2B (40) Trial 3: Cut#4 (61), Cut#2B (39) Average: Cut#4 (61), Cut#2B (39)

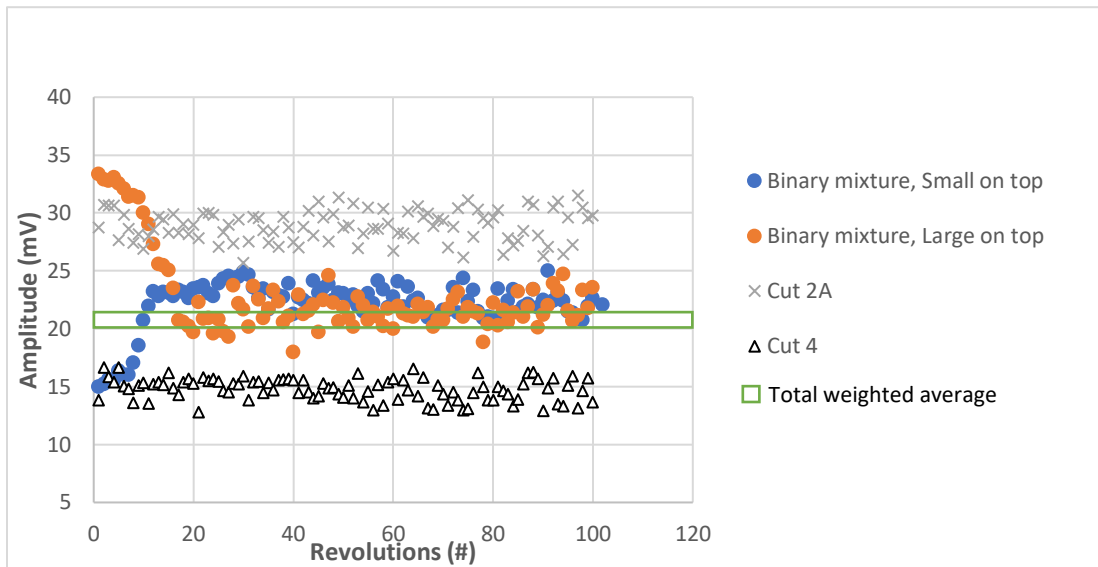
Appendix C: Starch granules combined trials with 50-50% binary mixture by mass ratio, Cut#2B (1.40 – 1.70 mm), Cut#4 (0.006 – 1.18 mm) horizontally loaded in the V-blender



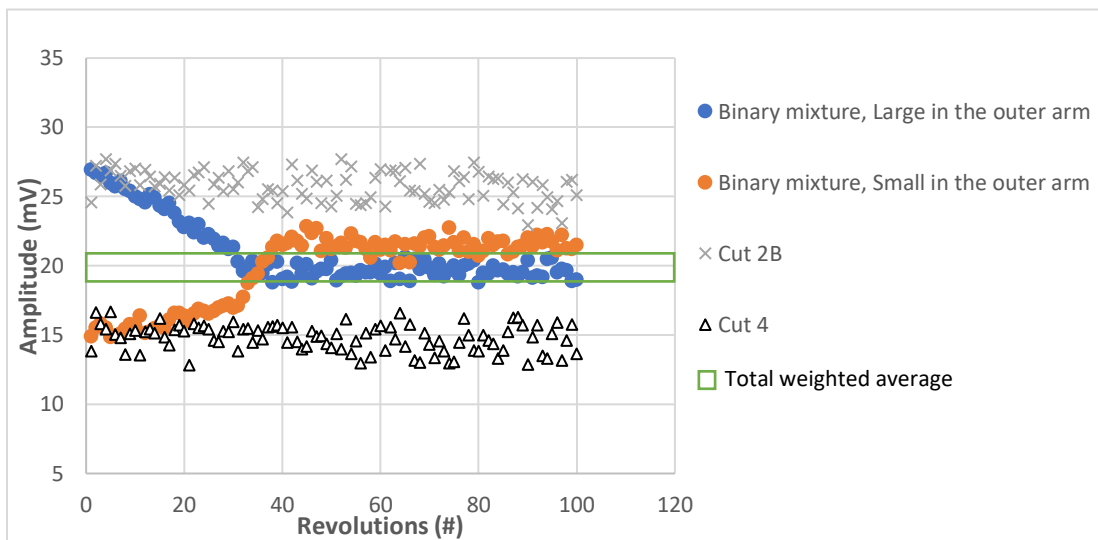
Appendix D: Starch granules combined trials with 50-50% binary mixture by mass ratio, Cut#1 (2.00 – 2.36 mm), Cut#3 (1.18 – 1.40 mm) horizontally loaded in the V-blender



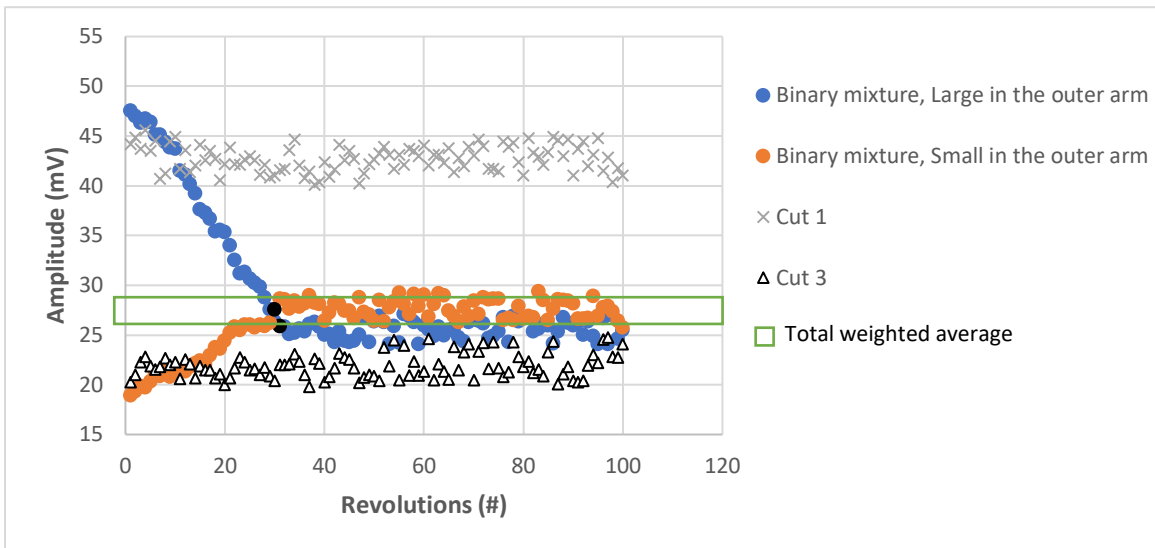
Appendix E: Starch granules combined trials with 50-50% binary mixture by mass ratio, Cut#2A (1.70 – 2.00 mm), Cut#4 (0.006 – 1.18 mm) horizontally loaded in the V-blender



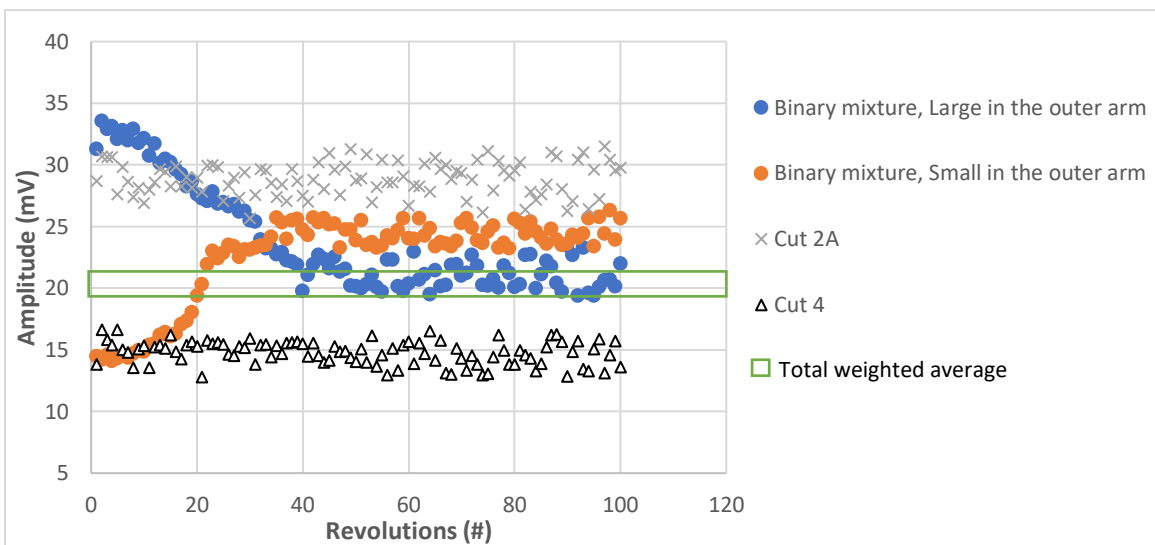
Appendix F: Starch granules combined trials with 50-50% binary mixture by mass ratio, Cut#2B (1.40 – 1.70 mm), Cut#4 (0.006 – 1.18 mm) vertically loaded in the V-blender



Appendix G: Starch granules combined trials with 50-50% binary mixture by mass ratio, Cut#1 (2.00 – 2.36 mm), Cut#3 (1.18 – 1.40 mm) vertically loaded in the V-blender



Appendix H: Starch granules combined trials with 50-50% binary mixture by mass ratio, Cut#2A ((1.70 – 2.00 mm), Cut#4 (0.006 – 1.18 mm) vertically loaded in the V-blender



Curriculum Vita

Name: Omar Salem

Post-secondary Education and Degrees:

Master of Engineering Science, Chemical Engineering
The University of Western Ontario
London, Ontario, Canada
2022-2024

Bachelor of Science, Pharmacy
German University in Cairo
Cairo, Egypt
2013-2018

Related Work Experience

Graduate Teaching Assistant
The University of Western Ontario
2022-2023